# Water Balance of the Maurikse Wetering

Niek Hunink

MSc. Thesis

TU Delft

Royal HaskoningDHV
Enhancing Society Together

# Water balance of the Maurikse Wetering

by

Niek Hunink

In partial fulfilment of the requirements for the degree of

**Master of Science**
in Civil Engineering

at the Delft University of Technology,
to be defended publicly on Friday July 19, 2019 at 12:00 p.m.

| | | |
|---|---|---|
| Student number: | 4014634 | |
| Thesis committee: | Dr. ir. M. Hrachowitz (chair) | TU Delft |
| | Dr. ir. M. Bakker | TU Delft |
| | Dr. ir. J. Bricker | TU Delft |
| | MSc. H. Vermue | Royal HaskoningDHV |



TU Delft

# Acknowledgements

Before you lies the final product of my master thesis. While this thesis is a personal work and only my name is listed as its author, it could not have been accomplished by myself alone. The support I received over the last year has been imperative for my success.

First of all, I would like to thank Han Vermue, who was my supervisor at Royal HaskoningDHV, for his tireless support and close supervision during this entire project. Han, your knowledge, insight and dedication cannot be understated. I could truly rely on you.

My sincere thanks go out to my supervisors at TU Delft, Markus Hrachowitz, Mark Bakker and Jeremy Bricker. Markus, your support, guidance and enthusiasm over the entire course of this project are greatly appreciated and I will be forever grateful for giving me the opportunity to work on this project. Without you this project would not have been possible. Mark and Jeremy, the insight you provided in your fields of expertise were invaluable.

From the Rivierenland Water Board I would like to thank Judith van Tol, Frank Weerts, Esther Vermue and Jef Willemsen. Judith and Frank provided me with any data I required as well as insight and advice on how to proceed. Esther, our chance encounter was among the luckiest events I had during this thesis. What started as a hallway greeting resulted in us meeting Jef, which led to us three cracking one of the most frustrating problems I encountered during this thesis.

I had a lot of help from my colleagues at Royal HaskoningDHV. Most of all I would like to thank Wouter Engel for all the work he put into with modelling the most crucial aspect of this thesis. Any questions I had, any additional data I required, Wouter was there. Thank you. I am thankful to all my colleagues at Royal HaskoningDHV, especially the Water Management team at Rotterdam. I want to mention Jacco Breedijk in particular, who initially put me into contact with his colleagues at Royal HaskoningDHV while I was still looking for a thesis subject, which resulted in the subject you see before you today. Jacco, you are a good friend, one that I can rely on.

Thank you Claudia Brauer, for helping with WALRUS, for providing me with literature as well as insight on how to proceed.

A special thanks goes out to my friends Maarten and Reijer, who helped me a lot in finishing this thesis.

These acknowledgements would not be complete without a shoutout to Hokje 1, and yes, also to Hokje 2, who were my student buddies, colleagues and most of all my friends.

I want to thank my parents Mark, Mariët, Ella and Pieter, as well as my sister Jolien and brothers Martijn and Timo, for always believing in me and helping me get through this. I love you all.

Last but not least, I want to express my sincere gratitude to my friends, for their support, advice, proofreading and/or for keeping my morale up. Jasper, Lisa, Ties, Jeroen, Nicael, Maud, Team Kickass and the Sleeping Saviors, and many more. Thank you.

It has been a long road, but I am very happy with the results. I hope this thesis can contribute to the reader's interest in the wonderful world of Hydrology.

*Niek Hunink*

*Delft, July 2019*

# Abstract

The Maurikse Wetering is a tributary of the Line river in the centre of the Netherlands. It is situated between the larger Nederrijn and Waal rivers, which roughly run parallel to the course of the Maurikse Wetering river. Due to the catchments' proximity to these rivers, intercatchment groundwater flow (IGF; groundwater flow crossing topographic divides) might have a significant influence on the water balance of the Maurikse Wetering catchment. As the IGF cannot be measured directly and due to the complex nature of the IGF, the IGF is considered to be one of the hardest fluxes to quantify in conceptual hydrological modelling. The objective of this thesis is to express the IGF as a function of easy-to-measure variables.

The most common method used to estimate the net IGF to a catchment, is to equate the IGF to the missing water in the water balance of the catchment. However, this is not possible for the Maurikse Wetering catchment, since the discharge data of the tilting weirs is erroneous. To quantify the IGF, the Maurikse Wetering catchment and the surrounding area is modelled in the groundwater model MORIA. The program iMOD is used to analyse and visualise the modelled data.

The direction of the groundwater flow as modelled by MORIA shows that the groundwater flow in the region is heavily influenced by the Nederrijn and Waal rivers. Thus, in order to relate the water level in either the Nederrijn or the Waal to the net IGF to the Maurikse Wetering catchment, a simple linear regression (SLR) analysis was performed. In the SLR, the modelled IGF data is expressed as a linear function of the water level in the rivers. Of the variables entered in the SLR analysis, the Nederrijn has the best fit to the IGF flux. This means that the IGF can be expressed in terms of the water level in the Nederrijn.

A multiple linear regression (MLR) analysis was performed to study the influence of variables affecting the water balance of the Maurikse Wetering, e.g. the water level in the Nederrijn, the groundwater level in the Maurikse Wetering catchment and the precipitation, on the IGF. According to the MLR analysis, the variables that influence the IGF flux are the Waal level, the average groundwater level in the catchment, the precipitation, the storage deficit in the unsaturated zone and the water level in the Maurikse Wetering.

The fact that multiple easy-to-measure factors have a relation to the IGF, shows that there are alternative methods to equating the IGF to the missing water in the water balance. This provides a basis for the usage of IGF relations in predictive modelling. If reliable discharge data for the Maurikse Wetering can be acquired, it is possible to validate the common method to measure IGF.

The IGF is often ignored in conceptual hydrological modelling. In order to analyse the effect it has on these models, the catchment is modelled in WALRUS. The catchment is once calibrated without IGF data, and once with the IGF as modelled by MORIA. The catchment is then modelled once without IGF data, and once with the IGF as modelled by the SLR relation with the Nederrijn.

Including the IGF in WALRUS shows an improvement in modelling the variation in groundwater level over smaller time steps compared to the WALRUS model without IGF, the latter only showing a seasonal change in groundwater level. During validation, the model with the IGF relation retains a higher efficiency in modelling the average groundwater level in the Maurikse Wetering than the model without an IGF flux. The results with and without the IGF incorporation into the model show that the IGF can contribute to significant improvements for conceptual hydrological models.

# TABLE OF CONTENTS

# List of abbreviations

| | |
|---|---|
| GWL | Groundwater level |
| IGF | Intercatchment groundwater flow |
| MLR | Multiple linear regression |
| NR | Nederrijn |
| NS | Nash-Sutcliffe |
| NSE | Nash-Sutcliffe efficiency |
| SLR | Simple linear regression |
| WA | Waal |

# 1 Introduction

On the 14th of December 2017, the Arkelse Damsluis lock between the Linge River and the Merwedekanaal channel was closed by the Rivierenland water board as maximum water levels were reached in the Merwedekanaal (Tanis, 2017). The most critical water levels in the Linge basin occurred in the Maurikse Wetering river, a tributary of the Linge. This event lay at the basis of this thesis. A conceptual hydrological model can be used to study the various fluxes in the Maurikse Wetering,

## 1.1 Project area

The Maurikse Wetering is a river in the province of Gelderland. It is a tributary of the Linge, the longest river fully in the Netherlands (Lingestreek, n.d.). To the north of the Maurikse Wetering catchment runs the Nederrijn and to the south the Waal, two of the largest rivers in the Netherlands. The course of these rivers is roughly parallel to the course of the Maurikse Wetering. The Linge runs between the Maurikse Wetering and the Waal, with the Nederrijn running adjacent to the catchment of the Maurikse Wetering. The Amsterdam Rijnkanaal, a canal connecting the port of Amsterdam with the Waal, effectively cuts the catchment in half. The Maurikse Wetering runs through a culvert beneath the Amsterdam Rijnkanaal. An overview is shown in Figure 1-1.

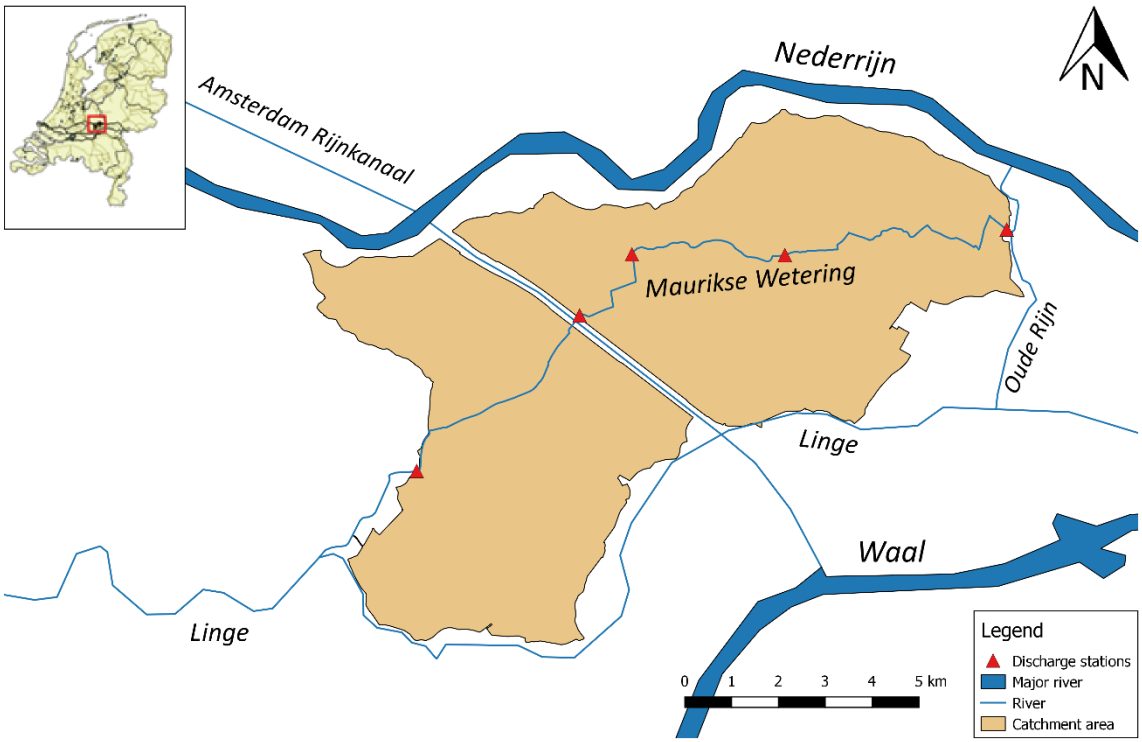


**Figure 1-1, overview of the catchment of the Maurikse Wetering and surrounding area**

### 1.1.1 Catchment characteristics

The catchment of the Maurikse Wetering is part of the larger Betuwe area and has a size of 84 km². The area mainly consists of agricultural area with a few villages. If the Maurikse Wetering has the same composition as the Betuwe, 55% of the area consists of agricultural area and 13% of built-up area (Hobbelt et al., 2018). The percentage of built-up area is likely lower for the Maurikse Wetering as the Betuwe contains larger cities like Tiel and part of Arnhem. In Figure 1-2 it can be seen that most of the Maurikse Wetering consists of agricultural area and pastures, with some urban area and fruit tree plantations. The catchment of the Maurikse Wetering covers most of the Buren municipality. Looking at the distribution of the population centers, from a total of 26.431 inhabitants in the municipality (Gemeente Buren, 2018) an estimated 20.000 people live in the Maurikse Wetering catchment.

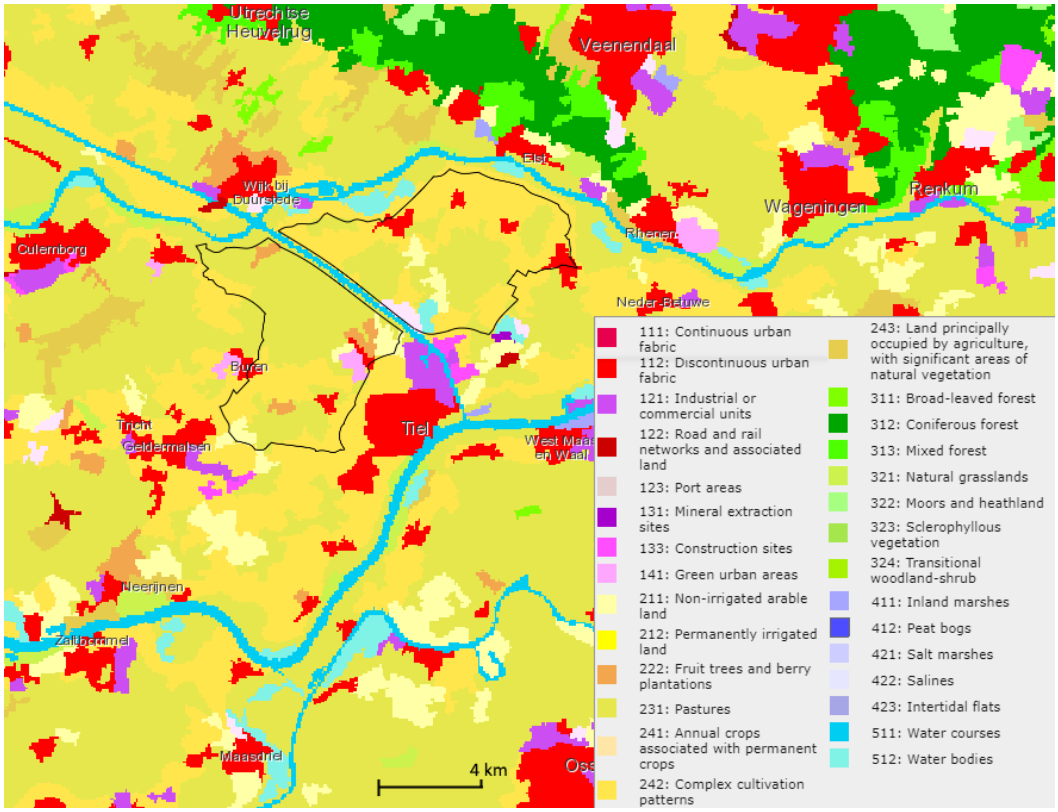


**Figure 1-2, land use in and around the Maurikse Wetering catchment (catchment borders in black)**

The topographic catchment of the Maurikse Wetering is effectively cut in half by the Amsterdam-Rijnkanaal, which runs roughly north by north west through the catchment with a culvert/sifon connecting the two halves of the catchment. A pumping station on the upstream side of the culvert can pump water to the Amsterdam-Rijnkanaal when the water level is deemed too high. Rijkswaterstaat is responsible for the culvert, while Rivierenland Water Board is responsible for the pumping station (Vis & Franssen, 2014).

During the summer months the river can run dry without an additional supply of water. This would have a negative effect on the agriculture in the region. To ensure that there is enough water in the system throughout the year, water is being let in from the Rhine through the Old Rhine. The Old Rhine runs south from the Nederrijn to the Linge, with a tilting weir at De Kat to discharge water into the Maurikse Wetering.

The catchment is divided in 83 levelling areas, where the groundwater is maintained to a certain level via a series of weirs connecting each area. These weirs are fixed, only in the Maurikse Wetering river do tilting weirs exist. These tilting weirs are adjustable from the control centre situated in Tiel.

## 1.1.2 Geohydrology

The Maurikse Wetering catchment is part of the old Rhine delta. The movement of the rivers through meandering or braiding since the Pleistocene resulted in so-called sand lanes (Cohen, 2009). These sand lanes can have an effect on the groundwater flow in the region. The sand lanes are shown in Figure 1-3.

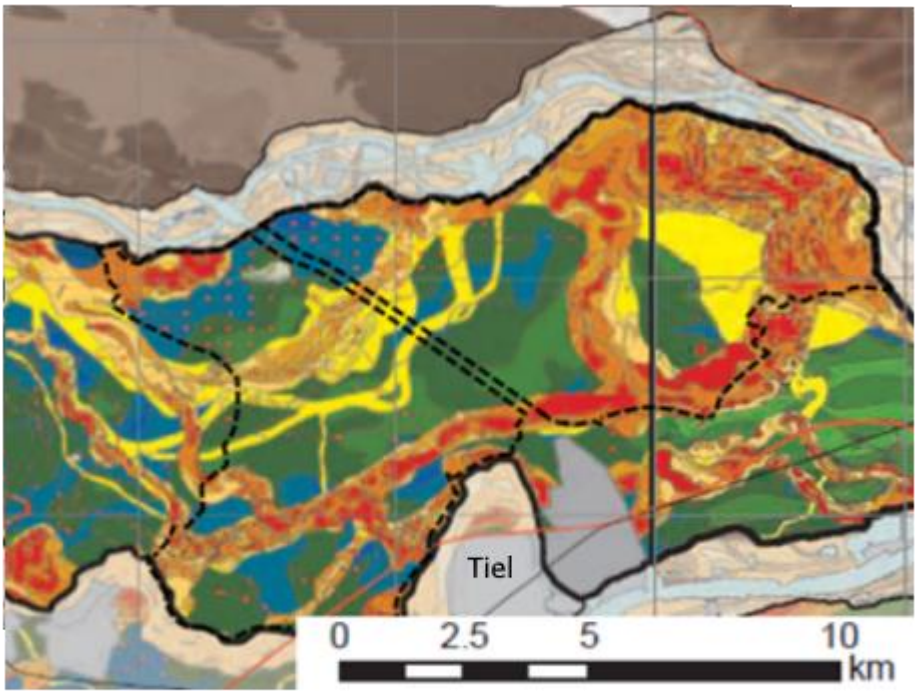


**Lanes within flood plains**

| | | |
|---|---|---|
| 1 | 0 - 1.0 m -mv | *River sand* |
| 2 | 1.0 - 2.0 m -mv | |
| 3 | 2.0 - 3.0 m -mv | |
| 4 | 3.0 - 4.0 m -mv | |
| 5 | 4.0 - 5.0 m -mv | |
| 6 | 5.0 - 6.0 m -mv | |
| 7 | 6.0 - 7.0 m -mv | |
| 8 | 7.0 - 8.0 m -mv | |
| 9 | 8.0 - 9.0 m -mv | |
| 10 | 9.0 - 10.0 m -mv | |

**Lanes outside flood plains**

| | | |
|---|---|---|
| 13 | 0 - 1.0 m -mv | *River sand* |
| 14 | 1.0 - 1.5 m -mv | |
| 15 | 1.5 - 2.0 m -mv | |
| 16 | 2.0 - 3.0 m -mv | |
| 17 | 3.0 - 6.0 m -mv | |

**Pleistocene afzettingen**

| | | |
|---|---|---|
| 401 * | 0 - 1.0 m -mv | |
| 20 | 0 - 1.0 m -mv | *River sand* |
| 21 | 1.0 - 2.0 m -mv | |
| 22 | 2.0 - 3.0 m -mv | |
| 23 | 3.0 - 4.0 m -mv | |
| 24 | 4.0 - 5.0 m -mv | |
| 25 | 5.0 - 6.0 m -mv | |
| 26 | 6.0 - 7.0 m -mv | |
| 27 | 7.0 - 8.0 m -mv | |
| 28 | 8.0 - 9.0 m -mv | |

**Figure 1-3, sand lanes. The borders of the Maurikse Wetering catchment are displayed as dotted lines.**

The soil profile in the subsurface beneath the Maurikse Wetering contains fault lines. These can be seen in Figure 1-4 at 3.9 and 9.4 km from point A (Point A being near the weir at Buren). The impermeable layers separating the aquifers are often discontinuous because of these fault lines, which allows for free exchange of groundwater between aquifers. This can make it more difficult to differentiate between the upper aquifer and lower aquifers.

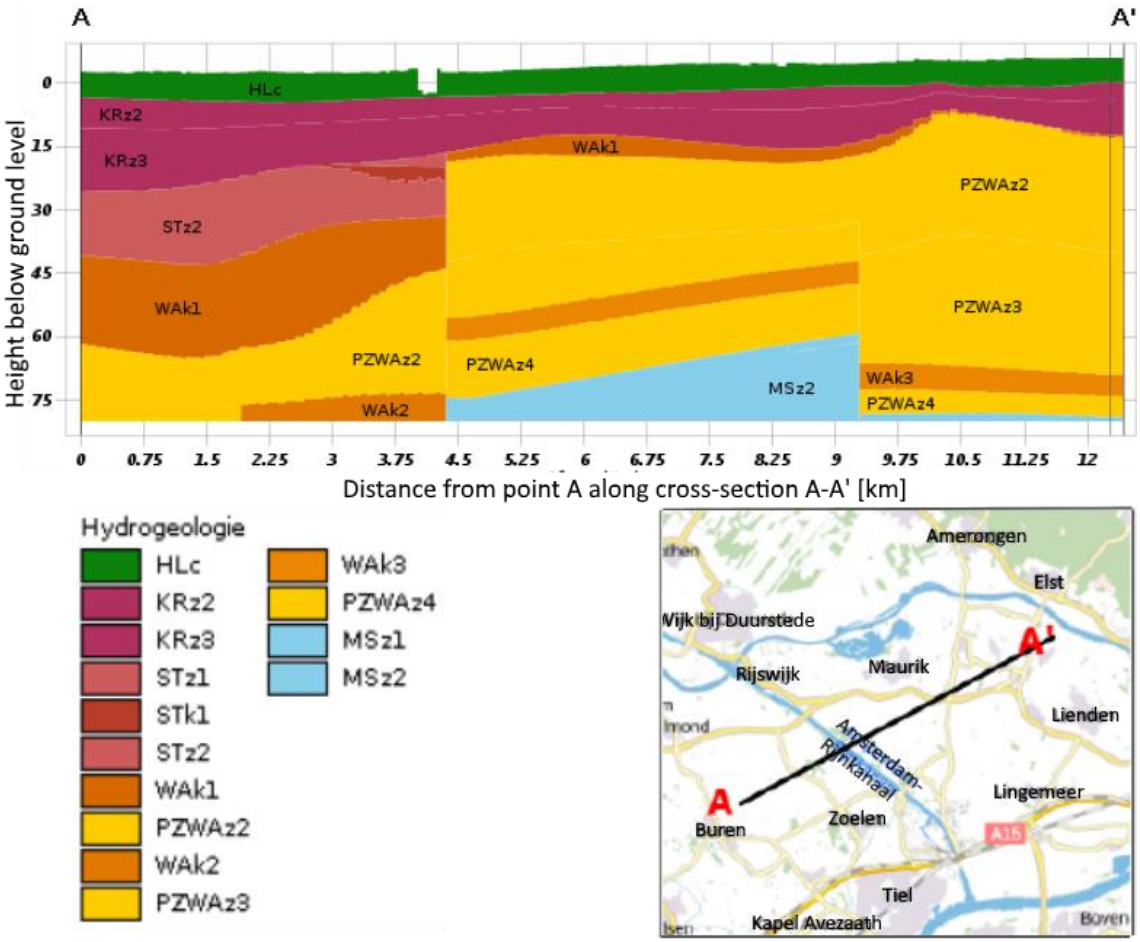


**Figure 1-4, cross-section of the Maurikse Wetering from Buren modelled by the REGIS II model. Taken from DINOloket (TNO, 2013).**

According to Hobbelt et al. (2018), groundwater withdrawals occur by Evides at Kerk-Averaath and between Buren and Zoelen. Combined these withdrawals consist of 3.8 million $m^3$ per year. These withdrawals occur in the second aquifer. In Figure 1-4, the upper aquifer consists of the purple KRZ2 and KRZ3, with the second aquifer consisting of the yellow PZWAz2 PZWAz3 and PZWAz4. The pink STz2 and brown WAK1 are poorly permeable layers (Swierstra & Kerckhoffs, 2018).

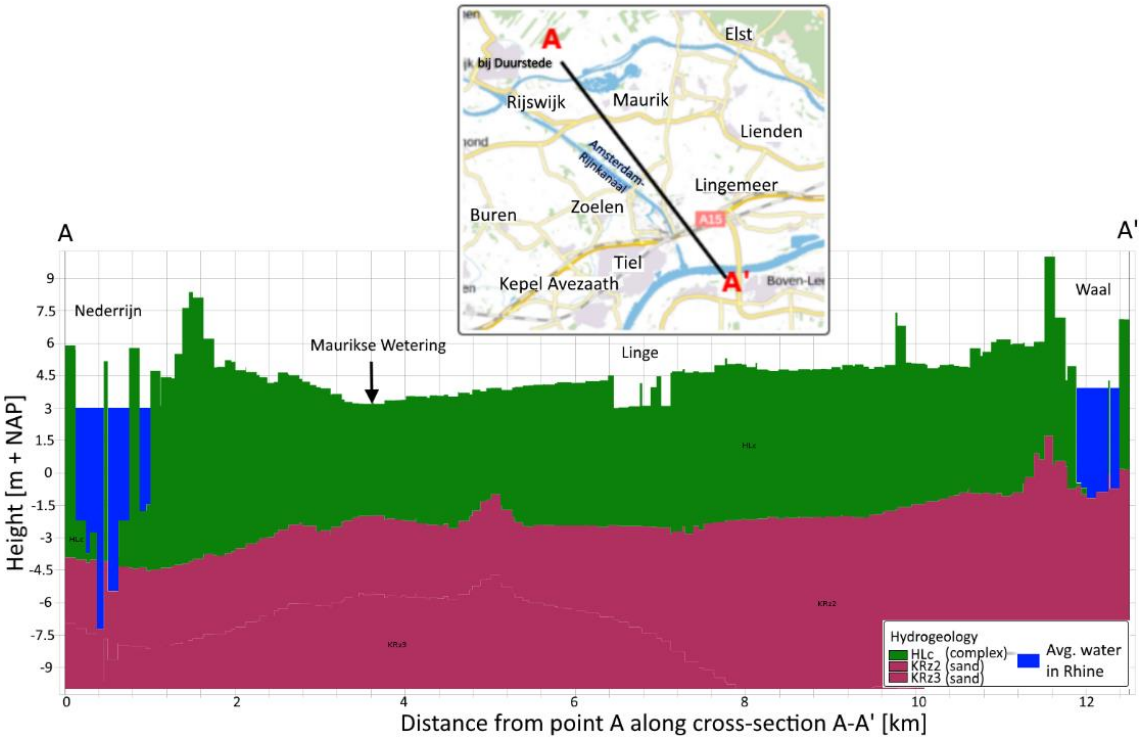


**Figure 1-5, cross section perpendicular to the Maurikse Wetering of the top layer, with average (mode) Nederrijn and Waal levels and the location of the Maurikse Wetering and the Linge.**

From Figure 1-5 it can be seen that the Nederrijn and Waal reach into the second, sandy, layer. The top layer is a complex mix of different soil types. Figure 1-5 shows that in this cross section, the Maurikse Wetering is roughly equal to the average Nederrijn level at approximately 3 m + NAP, and below the average Waal level at 4 m + NAP.

## 1.2 Intercatchment groundwater flow

Intercatchment groundwater flow refers to groundwater fluxes crossing topographic divides (Bouaziz et al., 2018). Bouaziz et al. (2018) explains how intercatchment groundwater flow (IGF), also called interbasin groundwater flow, can have a significant contribution to the water balance in a catchment, especially on smaller sub-catchments. The inner workings of IGF can be quite complex and it is considered to be one of the most difficult watershed fluxes to quantify (Genereux et al., 2005). Due to this level of difficulty, the IGF is often ignored. This can be one of the causes why water balances often don't close. By ignoring the IGF, the watershed can be seen as hydrologically isolated from its surroundings apart from outgoing, and sometimes incoming, surface water. However, the Netherlands almost entirely consist of lowland, with a dense network of artificial waterways and polders where the groundwater level is artificially maintained. Topographic (surface) catchment borders rarely overlap with geohydrological catchments borders. If seepage is taken into account, it is most often entered as a fixed additional flux of incoming or outgoing water without talking about its actual origin or destination (Veldkamp & Wiertz, 1997).

Vermue (2017) explains how the groundwater flow to/from the Linge catchment from/to adjacent catchments can be linked to the water level in the adjacent rivers. The net flux can either enter or exit the catchment depending on the water level in the rivers but whether the general direction is fixed is unknown. Cohen et al. (2009) shows sand lanes all over the Linge basin. These sand lanes possibly increase the difficulty in determining the average of processes in the groundwater reservoir, like groundwater level and groundwater fluxes. The effect these sand lanes have on the direction of flow is also difficult to determine.

It is important to know that not all water exits through a catchments' outlet, nor does all discharge in outlets originate in the catchment. For a narrow lowland catchment like the Maurikse Wetering with major rivers bordering it, this IGF might be significant for the entire catchment, something that can be seen in Vermue (2017) as well. In Vermue (2017), about 10% of the Linge catchment was modelled. This is roughly the area of the triangle Doornenburg-Huissen-Bemmel. Here it was found that the groundwater table is heavily influenced by the surrounding major rivers. For this catchment the average IGF flux was quantified. Besides the influence of major water bodies, the IGF coming from adjacent catchments can have a significant influence on a catchments' water balance, as can be seen in Bouaziz et al. (2018).

## 1.3 Scope

The position of the Maurikse Wetering catchment between the Nederrijn and Waal rivers leads to the question whether the Nederrijn and Waal influence the water balance of the Maurikse Wetering catchment through intercatchment groundwater flow (IGF).

As the IGF cannot be measured directly, it is one of the most difficult fluxes to quantify (Genereux et al., 2002) (Genereux et al., 2005). It is therefore often neglected in catchment studies (Genereux et al., 2002). A common method for determining the IGF is to equate the IGF to the "missing" water in the water balance (Genereux et al., 2002) (Genereux et al., 2005) (Bouaziz et al., 2018) (Pellicer-Martínez et al., 2015) as seen in equation (1.1). In equation (1.1) the ΔS is the difference in storage, P the precipitation, ET the evapotranspiration and Q the river discharge.

$$\boldsymbol{\Delta S = P - ET - Q - IGF} \qquad \textbf{(1.1)}$$

This method of determining the IGF will likely not be sufficient on the short term, as ΔS is hard to determine as it is a combination of the difference in storage in the groundwater reservoir and the surface water reservoir. The water balance is usually determined annually, as for long periods the difference in storage can be considered negligible. This would remove the ΔS term from equation (1.1). In Genereux et al. (2005) it is stated that: "[Water balance] studies may offer the most direct way to quantify the net effects of IGF on a given watershed, at least over the timescale of the budget period (usually a year)" (Genereux et al., 2005, pp. 2). Due to the difficulty of determining the ΔS term, it is difficult to, for instance, determine the effect a local heavy precipitation event has on the IGF.

If the IGF can be reliably expressed as an equation in terms of variables of which data is relatively easy to acquire, for instance the water level in the Nederrijn, this would help in understanding the behaviour of the IGF. This more direct method of determining the IGF flux concerns the physical workings of the IGF, rather than the indirect method of measuring the IGF by equating it to the error in the water balance. Not equating the IGF to the error in the water balance makes the IGF independent of any data errors in unrelated variables. Relating the IGF to easy-to-measure variables shows that this difficult process can be described in a relatively simple manner.

This results in the following research question:

*What is the influence of intercatchment groundwater flow in the Maurikse Wetering, and can a relation be established between independant variables and the intercatchment groundwater flow to the Maurikse Wetering?*

To model the groundwater fluxes, the groundwater model MORIA will be used. MORIA is developed by the Rivierenland Water Board, the province of Gelderland and drinking water company Vitens and is a groundwater model with highly detailed maps of the subsurface of the Rhine delta in Gelderland and Overijssel. The results of MORIA can then be analysed in Deltares'

iMOD (Vermeulen et al., 2018). Using iMOD, the spatial and temporal variation of groundwater fluxes in the region will be analysed and discussed. This includes fluxes from upstream (lowland) catchments. From the quantity and direction of the groundwater fluxes the net IGF can be determined. The net IGF is the net amount of water entering the catchment. If this number is positive, the catchment gains water via IGF. If it is negative, the catchment loses water.

If an IGF relation is found, it will then be applied to a conceptual hydrological model. WALRUS was chosen as the conceptual hydrological model as it is specifically designed to model lowland areas like the Maurikse Wetering catchment. WALRUS is also one of the most used models when it comes to studying lowland areas by Royal HaskoningDHV and the Rivierenland Water Board, under whose guidance this thesis is being written. This means that expertise and technical support will be readily available when needed.

## 1.4 Thesis outline

This thesis is divided into 4 main topics; The water balance, the intercatchment groundwater flow, the IGF relation and the WALRUS model.

Chapter 2 contains the methods used in this thesis for all chapters.

Chapter 3 contains the results of the water balance section, the data required for a conceptual hydrological model for the hydrologically isolated catchment (meaning without IGF) is analysed.

Chapter 4 contains the results of the intercatchment groundwater flow section, the IGF is quantified and analysed. The sources of IGF to the Maurikse Wetering catchment are determined and the direction of the groundwater flow is modelled and discussed.

Chapter 5 contains the results of the IGF relation section, a relation is drawn up between the IGF and variables which might influence the IGF via simple linear regression analyses and multiple linear regression analyses.

Chapter 6 contains the results of the WALRUS section, the conceptual hydrological model WALRUS is used to build a conceptual hydrological model of the Maurikse Wetering. The model is calibrated to the groundwater level and the discharge as modelled by MORIA.

Chapter 7 summarises the conclusions drawn from the previous chapters. Chapter 8 discusses the conclusions further, and chapter 9 provides recommendations and ideas for further research.

# 2 METHODS

## 2.1 Water balance

To see if the water balance closes and if the IGF can be estimated according to the common method of equating the IGF to the missing water in the water balance can be used, the data from various sources will be analysed.

### 2.1.1 Discharge data

10 years of discharge data was provided by the Rivierenland Water Board. There are 5 sites at which discharge data is available, which are shown in Figure 2-1. These sites all lay within the main river. Buren, Kribbrug, Adam Reinberg and De Kat are tilting weirs that measure discharge according to a stage-discharge relation, the pumping station at the Amsterdam Rijnkanaal (ARK) monitors the amount of water that is pumped and the culvert at the ARK has a stage-discharge relation. The weir at Buren is the main outlet of the catchment. The actual Maurikse Wetering river continues shorly before flowing into the Linge river, but the weir at Buren is the last location with discharge data and is thus seen as the system outlet. At De Kat water from the Rhine enters the system. At the pumping station to the Amsterdam Rijnkanaal a siphon runs beneath the Amsterdam Rijnkanaal. When the upstream water level is too high the pumping station is turned on and water is discharged onto the Amsterdam Rijnkanaal. Through an empiric formula there is an estimation of the discharge running through the culvert. However, this formula relies on downstream water levels which are not measured. Instead, the water levels are estimated by assuming the water levels to be equal to those at Buren plus the gradient over the distance. Thus, none of the stations with discharge data rely on direct discharge measurements, but rather on stage-discharge relations.

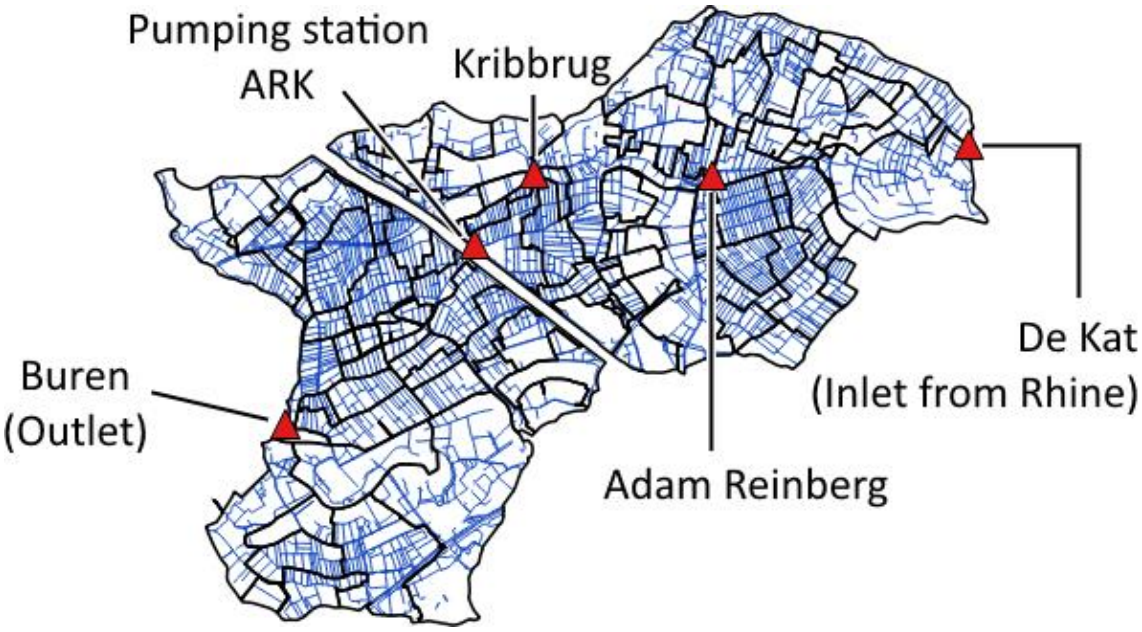


**Figure 2-1, The Maurikse Wetering catchment, with subcatchments (levelling areas) (in black), secondary waterways (in blue) and named discharge measurement stations (red).**

The discharge data will first be analysed in its provided form, with cubic metres per second ($m^3/s$) as the unit, before being converted to millimetres per day (mm/d) at the end of this analysis. The original unit notation refers to the water flowing through the river, while the latter refers to the discharge relative to the catchment area. This conversion is done as fluxes like the precipitation and evaporation are given as millimetres per day.

### 2.1.2 Aggregated values

The discharge data has a timestep of 15 minutes. Missing values were filled up by averaging the values of the timesteps before and after the missing values. The provided data also had inconsistencies on occasion regarding the timestep. From a total of 300460 measurements, 6959 measurements contain aggregated data. With aggregated data it is meant that two or more default timesteps of $\Delta t$ = 15 minutes are combined into one data point. The reason for this is unknown. These aggregated timesteps range from 30 minutes to several days. The corresponding discharge data is computed via the default formula to acquire discharge data in $m^3/s$ and multiplied by the number of seconds in the timestep. As no other data is available this value is assumed to be the total discharge during the time step, which is distributed evenly over said timestep. This needs to be adjusted as this discharge data is now summed into one timestep, shown as a peak in discharge.

Timesteps larger than the desired timestep (set at $\Delta t$ = 1 hour) can prove problematic during for instance the calibration and validation of the WALRUS model. It is therefore best to omit these values from the dataset. However, steps with a size $\Delta t$ smaller than or equal to $\Delta t$ = 1 hour, for instance $\Delta t$ = 30 minutes, can be kept as these fall within the desired range. When a timestep of for instance 30 minutes crosses from one hour into the next (for instance, from 12:45 to 13:15), the corresponding discharge needs to be distributed accordingly over both final timesteps instead of being added to the timestep corresponding to the dataset. Otherwise this would result in incorrect hourly data.

The chosen approach was to first divide all supplied data in timesteps of $\Delta t_{default}$ = 15 minutes, which is as said before the default timestep for the supplied data. For this purpose, the Aggregate value Agg is introduced. This value is the amount of default timesteps in every given timestep:

$$\boldsymbol{Agg_i = \frac{\Delta t_i}{\Delta t_{default}}} \tag{2.1}$$

A fictional example can be seen in Table 2-1.

The timestep $\Delta t_i$ will be split into a number of default timesteps equal to its Agg value. Each new timestep $\Delta t_{new}$ retains its Agg value. The corresponding discharge for $\Delta t_{new}$ = 15 minutes will be:

$$\boldsymbol{Q_{15\,min} = \frac{Q_{\Delta t_i}}{Agg}} \tag{2.2}$$

The new values are then summed up into the new timestep $\Delta t_{new}$ = 1 hour, as can be seen in Table 2-2, where the values from Table 2-1 are refined. The timesteps that are deemed outside of the desired range are new omitted. This is done via the average aggregated value $Agg_{AVG}$.

$$\boldsymbol{Agg_{AVG} = \frac{\sum(Agg_i)}{\frac{\Delta t_{new}}{\Delta t_{default}}}} \tag{2.3}$$

If this value $Agg_{AVG}$ is higher than a certain maximum value $Agg_{MAX}$ the corresponding hour will be deleted from the dataset as it is deemed too inaccurate. For now, this maximum value is set at the denominator of the formula for $Agg_{AVG}$. Now every remaining $Agg_{AVG}$ value will be larger than or

equal to the timestep $\Delta t_{new}$. Arguments can be made for a higher value, especially during dry weather flow, but for now this will not be evaluated further.

| Time | Q | Agg | Time (hr) | Q [m³/hr] |
|---|---|---|---|---|
| ***12:00*** | $Q_{t1}$ | 6 | 12:00 | $Q_{t1}$ |
| ***13:30*** | $Q_{t2}$ | 1 | 13:00 | $Q_{t2} + Q_{t3}$ |
| ***13:45*** | $Q_{t3}$ | 1 | | |

**Table 2-1, fictional example discharge data before refinement**

| Time | Q [m³/15 min] | Agg | Time (hr) | Q [m³/hr] | $Agg_{AVG}$ | Viable |
|---|---|---|---|---|---|---|
| ***12:00*** | 1/6 * $Q_{t1}$ | 6 | 12:00 | 4/6 * $Q_{t1}$ | 6 | No |
| ***12:15*** | 1/6 * $Q_{t1}$ | 6 | | | | |
| ***12:30*** | 1/6 * $Q_{t1}$ | 6 | | | | |
| ***12:45*** | 1/6 * $Q_{t1}$ | 6 | | | | |
| ***13:00*** | 1/6 * $Q_{t1}$ | 6 | 13:00 | 2/6 * $Q_{t1}$ + $Q_{t2} + Q_{t3}$ | 3.5 | Yes |
| ***13:15*** | 1/6 * $Q_{t1}$ | 6 | | | | |
| ***13:30*** | $Q_{t2}$ | 1 | | | | |
| ***13:45*** | $Q_{t3}$ | 1 | | | | |

**Table 2-2, fictional example discharge data after refinement with $Agg_{MAX} = 4$**

For the dataset given (2008 – 2017) the results are as follows:

- The total amount of events with aggregated quarters = 6959
- Total amount of events from original dataset with Agg_max > 4 = 2230
  These events amount to a combined timespan of 4465.5 hours.

After refinement and aggregation, the data deemed unreliable is deleted.

- In total 4669 hours are deleted from this dataset from a total of 81071 hours. This is equal to 5.8 %.
- If all aggregated data was simply deleted from the original set this would amount to 7695.75 hours, an amount equal to 9.5 % from the total. Additionally, the remaining dataset would likely have been of lesser quality due to gaps created by deleted rows. It can be seen that this way a part of the discharge is missing from comparing Table 2-1 and Table 2-2, when looking at the hourly discharge *Q [m³/s]*.

### 2.1.3 Fish ladder

In 2012 a fish ladder was constructed, allowing fish to pass the weir at Buren. This invokes issues with the discharge data, as an unknown amount of water passes at an uncalibrated section. During field measurements for calibration of the Q-h curve in 2016, the fish ladder was closed (Mulder & Maartense, 2017). The fish ladder is therefore uncalibrated and its precise effect is unknown. A rough estimate for the flow passing through the fish ladder is 15% of the total discharge. Due to this uncertainty, the fish ladder will not be taken up in this thesis.

### 2.1.4 Backwater curve and negative discharge

At the locations with discharge data (Buren, Kribbrug, Adam Reinberg and De Kat) the water flows over tilting weirs. Most of the time the downstream water level is lower than the weir level, which means that the downstream boundary conditions have no effect on the discharge over the weir making this a free flowing weir.

The possibility of a backwater curve exists if the downstream water level $h_{downstream}$ is higher than the weir level $h_{weir}$. With a backwater curve, the downstream boundary conditions influence the upstream water level. For this catchment, this can occur due to the weir being lowered to account for high water levels in the Maurikse Wetering. Another possible reason of a backwater curve occurring is due to events in the Linge, for instance when the sluice at Gorinchem is closed which decreases the discharge from the Linge into the Merwedekanaal, thus increasing the water level (Tanis, 2017), or even high water levels in the Waal propagating up to the Maurikse Wetering.

While positive discharge still occurs, when the downstream water level is higher than the weir level the data becomes less reliable as the Q-h relation will likely be disturbed. It appears that the Q-h relation was originally determined and calibrated according to a free-flowing weir, as the original formula for determining the discharge over the weir has no term for the downstream water level.

$$\boldsymbol{Q_{weir} = 1.7 * W * C * \left(h_{upstream} - h_{weir}\right)^{\frac{3}{2}}} \qquad \textbf{(2.4)}$$

In equation (2.4), W is the width of the weir and C the discharge coefficient.

A "drowning grade" (*"verdrinkingsgraad"*) is present in the eventual calculation of the discharge. This factor comes into play when the downstream water level exceeds the weir level and appears to be an empirical formula. But little documentation was given so it remains unsure whether or not the Q-h relation remains accurate during high downstream water levels. The exact influence of a possible backwater curve is unknown. Further analysis will not be possible as creating a new Q-h curve is outside the scope for this research.

If it turns out that the data is unreliable due to backwater curves disturbing the Q-h relation, this can have a significant effect on the quality of the supplied data as the downstream water level is above the weir level for 4655 hours out of the remaining 76378 hours. This equals 6.1 %.

When the downstream water level is higher than both the weir level and the upstream water level, water will enter the catchment at the weir instead of exiting it. This is modelled as negative discharge as the positive direction leads out of the catchment. However, the WALRUS model does not take downstream influences into account. Therefore, when negative discharge occurs these data points should be taken out of the dataset. Setting these to zero would not work, as the negative discharge is determined by the downstream boundaries, not necessarily the upstream water level. So it is highly likely that at least at a fraction of these events more than zero discharge is generated, making setting the discharge during negative discharge to zero a wrong assumption which would be detrimental to calibration. The total number of hours with negative discharge over the period 2008 – 2017 is 24 hours.

### 2.1.5 Water balance

A relatively simple but often very accurate water balance is the following formula:

$$\boldsymbol{\Delta S = P - ET_a - Q} \qquad \textbf{(2.5)}$$

In equation (2.5), ΔS is the change in storage, P the total precipitation, $ET_a$ the actual evapotranspiration and Q the discharge at the system outlet.

When looking at long time steps, the expected change in storage is negligible. Therefore, the easiest water balance is Q = P, with Q being the summation of the discharge over a hydrological year and P the total precipitation over the same hydrological year. A hydrological year is defined as ranging from the 1st of April to the 31th of March of the next year, so the hydrological year of 2017 is set from 1-4-2017 to 31-3-2018. To get to the same unit as the precipitation, the discharge data, which is given in $m^3$, is divided by the area of the catchment and multiplied by 1000 to get the unit mm. The area of the catchment is 84.5 $km^2$ as calculated by QGIS. The precipitation and potential evaporation data are taken from the Royal Dutch Meteorological Institute (KNMI). The data from the KNMI stations around the Maurikse Wetering catchment is used to see how they differ. These are the stations Herwijnen, Volkel, Deelen and De Bilt. Their locations are shown in Figure 2-2. The data from the station closest to the Maurikse Wetering, station Herwijnen, is taken as the most representable meteorological data for the Maurikse Wetering catchment. Now the fluxes in the water balance are available, however the discharge data includes external surface water fluxes. The water balance requires the net discharge.

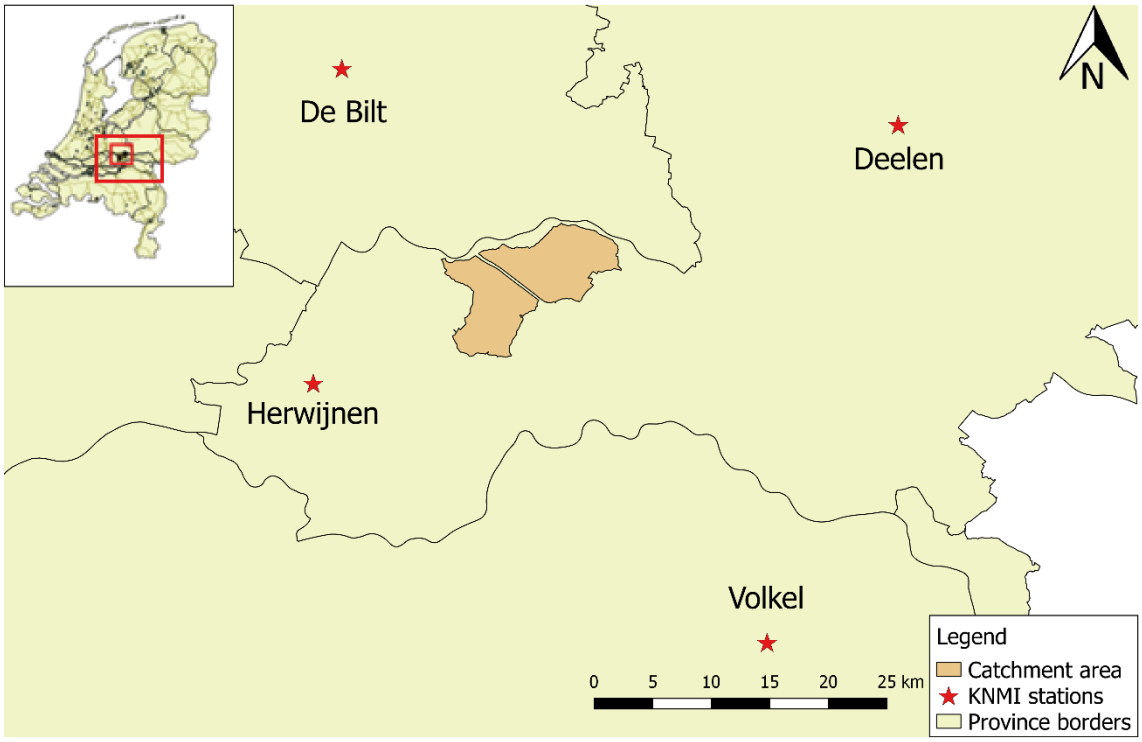


**Figure 2-2, locations of the KNMI stations closest to the Maurikse Wetering catchment**

To get the net discharge, meaning discharge generated in the catchment, all surface water in- or outlets are summed up into one discharge term. Other than the outlet at Buren, these are the inlet at De Kat and the pumping station at the Amsterdam Rijnkanaal. The inlet at De Kat lets in water coming from the Rhine to satisfy the water demands of the agriculture in the region during dry periods. The discharge at De Kat needs to be subtracted from the discharge term as it is not part of the discharge generated in the catchment. The order of magnitude of this term is approximately 10 % of the discharge at Buren. The pumps of the Amsterdam Rijnkanaal pumping station will only be turned on if the upstream water level is too high. This is done to prevent flooding in the upstream section as the culverts going underneath the Amsterdam Rijnkanaal are a bottleneck during high water.

Including the evaporation term sets the annual water balance to $Q = P - ET_a$. This is a common approximation for the water balance in a catchment. Here the actual evaporation $ET_a$ is a fraction of the potential evaporation $E_P$. As the potential evaporation is calculated by the KNMI and

assuming the annual storage difference being negligible, the annual actual evaporation can be computed by means of the following:

$$Q = P - ET_a \rightarrow Q = P - X * ET_P \rightarrow$$
$$X = \frac{P - (Q_{Buren} - Q_{Kat} + Q_{gemaal})}{ET_P} \quad (2.6)$$

### 2.1.6 Budyko curve

The Budyko curve plots the ratio of actual evapotranspiration over precipitation, also known as the evaporation ratio $ET_a$ / P, against the potential evaporation over precipitation. The ratio potential precipitation over precipitation ($ET_P$ / P) is also known as the dryness index ϕ. Every catchment in the world roughly follows the curve describing the relation between these ratios (Arora, 2002). The $ET_P$ is estimated by the KNMI using Makkink (KNMI, n.d).

## 2.2 Intercatchment groundwater flow

This section describes the methods used with the groundwater model MORIA and program iMOD in order to acquire the modelled IGF data.

### 2.2.1 Rhine level

Rhine level data is taken from Rijkswaterstaat's Waterinfo (Rijkswaterstaat, 2019). The measuring sites are shown in Figure 2-3. A list of these stations and their data are presented in Appendix A. The stations which will be taken for most of the analysis are station 2, which is 'Beneden Amerongen' in the Nederrijn river, and station 6, which is 'Tiel Waal' in the Waal river. These stations are the stations closest to the catchment within the two main rivers and thus the water levels here will likely have the largest influence on the Maurikse Wetering catchment.

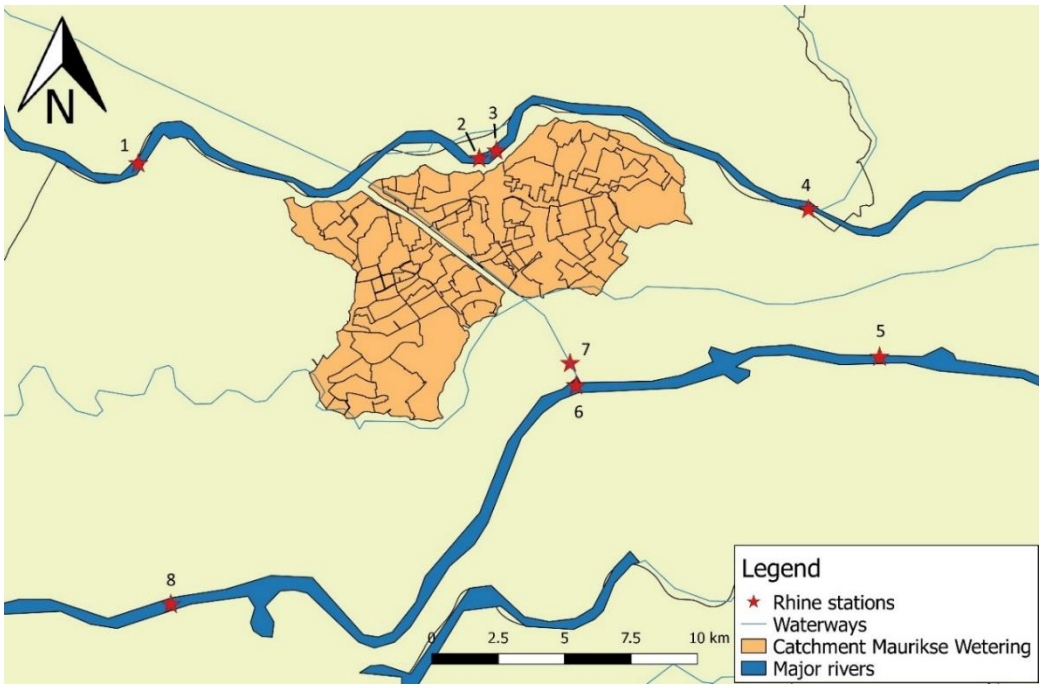


**Figure 2-3, water level measuring stations in the Nederrijn, Waal and Amsterdam Rijnkanaal. Stations 2 and 6, Beneden Amerongen and the Waal at Tiel respectively, are deemed the most relevant to this study.**

As the map shown in Figure 2-3 doesn't show the exact course of the Nederrijn and Waal, the position of the stations is changed in the figure. The exact location of the stations according to their coordinates are presented in Appendix A.

### 2.2.2 IGF quantity

The groundwater model MORIA consists of a number of hydrogeological layers. Horizontally it is divided into cells of a chosen resolution. When run, MORIA models the hydraulic head in each cell and the fluxes between the cells. The relevant fluxes for this project are given in Table 2-3.

| Flux | Name |
|---|---|
| *FRF* | Flux Right Face, the horizontal flux in the left-right direction |
| *FFF* | Flux Front Face, the horizontal flux in the up-down direction |
| *FLF* | Flux Lower Face, the vertical flux at the bottom of each layer |
| *RIV* | River, drainage/infiltration related from/to the surface water. Here only in layer 1 |
| *DRN* | Drainage, drainage to the surface water (no infiltration). Here only in layer 1 |

**Table 2-3, names of the fluxes in iMOD's water balance module**

A schematic overview in Table 2-3 is given in Figure 2-4. As can be seen, flow towards the system/cell is positive, an outgoing flux is negative. As can be seen in Figure 2-4, the drainage flux DRN does not have a positive (incoming) direction, as this flux relates to drainage pipes and drainage ditches. These remove water from the model when the modelled head in a layer (for this catchment this is only the first layer) exceeds the elevation of the drainage system (Vermeulen et al., 2018). No infiltration is possible in the drainage module. The river flux RIV represents the presence of rivers/streams from which water may infiltrate or to which water may discharge.

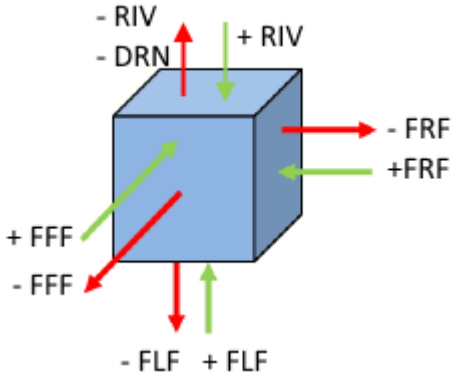


**Figure 2-4, fluxes in iMOD's water balance module (source: Vermeulen et al. (2018), p.390). Names of these fluxes are shown in Table 2-3.**

The chosen cell resolution in MORIA for this project is 100 x 100 m. A courser grid would decrease model reliability and could possibly omit valuable detailed information regarding the direction of IGF. A smaller grid is not necessary for this research and would greatly increase runtimes.

There are 19 soil layers in this dataset. MORIA uses geological and hydrogeological data from the REGIS II model (Vernes et al., 2005). Formations in REGIS II are combined in MORIA, based on parameters like height below ground level and hydraulic conductivity (Swierstra & Kerckhoffs, 2018). This is shown in Table 2-4. Table 2-4 also shows the separating layer, corresponding to the vertical conductivity, which can differ from the horizontal conductivity. If a REGIS-formation is not

present in a cross-section, the layer will have a thickness of 0, meaning that the vertical flux from the layers above and below still pass through the layer, although this has no influence on the flow.

| Layer in MORIA | REGIS-formation | Separating layer REGIS |
|---|---|---|
| *1* | HLC (GEOTOP) | HLC (GEOTOP) |
| *2* | Bxz2 | Bxlmk1, bxk1 |
| *3* | Bxz3 | BXk2, krwyk1, krk1, berok1 |
| *4* | Bxz4, krz2, krz3, bez1, bez2, bez3 | Bek1, bek2, wvb1, eek1 |
| *5* | Eez1, eez2, eez3 | Krzuk1 |
| *6* | Krz4 | Krtwk1 |
| *7* | Krz5, drz1, drz2, drz3 | Druik1, drgik1 |
| *8* | DTC(GEOTOP) | DTC (GEOTOP) |
| *9* | Dnz1, urz1, urz2, urz3, urz4, urz5, stz1 | Urk1, stk1 |
| *10* | Stz2, syz1 | Syk1 |
| *11* | Syz2 | Syk2 |
| *12* | Syz3, syz4, pzwaz1 | Wak1 |
| *13* | Pzwaz2 | Wak2 |
| *14* | Pzwaz3 | Wak3 |
| *15* | Pzwaz4, msz1 | Msk1 |
| *16* | Msz2 | Msk2 |
| *17* | Msz3, msc****, msz4, kiz1 | Kik1 |
| *18* | Kiz2, kiz3, kiz4, kiz5, ooz1 | Ook1, ooc |
| *19* | Ooz2, ooc, brz1 | - |

**Table 2-4, which REGIS-formations correspond to which layer in MORIA. The column "Regis-formation" refers to the horizontal conductivity. The column "separating layer" refers to the vertical conductivity. Taken from Swierstra & Kerckhoffs (2018).**

After MORIA data has been provided with the modelled hydraulic head in all layers and the fluxes between cells, the data will be loaded into iMOD. This is done per hydrological year to prevent iMOD from crashing. To quantify the IGF fluxes for the Maurikse Wetering, the boundaries for the catchment need to be determined. For this project, the area of interest is the upper aquifer and the surface.

For the Maurikse Wetering it is known that the upper aquifer and its dependable layers (meaning layers with the same hydraulic head) consists of layers 1 – 11. Only these layers will be used in the iMOD analysis. To check if this assumption is valid, the hydraulic head of the layers 1 – 19 from a cross-section will be plotted. The upper aquifer and second aquifer should show a difference in

hydraulic head, from which the bottom of the upper aquifer/groundwater bucket can be determined.

When the boundaries of the groundwater reservoir of the Maurikse Wetering catchment are determined, the groundwater fluxes can be quantified. Using iMOD's water balance tool, the fluxes entering and exiting the catchment can be modelled, as the outline of the catchment was entered as the boundary of the system. This provides the lateral and vertical IGF.

It is said that layer 4 is the main aquifer, this will be tested by plotting the horizontal IGF. As the main aquifer will have the highest permeability, the horizontal IGF will be the highest in the main aquifer. For further analyses, unless stated otherwise the groundwater level will be equal to the hydraulic head in layer that is determined to be the main aquifer.

As the catchment is effectively split by the Amsterdam Rijnkanaal it was checked if the fluxes underneath the canal from the upstream (eastern) part of the Maurikse Wetering catchment to the downstream (western) part of the catchment are not accidentally counted as external groundwater fluxes. It was clear that this was not the case. This is elaborated on in Appendix B.

The shapefile of the Maurikse Wetering catchment is loaded into iMOD. In iMOD's water balance tool, the horizontal IGF is modelled first, by setting the boundaries to the catchment shapefile and all layers until the layer determined to separate the upper aquifer from the second aquifer. This provides the incoming and outgoing FFF and FRF (see Table 2-3) for the entire catchment. The FLF (see Table 2-3) is modelled by setting the boundaries to the catchment shapefile and the layer determined to separate the aquifers. The horizontal and vertical fluxes cannot be quantified in this way simultaneously, as only the flux at the underside of the deepest MORIA layer can be used as the FLF otherwise the FLF fluxes for all layers are taken in with the analysis too. The net IGF fluxes are calculated by summing the (positive) incoming fluxes and its respective (negative) outgoing flux.

After this, the RIV and DRN packages are used to model the infiltration/drainage to/from the surface water and drainage to drainage ditches and drainage pipes in the system.

As an option for averaging groundwater level over a shapefile was not found in iMOD, the average groundwater head is determined by taking the spatially distributed data from iMOD, converting it to a .ASC file and using Python to overlay a catchment .ASC file to only keep the cells within the catchment borders. The resulting head data was then averaged for daily groundwater head values for layer 4.

### 2.2.3 Groundwater flow direction

To study the spatial behaviour of the IGF, the flow direction is plotted. This is a function in iMOD, which plots the direction of the resultant of the FFF and FRF for each cell. From the resulting plots the behaviour of the groundwater flow can be studied, and patterns and areas of interest can be distinguished. As the result plotted in a 100 x 100 m resolution is too detailed for visual analysis and clear reporting, after the model has been run the hydraulic head and flow direction will be averaged over a cell size of 1 x 1 km. These maps will provide clarity on the origins and flow paths of the groundwater.

Looking at the summed IGF quantity as modelled by MORIA, periods with high, average and low IGF will be plotted to see what differences occur. It will also be seen if periods with similar IGF quantities during different years have similar groundwater flow directions. Looking at the Nederrijn and Waal data, it will be seen if high, average and low IGF occurs during high, average and low water levels in the rivers respectively. This will show the influence these rivers have on the IGF.

### 2.2.4 Spatial variation IGF

The hydraulic head in the upper and second aquifer were plotted in iMOD and compared to see if any notable differences between the hydraulic head in both aquifers occur that can cause a difference in vertical groundwater flow between the aquifers at certain locations.

To see the spatial variation in net IGF (both lateral and vertical), a 1 x 1 km grid was drawn over the project area and loaded into iMOD. Despite the Maurikse Wetering catchment being divided into subcatchments/levelling areas, these subcatchments have an irregular shape and size and might give an incorrect view of the spatial variation in net IGF. This grid was overlaid with the MORIA data to see the fluxes going in and out. The resulting net change was saved and added to the 1 x 1 km grid shapefile, which was entered in QGIS to provide a map with the results.

There are two distinct periods in the IGF data (chapter 4), with the change occurring in June 2015. For this reason, one year of each period is chosen to examine. These years are 2013 and 2017. In each year two months were selected, one with a high IGF flux and one with an average IGF flux. For 2013, the high flux occurred in June and the chosen 'average' month is September. For 2017, the high flux occurred in December and the chosen 'average' month is August. For these months the average IGF flux of the entire month was taken. This approach using the monthly average rather than daily values was done to limit the effects of local precipitation events which could disturb the data, and to get a clear overview of the effects which can be expected during similar situations rather than a single point in time.

## 2.3 IGF relation

To establish a relation between easy to quantify variables, it must be determined which processes, fluxes and/or occurrences within the region influence the IGF. The independent variables which influence the water balance are plotted against the IGF to see if a relation exists, and a multiple linear regression analysis will be performed to see how multiple variables relate to the IGF.

### 2.3.1 Relation between water levels

To see how the water levels (Nederrijn, Waal, Maurikse Wetering, groundwater level and storage deficit in the groundwater reservoir) relate to each other, the water levels of the Nederrijn and Waal are plotted against each other or against the net IGF, and on the z-axis against the groundwater level (the hydraulic head in the main aquifer) and the storage deficit of the unsaturated zone. The latter was chosen to represent the soil moisture in the unsaturated zone, as soil moisture data is not available. The storage deficit was taken by modelling the catchment in WALRUS with IGF data as modelled by MORIA (see chapter 6).

### 2.3.2 Simple/multiple linear regression analysis

A simple linear regression (SLR) analysis generates an equation which describes the statistical relation between an independent predictor variable and a dependant response variable (Seltman, 2018). The adjective "simple" refers to the outcome variable being related to a single predictor, rather than a multiple linear regression where more than one predictor variable is used. A multiple linear regression (MLR) analysis generates an equation which describes the statistical relation between several independent predictor variables and a dependent response variable (Preacher, Curran & Bauer, 2006).

For both the SLR and the MLR, the response variable is the net IGF flux as modelled by MORIA. The independent predictor variables are the acquired independent variables related to the water

balance: Precipitation (P), potential evaporation ($ET_{pot}$), Nederrijn level at Beneden Amerongen (NR), Waal level at Tiel (WA), storage deficit in the vadose zone ($d_V$), average Maurikse Wetering level (MW) and average groundwater level as modelled by MORIA ($d_G$). The ordinary least squares (OLS) method is used. The OLS method chooses the line which minimizes the sum of the squared residuals as the best fit line. The residuals are the differences between the values of the predictor data points and the fitted regression line (Seltman, 2018).

The t-test is used to determine if the sampling error $\mathbf{b_k} - \overline{\boldsymbol{\beta_k}}$ is too large, where $b_k$ is the OLS estimate of some known value $\overline{\boldsymbol{\beta_k}}$ of the null hypothesis (Hayashi, 2000), where $\beta_k$ is the slope of the regression line:

$$\boldsymbol{t_k = \frac{b_k - \overline{\beta_k}}{SE(b_k)}} \tag{2.7}$$

Here $SE(b_k)$ is the standard error of the OLS estimate of $\beta_k$. From this the p-value for each predictor variable can be calculated. The p-value tests the null hypothesis for each term, the null hypothesis being that the coefficient for the variable is equal to zero. This would mean that the variable has no effect/no correlation with the response. The p-value (probability value) is the probability that the null hypothesis is true.

$$\boldsymbol{p = \mathbf{Prob}(t > |t_k| * 2)} \tag{2.8}$$

A low p-value indicates that the null hypothesis can be rejected. This threshold p-value below which the null hypothesis can be rejected is taken as 0.05, as this is the most common value used (Wasserstijn & Lazar, 2016). Variables with p-values smaller than 0.05 are likely a meaningful addition to the model as this indicates that changes in the independent predictor variable are correlated to changes in the response variable. Therefore, variables where the p-value is above 0.05 and thus variables where the null hypothesis cannot be discarded will be taken out of the SLR/MLR.

It will also be seen if the f-test is satisfied, and if removing variables via their p-value increases the f-value. The f-test can be seen as an overall p-test for the entire MLR analysis. If an f-value is above a certain critical f-value, the null hypothesis can be rejected (Lomax, 2007). This can be expressed as the probability Prob > F. If this probability is low enough, the null hypothesis can be rejected. This probability is usually taken as 0.05 as well.

The resulting equation of the MLR can be written as:

$$\boldsymbol{y = c_1 * x_1 + c_2 * x_2 + \cdots + c_i * x_i + c_0} \tag{2.9}$$

Here y is the dependent response variable and $x_1$ through $x_i$ are the predictor variables. $C_1$ through $c_i$ are the corresponding regression coefficients. Regression coefficients can be thought of as the slope of the relation of one predictor variable to the response variable. It represents the mean change of the response variable for one predictor variable while the other predictor variables are held constant. A constant $c_0$ is added, this is the y-intercept.

To see how well the analysis estimate the response variable, the goodness of fit will be determined. The coefficient of determination (R-squared or $R^2$) will be used to determine the goodness of fit for the SLR (Young, 2000):

$$\boldsymbol{R^2 = 1 - \frac{VAR_{res}}{VAR_{tot}} = 1 - \frac{\frac{SS_{res}}{n}}{\frac{SS_{tot}}{n}}} \tag{2.10}$$

The R-squared cannot determine if the predictor coefficients are biased. For this reason, the residual plots must be plotted and analysed. No matter the R-squared value, if the residual plot is not randomly scattered but for instance patterns can be seen around the curve then the fit is biased, which would mean a bad fit. An example of such patterns is that in one part of the graph, all the residuals are above the regression line.

Other than the t-test, deciding which variables are to be discarded in the MLR analysis will be checked with a second method, by means of the adjusted R-squared (Shieh, 2007):

$$\boldsymbol{Adj.R-squared = \bar{R}^2 = 1 - \frac{\frac{SS_{res}}{df_e}}{\frac{SS_{tot}}{df_t}} = 1 - \frac{\frac{SS_{res}}{n-p-1}}{\frac{SS_{tot}}{n-1}}} \quad \textbf{(2.11)}$$

Here $df_t$ relates to the degrees of freedom of the variance of the estimate of the dependent variable. $Df_e$ relates to the degrees of freedom of the estimate of the error variance. The adjusted R-squared can be seen as an unbiased estimator of the R-squared as it takes into account the number of used variables. To acquire the highest adjusted R-squared value and thus the best fit, all possible combinations of variables will be run in the MLR analysis. From these outcomes, the highest adjusted R-squared value will be found and its corresponding combination of variables will be analysed to see if it matches the manual selection process of discarding variables according to their p-values. This method works for the SLR analysis as well, however as the SLR analysis only consists of one predictor variable, the R-squared and adjusted R-squared values are equal for the SLR analysis.

Moriasi et al. (2007) does not provide a performance rating table for the R-squared value or the adjusted R-squared value like it does for the Nash-Sutcliffe efficiency. To get an idea of the performance rating for the R-squared value and adjusted R-squared value of the regression plot, the performance rating for the Nash-Sutcliffe efficiency from Moriasi et al. (2007) will be used. These are shown in Table 2-5.

| **Performance rating** | **(Adjusted) $R^2$** |
|---|---|
| *Very good* | $0.75 \leq R^2 \leq 1.00$ |
| *Good* | $0.65 \leq R^2 \leq 0.75$ |
| *Satisfactory* | $0.50 \leq R^2 \leq 0.65$ |
| *Unsatisfactory* | $R^2 \leq 0.50$ |

**Table 2-5, performance ratings for (adjusted) R-squared values**

The units of the predictor variables and the response variable will be the same as the units used in the dataset for the WALRUS model. T the groundwater level (GWL, or dG in WALRUS) will be in mm beneath ground level instead of m + NAP. The water level in the Maurikse Wetering (MW) will be in mm above the channel bottom.

To model the simple linear regression and the multiple linear regression the python module statsmodels is used (Statsmodels, n.d.). The statsmodels module can also be used to plot the partial regression plots (also known as added variable plots). In a partial regression plot, the relationship between one dependant variable and the response variable is shown.

In the partial regression plot the slope of the regression line is $\beta_k$, the constant for the plotted independent variable computed in the MLR. The y-intercept in the partial regression plot is zero. The x-axis shows $x - \bar{x}$, where $\bar{x}$ is the mean value of the independent variable. The y-axis shows

the difference for each point from x = 0 on the regression line. From the partial regression plot, the residuals can be seen for each independent variable around the regression line. This is similar to a residual plot, however the residual plot has a slope of 0 whereas the partial regression plot has a slope $\beta_k$.

## 2.4 WALRUS model

During this thesis the WALRUS model will be used to build a hydrological model of the Maurikse Wetering. The Wageningen Lowland Runoff Simulator or WALRUS (Brauer et al., 2014a,b) is a conceptual hydrological model developed by Claudia Brauer from the Wageningen University and intends to: "fill the gap between complex, spatially distributed models which are often used in lowland areas and simple, parametric (conceptual) models which have mostly been developed for mountainous catchments" (Brauer, Torfs, & Teuling, 2017, p. 1).

The model consists of 4 reservoirs or 'buckets', these being the unsaturated/vadose zone reservoir, the groundwater reservoir, the quickflow reservoir and the surface water reservoir, with fluxes between these reservoirs. A schematic overview can be seen in Figure 2-5.

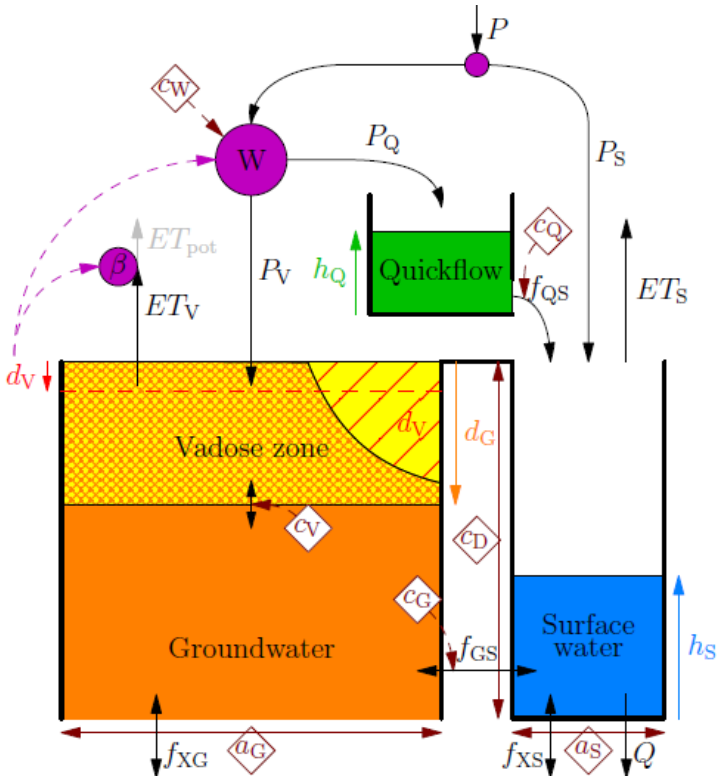


**Figure 2-5, schematization of the WALRUS model (Brauer et al., 2014a)**

In WALRUS, part of the precipitation quickly flows to the surface water via quickflow, e.g. cracks, macropores and drainage pipes. This is represented by the quickflow reservoir. The quickflow parameter $c_Q$ determines the average time during it takes for this water to reach the surface water. The remaining precipitation infiltrates in the upper part of the soil, the vadose zone. The fraction of the precipitation directed to the quickflow reservoir is determined via the wetness index W. This value is determined by a function of the wetness parameter $c_W$ and the storage deficit (dryness) in the vadose zone $d_V$.

If the storage deficit is less than the equilibrium storage deficit $d_{V,eq}$, water from the vadose zone percolates to the groundwater reservoir. If the storage deficit is higher than the equilibrium storage deficit (the ground is too dry), this flux goes from the groundwater reservoir to the vadose zone

through capillary rise. The quantity is determined by the vadose zone relaxation time $c_V$. Water can also leave the vadose zone via evapotranspiration $ET_a$, named $ET_V$ in Figure 2-5.

From the groundwater reservoir the groundwater can drain to the surface water reservoir via the flux $f_{GS}$ if the groundwater level is above the surface water level, or the surface water infiltrates to the groundwater if the groundwater level is below the surface water level. The quantity of this flux is determined by the groundwater reservoir constant $c_G$.

From the surface water reservoir, water can leave the system via discharge. Evaporation from and precipitation to the surface water reservoir is taken into account as well.

To build a conceptual hydrological model of the Maurikse Wetering in WALRUS, the default discharge formula needs to be changed and WALRUS's parameters need to be calibrated.

The IGF can be added via the external groundwater flux $f_{XG}$, which can be seen in Figure 2-5. The incoming water from De Kat, as well as the water pumped out via the pumping station at the Amsterdam Rijnkanaal, can be added via the external surface water flux $f_{XS}$.

### 2.4.1 Channel depth and discharge formula

The maximum contact area between the surface water and the groundwater is determined by the channel depth $c_D$. This is therefore important in the geohydrology.

Setting the channel depth $c_D$ to the depth of the river at the weir at Buren would work if the river is the only source of surface water in the system. At Buren the channel depth is roughly equal to the average channel depth of the entire Maurikse Wetering. However, Brauer et al. (2017) states that WALRUS requires: "An estimate of the characteristic channel depth: how deep are the channels generally incised in the landscape or how deep are the channel bottoms below the land surface (cD)" (p20). The "channels generally incised in the landscape" contain all channels, including secondary and tertiary waterways. An average channel depth including these waterways results in a lower $c_D$ than merely averaging the Maurikse Wetering. An import aspect of the $c_D$ value is how it governs the relation between the surface water and the groundwater. A higher $c_D$ will have a larger contact area between surface- and groundwater. Therefore, it is important to get a good estimate of the channel depth $c_D$.

The tilting weir at Buren complicates this. Despite this data being wrong as shown in chapter 3, the weir is important in keeping the water level in the Maurikse Wetering at a desired level. Removing the weir from the model allows for a free-flowing river, which results in a lower water level. This in turn will have an impact on the interaction with the groundwater, making for an unrealistic model.

The discharge is determined according to the weir formula for the weir at Buren in equation (**2.12**) as given in Mulder & Maartense (2017). The parameters in this formula are described in Table 2-6.

$$\boldsymbol{Q = 3.026 * B_0 * (\max(h - h_s, 0))^{\frac{3}{2}}} \qquad (2.12)$$

| Parameter | Description | Unit |
|---|---|---|
| $Q$ | Discharge | [m³/s] |
| $B_o$ | Width | [m] |
| $h$ | Water level | [m] |
| $h_S$ | Weir level | [m] |

**Table 2-6, parameters of the weir formula in equation (2.12)**

Changing the channel depth but not altering the weir level $h_S$ isn't feasible. In the best-case scenario this will result in disproportionate changes in discharge, but more likely this will either cause the weir level to rise above the surface or cause the weir level to be lower than the channel depth, resulting in errors.

Therefore, the weir level needs to be multiplied by a factor equal to the new channel depth $c_{D1}$ divided by the original channel depth $c_{D0}$. With this, the fact that the weir level is given in [m + NAP] has to be taken into account. This needs to be accounted for by subtracting the bottom level of the original channel depth from the weir level $h_s$. Previously having both h and $h_s$ in [m + NAP] circumvented this effect, but now the weir is set to ground level. This means that the factor $\frac{c_{D,1}}{c_{D,0}}$ must be multiplied by the height of the entire weir or the relation will be wrong. Parameters $c_{D1}$ and $c_{D0}$ are given in Appendix C.

There is also the problem of width. If the change in height of the weir is decreased by a certain factor, the width in the weir formula needs to be changed as well, otherwise the influence of the weir on the discharge will be diminished. The width also cannot be overestimated, or the influence of the weir level will be too high. To solve this, the new width needs to counter the alteration in the channel depth in the weir formula.

$$\boldsymbol{B_0 * f(h, h_{s,0}) = B_1 * f(h, h_{s,1})} \tag{2.13}$$

Filling in the new factor in the function for h and some simple algebra results in the following formula for the new width:

$$\boldsymbol{B_1 = \left(\frac{1}{\frac{c_{D,1}}{c_{D,0}}}\right)^{\frac{3}{2}} * B_0 = \left(\frac{c_{D,0}}{c_{D,1}}\right)^{\frac{3}{2}} * B_0} \tag{2.14}$$

As the weir level data is incorrect (as will be explained in chapter 3), the discharge formula cannot be built around the weir level data. As the water level data is deemed reliable, the water level data will be used instead. The weir level will instead be set as a variable. This leads to the new discharge formula:

$$\boldsymbol{Q = [Conversion\ factors] * 3.026 * \left(\frac{c_{D,0}}{c_{D,1}}\right)^{\frac{3}{2}} * B_0 * \left(\max\left(h - \frac{c_{D,1}}{c_{D,0}} * h_s, 0\right)\right)^{\frac{3}{2}}} \tag{2.15}$$

| Parameter | Description | Unit |
|---|---|---|
| $Q$ | Discharge | [mm/d] |
| $h$ | Average water level in catchment | [m] |
| $h_S$ | Weir level at Buren | [m] |
| $c_{D,0}$ | Channel depth at Buren | [mm] |
| $c_{D,1}$ | Average channel depth | [mm] |
| $B_0$ | Width weir Buren | [m] |

**Table 2-7, parameters revised weir discharge formula in equation (2.15)**

In WALRUS, this new weir level was implemented slightly different, in a way that resulted in the same output but required less adaptation of WALRUS scripts. The water level data was entered as input as the weir level data $h_S$. In every process related to the water level (for example, exchange between groundwater and surface water) the parameter 'water level' was changed to 'weir level', thus remaining the same. The modelled "water level" minus the input "weir level" is the difference which determines the discharge, only now this difference is modelled above the water surface instead of below it to the weir level. If necessary, the modelled weir level can then be derived via the following formula:

$$\boldsymbol{weir\ level_{mod} = h_s - (h - h_s)} \tag{2.16}$$

## 2.4.2 WALRUS calibration

The model is calibrated using a Monte Carlo analysis, in which the WALRUS model is run with many random parameter sets. The Nash-Sutcliffe efficiency (NS or NSE) (Nash & Sutcliffe, 1970) is used to determine the goodness of fit of modelled data with the observed input, in this case the modelled groundwater level by WALRUS with the 'observed' data from the average groundwater level as modelled by MORIA. Simultaneously the NS efficiency for the modelled discharge and the discharge as modelled by MORIA is calculated.

$$\boldsymbol{NS = 1 - \frac{sum((data_{obs} - data_{mod})^2)}{sum\left(\left(data_{obs} - mean(data_{obs})\right)^2\right)}} \tag{2.17}$$

The 4 parameters that are calibrated are $c_W$, which influences the amount of water that goes to the quickflow reservoir or the groundwater bucket/reservoir, $c_V$, which influences the exchange between the unsaturated zone and the groundwater bucket, $c_G$, which influences the exchange between the groundwater and surface water, and $c_Q$, which influences the time it takes for the water in the quickflow reservoir to reach the surface water.

The parameter boundaries were first set using values from examples in the WALRUS tutorial (Brauer et al., 2018), shown in Appendix E. A Monte Carlo analysis was then performed with a limited number of parameter sets, usually 1000, which were then plotted over the NS efficiency. This amount is sufficient to show the course of the parameter sets to the maximum NS value, from which it can be determined if the boundaries need to be increased. For instance, in Figure 2-6 the left graph has sufficient boundary conditions as the maximum is within the limits (assuming that, at most, one maximum will occur). The right graph of Figure 2-6 however shows a maximum on the upper boundary, a course which will likely continue if the upper boundary is increased. The boundary conditions for this parameter are therefore insufficient and the upper limit needs to be increased.

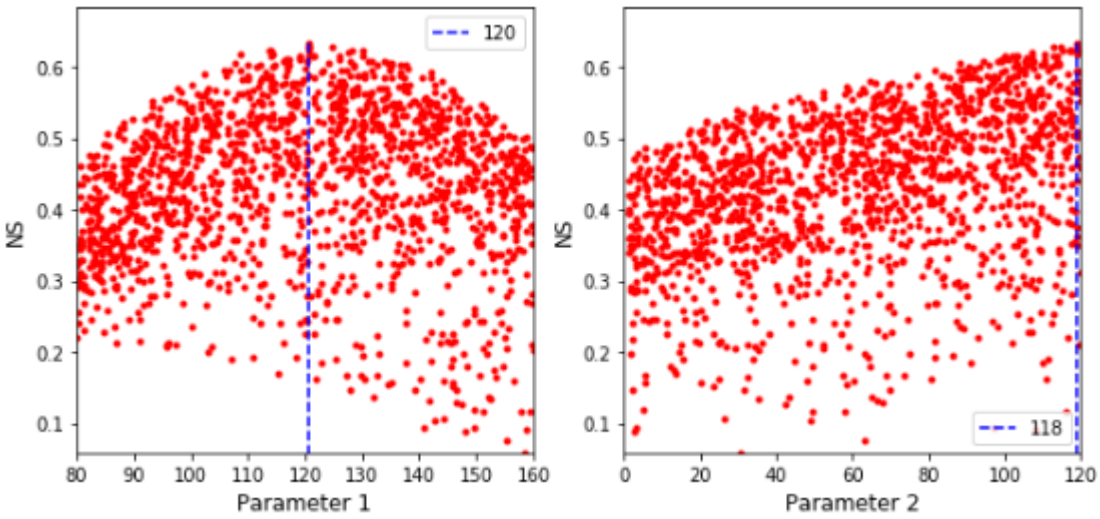


**Figure 2-6, examples boundaries check during calibration. Left: Boundaries sufficient (clear maximum). Right: Boundaries insufficient (no maximum).**

This process is repeated until suitable boundary conditions are found for all 4 relevant parameters in the WALRUS model. If the course is horizontal (and remains horizontal after adjusting the parameter boundaries), this indicates that the model is insensitive to that parameter. This means that no matter what value that parameter has, it has no influence on the model outcome. This occurs when the parameter influences a process that has no influence on what the model is being calibrated to.

As the best fit model does not have a perfect fit with the data from MORIA, the best fit in WALRUS is insufficient to confidently predict every outcome. It is therefore better to additionally show a spread in which the actual values lie, as the best fit is only an approximation.

MORIA modelled the exchange between groundwater and surface water as well as quickflow through the soil. This combined flux from MORIA is assumed to be equal to the discharge. The WALRUS model is also calibrated to this discharge flux. Looking at two processes during calibration increases the accuracy of the model and rules out any possibilities of the model fitting one process well but the other processes badly.

After the Monte Carlo analysis, the results are analyzed. The parameter sets which resulted in an NS efficiency for both groundwater level and discharge which are deemed “good” by Moriasi et al. (2007), meaning an NSE > 0.65, are kept while the others are discarded. The WALRUS model is run for all parameter sets with an NS value equal to or higher than this set boundary of 0.65 for both groundwater level and discharge as modelled by MORIA. The resulting datasets are saved separately and loaded into Python. In Python, the maximum and minimum values of the groundwater level and discharge as modelled by WALRUS are saved in separate columns for each timestep. These columns are added to the data file for the parameter set with the best fit for both parameters, which is then loaded back into Rstudio.

The default file for creating figures in WALRUS is changed to incorporate the spread between minimum and maximum values as a band, as well as plotting the outcome of the best fitting parameter as a line.

The IGF relation established earlier between the intercatchment groundwater flow and the Nederrijn level in section 2.3 will now be tested. As the model is already calibrated to the IGF data it will not be calibrated using a Monte Carlo analysis again, as the IGF relation is only an approximation of the IGF as modelled by MORIA. Calibrating the model to this would divert the WALRUS model away from reality. The input IGF data, being the IGF as modelled by MORIA, is

replaced by the IGF relation to the Nederrijn level with the Nederrijn level as input. This relation could be implemented directly in the WALRUS source files, but it was found to be easier to compute the IGF data from the relation separately using Nederrijn data and add it as the external groundwater flux $f_{XG}$.

### 2.4.3 Resulting WALRUS model

The parameters with the highest NS efficiency to both the average groundwater level and the discharge as modelled by MORIA from the calibration will be entered in WALRUS. The WALRUS output consists of 4 graphs, as can be seen in the example in Figure 2-7. The discharge data measured at the weir at Buren ($Q_{observed}$) is shown in the top graph, along with the discharge as modelled by WALRUS ($Q_{WALRUS}$) and the precipitation (P). The second graph shows the actual and potential evaporation, as well as the wetness W. The third graph shows the storage deficit in the unsaturated zone ($d_V$), the groundwater level as modelled by MORIA ($d_{G,MORIA}$), the groundwater level as modelled by WALRUS ($d_{G,WALRUS}$) and the water level, expressed as the difference between the channel bottom and the water level ($c_D - h_S$). The fourth graph shows the discharge as modelled by MORIA ($Q_{MORIA}$), the discharge as modelled by WALRUS ($Q_{WALRUS}$), the exchange between the groundwater and the surface water ($f_{GS}$), the IGF and the incoming surface water from De Kat ($f_{De\ Kat}$).

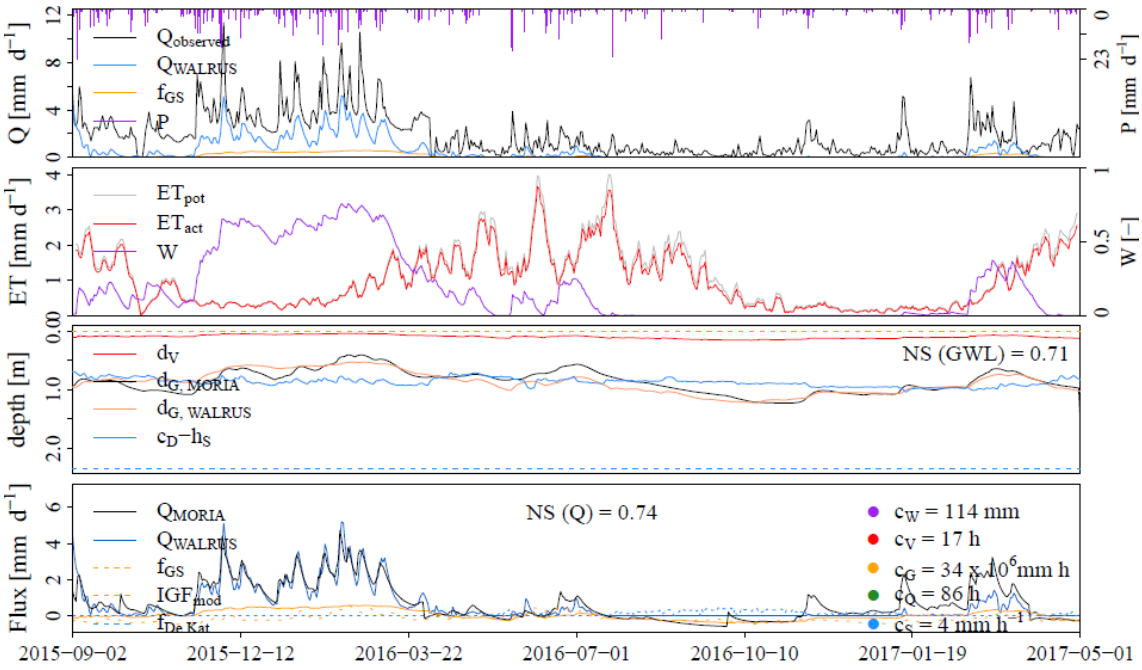


**Figure 2-7, example WALRUS model output. Top graph: Measured discharge data at weir Buren, modelled WALRUS discharge, groundwater flux and precipitation. Second graph: Evaporation and wetness. Third graph: groundwater level, water level above channel bottom and storage deficit. Bottom graph: Discharge modelled by MORIA and WALRUS, IGF, incoming water at De Kat and groundwater-surface water exchange.**

The NS efficiency for the groundwater level is displayed as "NS (GWL)" in the third graph of the WALRUS output, and the NS efficiency for the discharge will be shown as "NS (Q)" in the fourth graph. The parameters are displayed in the fourth graph as well.

# 3 WATER BALANCE

This chapter will explore the internal processes and provided data within the Maurikse Wetering. The provided data is checked for inconsistencies and altered when necessary. We will see if the water balance closes with the provided data and draw a Budyko curve to see if the results are as expected for this climate.

## 3.1 Discharge data

The original dataset from the discharge data from the weir at Buren can be seen in Figure 3-1. This figure is cut off at Q = 500 m³/s. The largest peak in this set is Q = 1028 m³/s.

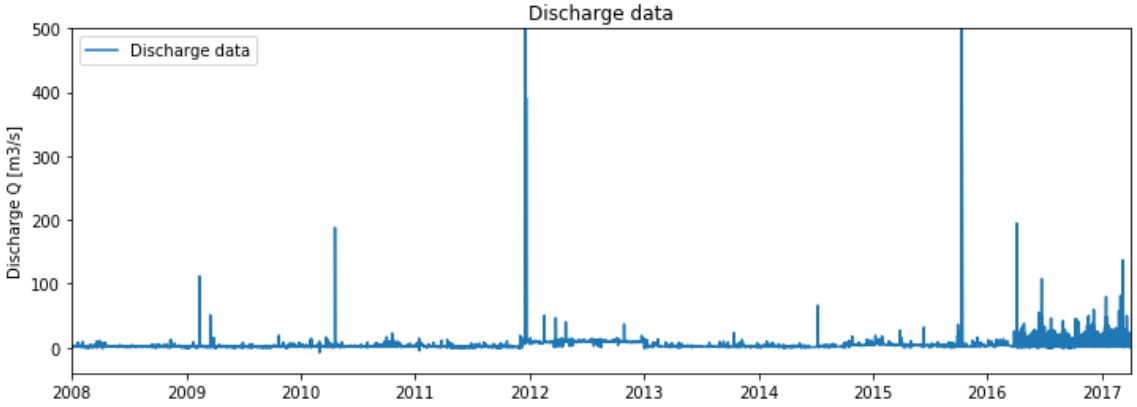


**Figure 3-1, original discharge data from the weir at Buren (cut off at Q = 500 m³/s). Significant peaks, uncharacteristic for a 9.5 meter wide weir, are clearly visible.**

Out of a total of 81071 hours of data, 4693 hours were deleted due to insufficient resolution or incompatibility with WALRUS. This amounts to 5.8 % of the data being deleted. The effects of this can be seen in Figure 3-2.

As can be seen in Figure 3-2, the hydrological year of 2016 is most affected by this revision, whereas the period from 2008 – 2015 sees more sporadic revision of peaks. For the hydrological year of 2016 84% of data consists of aggregated data, starting at 3-4-2016 at 22:00 hours and the last aggregate occurring at 31-3-2017 at 22:00 hours.

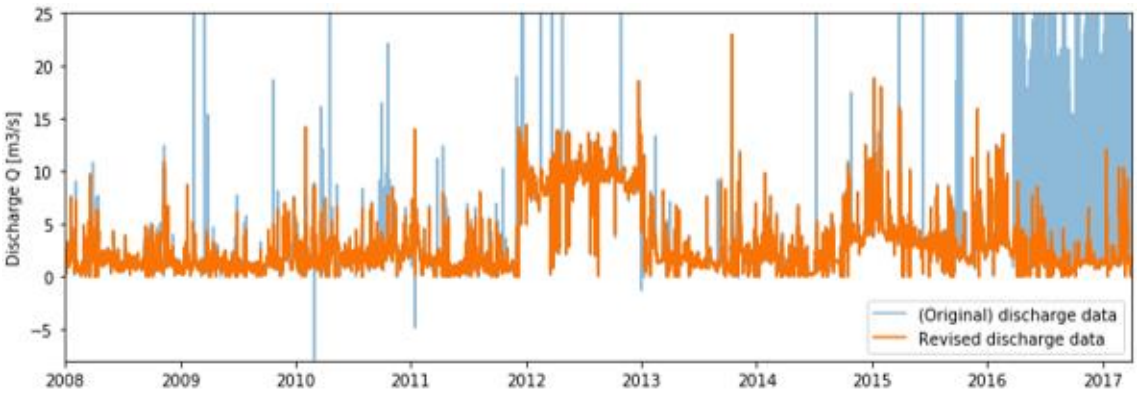


**Figure 3-2, revised discharge data from the weir at Buren, with the raw discharge data on the background.**

Figure 3-2 also shows a significant increase in the discharge data for the year 2012. In this year, the baseflow is approximately 10 $m^3/s$, compared to a baseflow between 1 and 3 $m^3/s$ for the other years. As the meteorological data for 2012 does not appear to differ from the other years, the data for 2012 is likely erroneous. To see which sections of data are correct, further analysis is needed. This is done in the next section, where the discharge quantity is tested via the water balance to see if the water balance closes.

## 3.2 Budyko curve and water balance

The annual precipitation for the year 2017 is 800 mm for station Herwijnen, which is the KNMI station closest to the Maurikse Wetering. The main exit of the catchment is at Buren, where the discharge is measured. The annual sum of these measurements over the year is 69 million $m^3$ for 2017. This equals an annual discharge of 825 mm in 2017.

Immediately, an interesting observation is made. When dividing the sum of the discharge over sum of the precipitation, the ratio is Q/P = 1.03. If the data is correct, this means that around the same amount of precipitation falls on the catchment as leaves through the main stream outlet. This not a sign of an ordinary isolated catchment, as through evaporation alone this ratio should be significantly lower.

The factor of the actual evaporation $ET_a$ over the potential evaporation $ET_P$ (called factor X in Table 3-1) according to the data of the surrounding KNMI stations is shown in Table 3-1.

| **Station** | **P** | **$ET_P$** | **X (%)** | **$ET_A$ [mm] (calculated)** |
|---|---|---|---|---|
| ***Herwijnen*** | 800 | 610 | 8.9 | 54 |
| ***De Bilt*** | 914 | 586 | 24.8 | 145 |
| ***Deelen*** | 909 | 561 | 25.3 | 142 |
| ***Volkel*** | 749 | 606 | 2.3 | 14 |

**Table 3-1, actual evaporation to fit the water balance for 2017**

For a temperate climate as exists in the Netherlands, the factors and values shown in Table 3-1 appear too low. A Budyko curve is drawn up to check whether these results fit expectations for such a catchment.

### 3.2.1 Budyko curve

The resulting Budyko curve for 2017 with actual evaporation rates calculated from the factors from Table 3-1 is shown in Figure 3-3.

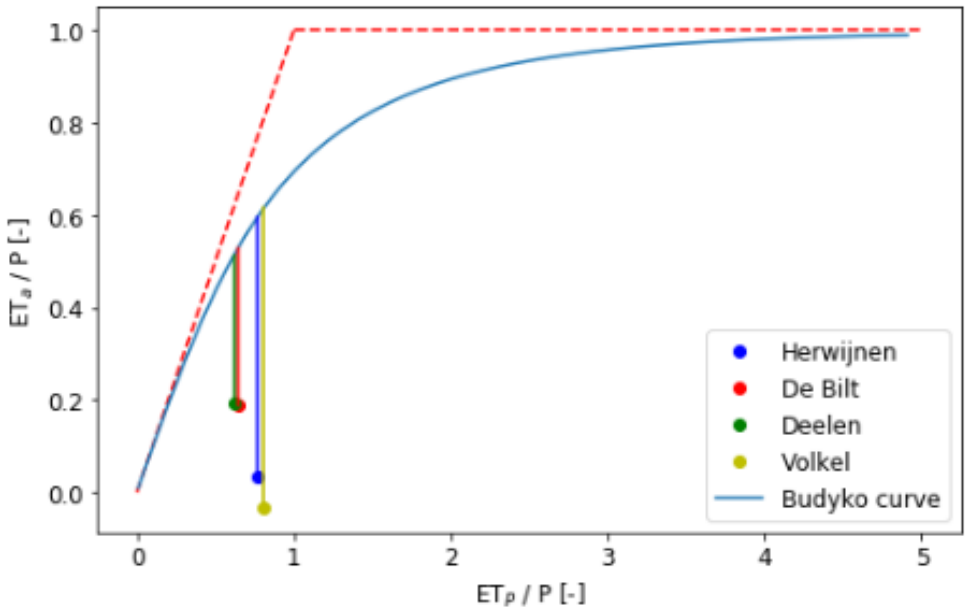


**Figure 3-3, Budyko curve for 2017 for the KNMI stations closest to the Maurikse Wetering with actual evaporation ratio against potential evaporation ratio for the closest 4 KNMI stations**

| KNMI station | Error calculated evaporation compared to Budyko curve |
|---|---|
| *Herwijnen* | 95 % |
| *De Bilt* | 64 % |
| *Deelen* | 63 % |
| *Volkel* | 106 % |

**Table 3-2, difference calculated and Budyko actual evaporation, relative to the Budyko curve**

Figure 3-3 also shows the error that follows from this data, the values of which are given in Table 3-2. Here the meaning of 'error' refers to the difference between the actual evaporation ratio and the expected evaporation ratio according to Budyko.

$$'Error' = \frac{\left(\frac{ET_a}{P}\right)_{Budyko} - \left(\frac{ET_a}{P}\right)_{data}}{\left(\frac{ET_a}{P}\right)_{Budyko}} \qquad (3.1)$$

This error is the amount of water that is missing from the water balance if the system in reality follows the Budyko curve more closely. The latter is expected because of the regular appearance of the catchment with for instance a relatively low fraction of the surface area being paved. From the way the actual evaporation is calculated, this would mean an additional (significant) flux into the system that is hidden by the standard water balance equation of Q = P – ET.

### 3.2.2 Water balance

From chapter 3.2.1 it is clear that the water balance doesn't close with standard evaporation levels for the Netherlands. It will now be seen how much water is missing, and what conclusions can be drawn from this.

In Table 3-3 the external fluxes to the Maurikse Wetering catchment are shown. The incoming fluxes are precipitation and the surface water entering at De Kat. The outgoing fluxes are evaporation, where actual evaporation is taken at an estimated 80 % of potential evaporation, and the pumping station at the Amsterdam Rijnkanaal (ARK), which pumps water to the Amsterdam Rijnkanaal if water levels in front of the culvert running underneath it are too high.

The flux of De Kat and the pumping station at the Amsterdam Rijnkanaal are given in $m^3$ as this is a fixed value, whereas the corresponding amount in millimeter differs depending on which weir is observed as this changes the corresponding catchment area.

| Hydrological year | De Kat [$m^3$] | ARK [$m^3$] | P [mm] (Herwijnen) | Actual evaporation [mm] (Herwijnen) |
|---|---|---|---|---|
| *2008* | 15763017 | 1059351 | 713 | 500 |
| *2009* | 4372425 | 1991619 | 704 | 538 |
| *2010* | 20103468 | 1937540 | 716 | 523 |
| *2011* | 4074025 | 519099 | 840 | 523 |
| *2012* | 1428606 | 1179771 | 882 | 489 |
| *2013* | 4043697 | 785565 | 705 | 514 |
| *2014* | 3071221 | 726398 | 840 | 520 |
| *2015* | 3417588 | 1010367 | 952 | 533 |
| *2016* | 7988803 | 259670 | 664 | 542 |
| *2017* | 7145587 | 2983230 | 800 | 520 |

**Table 3-3, external surface water fluxes per hydrological year**

The water balance is now computed for Buren and Kribbrug, where discharge is the summed discharge per hydrological year. Net discharge is the discharge over one year minus the external surface water flux of De Kat. For the net discharge at Buren the discharge over the pumping station at the Amsterdam Rijnkanaal is added, as this is discharge generated within the catchment but not measured at Buren. For Kribbrug the discharge of the pumping station is not added, as the Amsterdam Rijnkanaal is downstream of Kribbrug.

| Hydrological year | Discharge Buren [mm] | Net discharge Buren [mm] | Water balance deficit [mm] |
|---|---|---|---|
| *2008* | 945 | 375 | -163 |
| *2009* | 571 | 519 | -353 |
| *2010* | 935 | 697 | -459 |
| *2011* | 1334 | 1286 | -969 |
| *2012* | 3017 | 3000 | -2606 |
| *2013* | 736 | 688 | -496 |
| *2014* | 1162 | 1125 | -805 |
| *2015* | 1250 | 1210 | -791 |
| *2016* | 621 | 526 | -386 |
| *2017* | 824 | 740 | -460 |

**Table 3-4, water balance per hydrological year for the weir at Buren**

| Hydrological year | Discharge Kribbrug [mm] | Net discharge Kribbrug [mm] | Water balance deficit [mm] |
|---|---|---|---|
| *2008* | 484 | 27 | +185 |
| *2009* | 563 | 437 | -270 |
| *2010* | 505 | -77 | +315 |
| *2011* | 821 | 703 | -386 |
| *2012* | 374 | 333 | 61 |
| *2013* | 1198 | 1081 | -889 |
| *2014* | 1424 | 1335 | -1015 |
| *2015* | 1234 | 1135 | -717 |
| *2016* | 1284 | 1052 | -912 |
| *2017* | 1405 | 1198 | -918 |

**Table 3-5, water balance per hydrological year for the weir at Kribbrug**

In Table 3-4 and Table 3-5 the value given at "Water balance deficit" represents the change in storage assuming the water balance closes. This means that a negative number represents a surplus in discharge compared to influx, which would mean a decrease in storage.

While the water balance of Kribbrug at a first glance appears to close for the period 2008 – 2012, the fluctuations are extremely high, with a discharge generated within the catchment itself being - 77 mm in 2010. Approximately the same amount of precipitation fell in that year as did in 2008 and 2009, making this rather unlikely. The amplitude of this difference in storage should not be this extreme for a catchment such as the Maurikse Wetering.

## 3.3 Analyzing revised data

Looking back at Figure 3-2, the period of 2012 to 2013 appears to be the most erroneous. For Buren this results in a huge deficit in the water balance. At Kribbrug there is only one datapoint that year, on January 1st. The water balance as shown is the result of starting on April 1st, the start of a hydrological year, which does not include the data point. The values for this year are the summation of the data from 1-1-2013 to 31-3-2013.

Without probable cause and little other data to support this, the average discharge increases by a huge margin, comparable to significant rain events. In the winter of 2014 – 2015 the dry weather flow significantly increases as well.

It is possible that weir levels or water levels were not properly monitored during these periods. Looking at Figure 3-4, in the period 2013 – 2016 it often occurred that the weir level was significantly higher than the downstream water level, up to +1 meter. This raises the suspicion that in 2012 something occurred that upset the measuring system of the tilting weir. This may have something to do with the construction of the fish ladder.


**Figure 3-4, weir level and upstream water level at Buren between January 2008 – April 2018.**

As told by the system operator at Rivierenland Water Board, there is no other influx of surface water into the Maurikse Wetering catchment other than the already known inlet at De Kat. The weir at Buren has a lowest possible crest level of 1.02 m + NAP. This is the level when the weir is fully opened. However, the provided data as can be seen in Figure 3-4 shows levels consistently below that level during the entire 10 years of recorded data, with the lowest level being 0.602 m + NAP. As a result of this the weir data was deemed unreliable. As the discharge data is a function of the difference between the weir level and the water level through a stage-discharge relation (Mulder & Maartense, 2017), erroneous weir level data results in erroneous discharge data. Due to a recent switch in operating systems, archived data other than the acquired dataset will be hard to come by and so the origin of the error is unknown.

## 3.4 Amsterdam Rijnkanaal

Contrary to the discharge measurements at the other stations, the discharge data at the culvert beneath the Amsterdam Rijnkanaal doesn't rely on a weir. The problem here is that while upstream water level is automatically measured, the downstream water level is not. The downstream water level is estimated as being equal to the upstream water level at Buren plus the gradient over the distance (Rivierenland Water Board, n.d.). This gradient from the weir at Buren to the culvert is set to 5 centimeters.

However, it turns out that this method measures a cumulative gross discharge of approximately 50 mm/year for an area of 45 km². This means that most, if not all, of the discharge entering the catchment at the inlet at De Kat does not reach the culvert, as does almost all of the precipitation. This is an unrealistic scenario, as it seems unlikely that the area generates next to no discharge in the Dutch climate.

## 3.5 Chapter summary

In this chapter, the data required for creating a conceptual hydrological model (without an IGF flux) is analysed. It was found that the water balance for the Maurikse Wetering does not close.

As the annual precipitation and potential evapotranspiration data corresponds to expected values for the Netherlands (KNMI, n.d.), there is either a significant influx of IGF or the discharge data is incorrect. This will be tested in chapter 5 by means of the MORIA groundwater model. As the weir level data appears to be incorrect, as the data frequently falls below the minimum possible weir level, until proven otherwise it is assumed that the discharge data is false.

If the IGF flux turns out to not be significant, this means that with the available data for the Maurikse Wetering, the IGF cannot be expressed as the 'missing' water in the water balance as was done in Genereux et al. (2005) and Bouaziz et al. (2018).

# 4 INTERCATCHMENT GROUNDWATER FLOW

In this chapter the workings of intercatchment groundwater flow or IGF will be explored. As the major rivers the Nederrijn and the Waal surround the Maurikse Wetering catchment, they are likely the main source of intercatchment groundwater flow. We will see how the IGF changes in both volume and direction over the year, what causes these changes and if a relation exists between surface parameters and the IGF.

## 4.1 Rhine level

Figure 4-1 and Figure 4-2 show that the Nederrijn is more regulated than the Waal. This is done via a lock between stations 2 and 3, Beneden Amerongen and Boven Amerongen. This way, the Nederrijn has a more constant water level whereas the Waal is free-flowing and shows more fluctuations in its water level throughout the year.

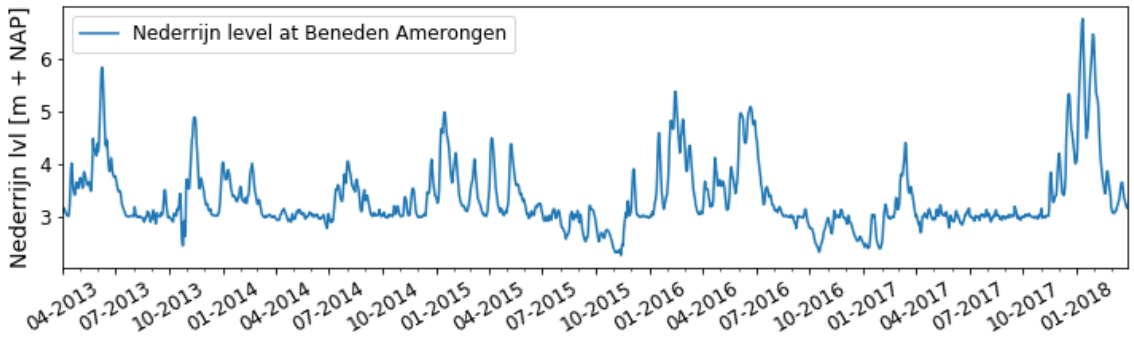


**Figure 4-1, water level at station 2: the Nederrijn at Beneden Amerongen**

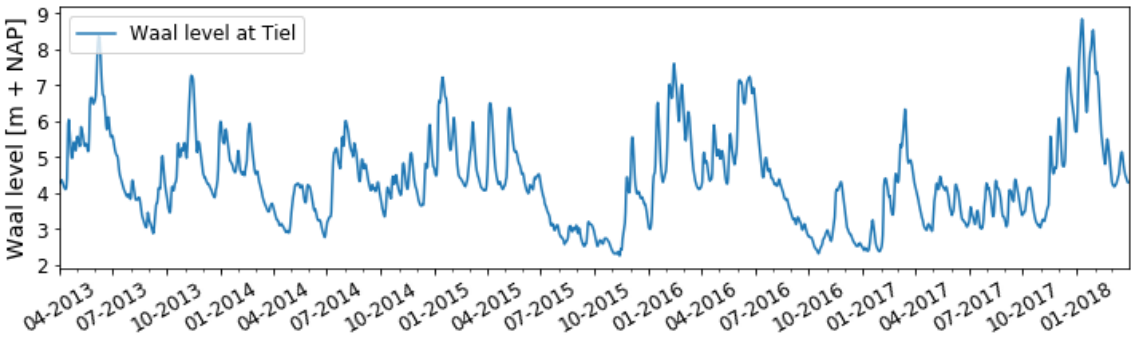


**Figure 4-2, water level at station 6: the Waal near Tiel**

## 4.2 IGF quantity

To determine the amount of IGF, first the boundaries need to be determined which are to be used in the iMOD analysis of the MORIA model results. After that, the gross and net IGF flux can be quantified.

### 4.2.1 Groundwater reservoir boundaries

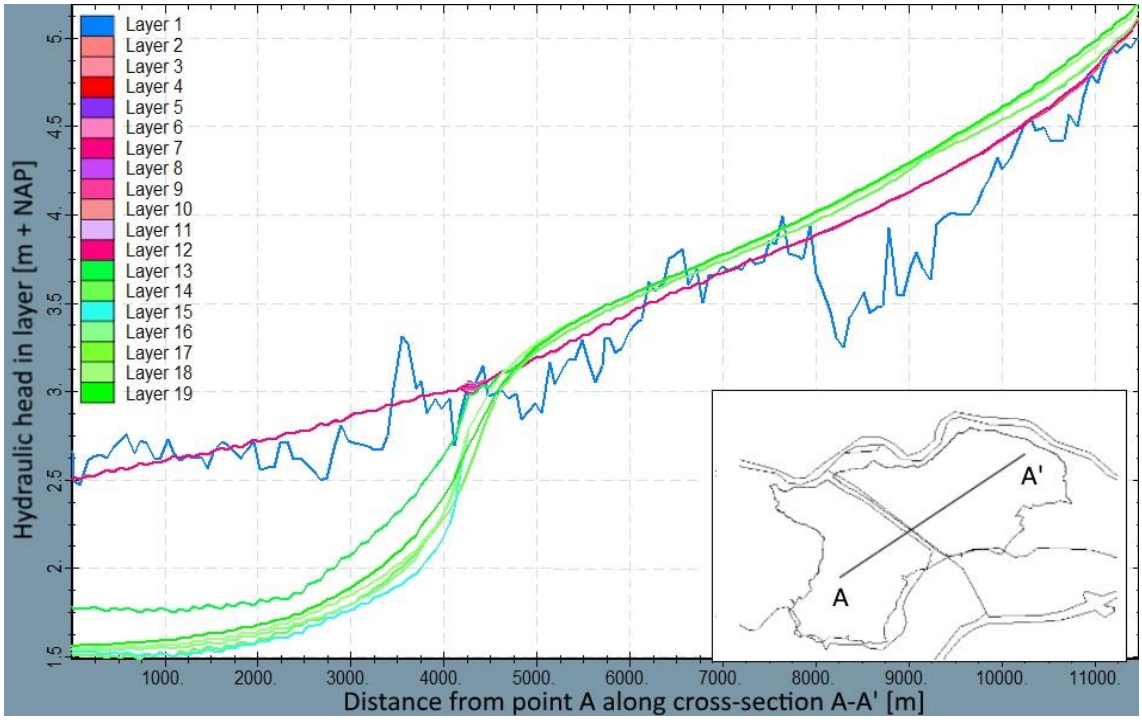


**Figure 4-3, hydraulic head as modelled by MORIA in layers 1-19 on 1-4-2013 over a cross-section, which is depicted in the lower right. 3 distinct groups can be seen, layer 1 (blue), layers 2-12 (shades of red) and layers 13-19 (shades of green). This grouping shows which layers make up different aquifers.**

In Figure 4-3 the hydraulic head of layers over a cross-section is shown. There are 3 distinct groups, being the top layer, layer 1, which is the unsaturated zone and therefore has a relatively high spatial and temporal variability. Layers 2-12 appear to be grouped together and layers 13 – 19 as well. This means that the latter group is a lower aquifer, separated by a poorly permeable or impermeable layer. As the bottom of layer 11 lies on top of the main impermeable layer between the two aquifers, layer 12, and the incoming/outgoing vertical flux is modelled at the bottom of the layer, layer 11 will be set as the bottom of the groundwater bucket. The vertical flux FLF is taken as the vertical IGF.

The borders of the groundwater bucket are now set. The depth of the groundwater bucket is the depth of layers 1 to 11. The (horizontal) surface of the groundwater bucket is set equal to the topographic catchment of the Maurikse Wetering, an area of 84.5 km². From Figure 4-4 it is clear that the main aquifer in this profile is layer 4, which carries most of the lateral IGF flow. This is due to this layer being thick in this area as can be seen in Figure 1-4 (REGIS layers Krz2 and Krz3, as taken from Table 2-4), as well as being relatively highly permeable. Unless stated otherwise, from this point on the groundwater level is set to the hydraulic head in layer 4.

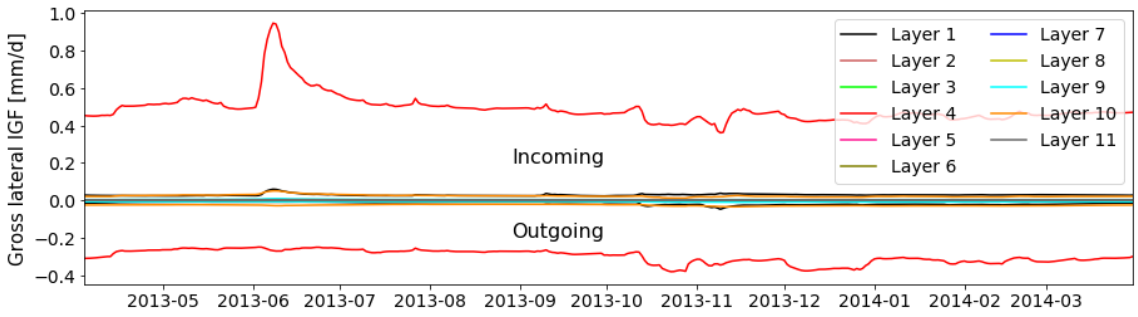


**Figure 4-4, horizontal IGF fluxes in each layer for layers 1-11 for the hydrological year 2013. Each layer has an incoming and outgoing element, with the positive values being incoming IGF and negative values outgoing IGF. Layer 4 (red) sees the vast majority of both the incoming and outgoing flow.**

The vertical flux coming from lower layers is taken as the FLF flux of layer 11. The lateral IGF is taken as the sum of the FFF (flux front face) and FRF (flux right face) of layers 1 to 11.

### 4.2.2 Net IGF flux

With the boundaries set, iMOD can be used to model the IGF fluxes. The gross IGF fluxes, meaning the total incoming and total outgoing fluxes, are plotted in Figure 4-5. Figure 4-5 shows that the lateral fluxes are significantly higher than the vertical fluxes.

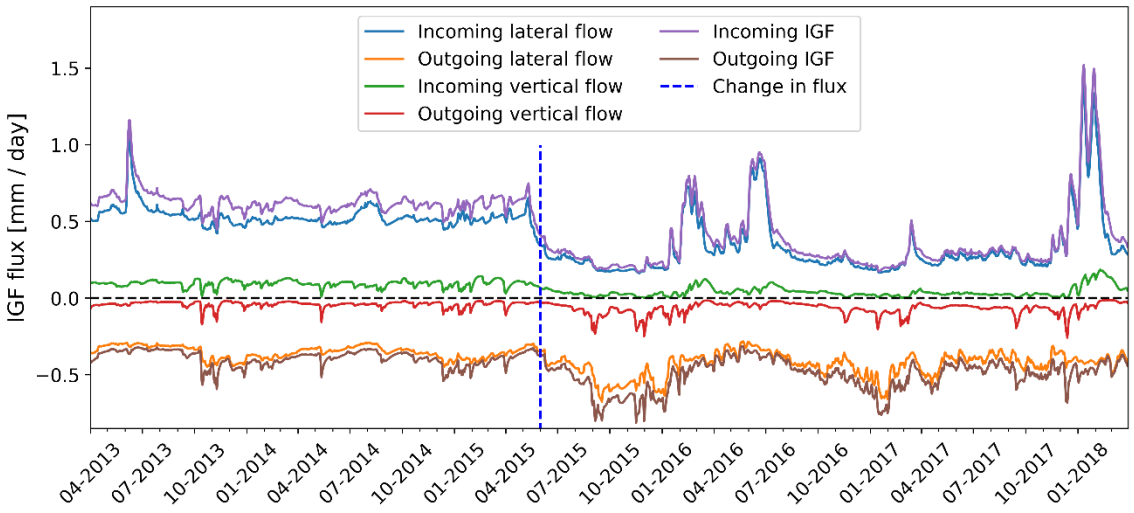


**Figure 4-5, gross IGF fluxes. The lateral fluxes are significantly higher than the vertical fluxes. Around June 2015 there is a significant change in quantity and behaviour of the IGF, especially the incoming lateral flow. This moment is marked by the blue dotted line.**

From the gross IGF fluxes, the net IGF fluxes can be computed. The different lateral net IGF fluxes are plotted in Figure 4-6. As can be seen, the net right flux and net front flux follow a similar course, only the front flux FFF has a higher amplitude. This will be expanded upon later in this section. The conclusion that can be drawn from Figure 4-6 is that the cause of fluctuations in the IGF can be found in the 'Front' direction, meaning flow in the north-south direction, as Figure 2-4 shows.

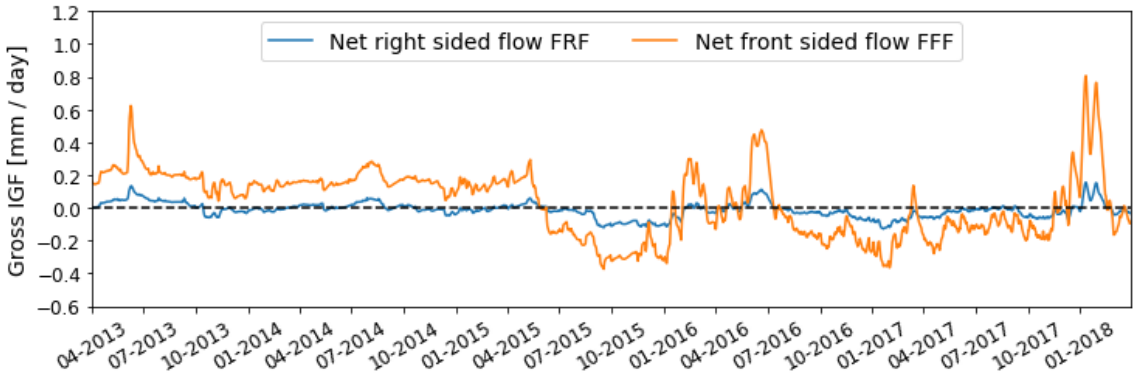


**Figure 4-6, net lateral IGF fluxes, front and right faced, to the Maurikse Wetering catchment. A positive value indicates water flowing to the Maurikse Wetering catchment (net gain).**

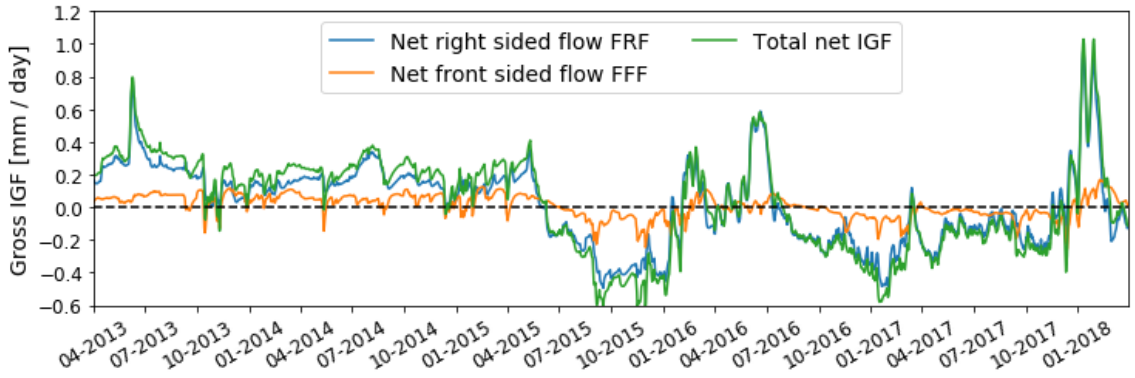


**Figure 4-7, vertical, lateral and total net IGF fluxes to the Maurikse Wetering catchment. The net IGF is the sum of all IGF fluxes over the catchment borders.**

From Figure 4-7 it can be seen that the lateral IGF flux is significantly higher than the vertical IGF flux. The vertical IGF flux also roughly follows the course of the lateral IGF flux, changing from a net gain to the catchment a net loss at roughly the same time. The annual sum of the net IGF for each year is given in Table 4-1.

| Hydrological Year | Net IGF [mm/yr] | Water balance deficit [mm/yr] | % of missing water in water balance |
|---|---|---|---|
| *2013* | 92.4 | -496 | -18.6 |
| *2014* | 77.3 | -805 | -9.6 |
| *2015* | -61.8 | -791 | 7.8 |
| *2016* | -45.2 | -386 | 11.7 |
| *2017* | -16.1 | -460 | 3.5 |
| *Average* | 9.3 | -496 | -1.0 |

**Table 4-1, annual sum of the net IGF flux as modelled by MORIA and average annual sum for this dataset. This is compared to the water balance deficit for each hydrological year from Table 3-4, showing that the IGF as modelled by MORIA is not enough to close the water balance with the available data. A positive number in the last column means the IGF works towards closing the water balance, a negative number worsens it.**

From Table 4-1 it can be seen that 2013 and 2014 see a net IGF gain, whereas the hydrological years 2015 to 2017 see a net IGF loss. Looking at chapter 3.2, the net IGF loss in 2017 confirms the hypothesis that the discharge data is erroneous and the IGF cannot be estimated as the missing water in the water balance. Table 4-1 shows that the contribution of IGF to the water balance does not close the water balance with the provided data. For the years 2015 to 2017 the catchment even loses water to IGF. This confirms that at least one dataset is erroneous. Combined with the results from chapter 3, it can be stated that the discharge data is erroneous.

Now that the IGF is quantified using MORIA, it can be seen which variables influence the IGF flux. The variables that are observed in this analysis are the precipitation, the average groundwater level in the catchment and the water level in the two major rivers; the Nederrijn and the Waal. The course of these variables are compared to the incoming IGF.

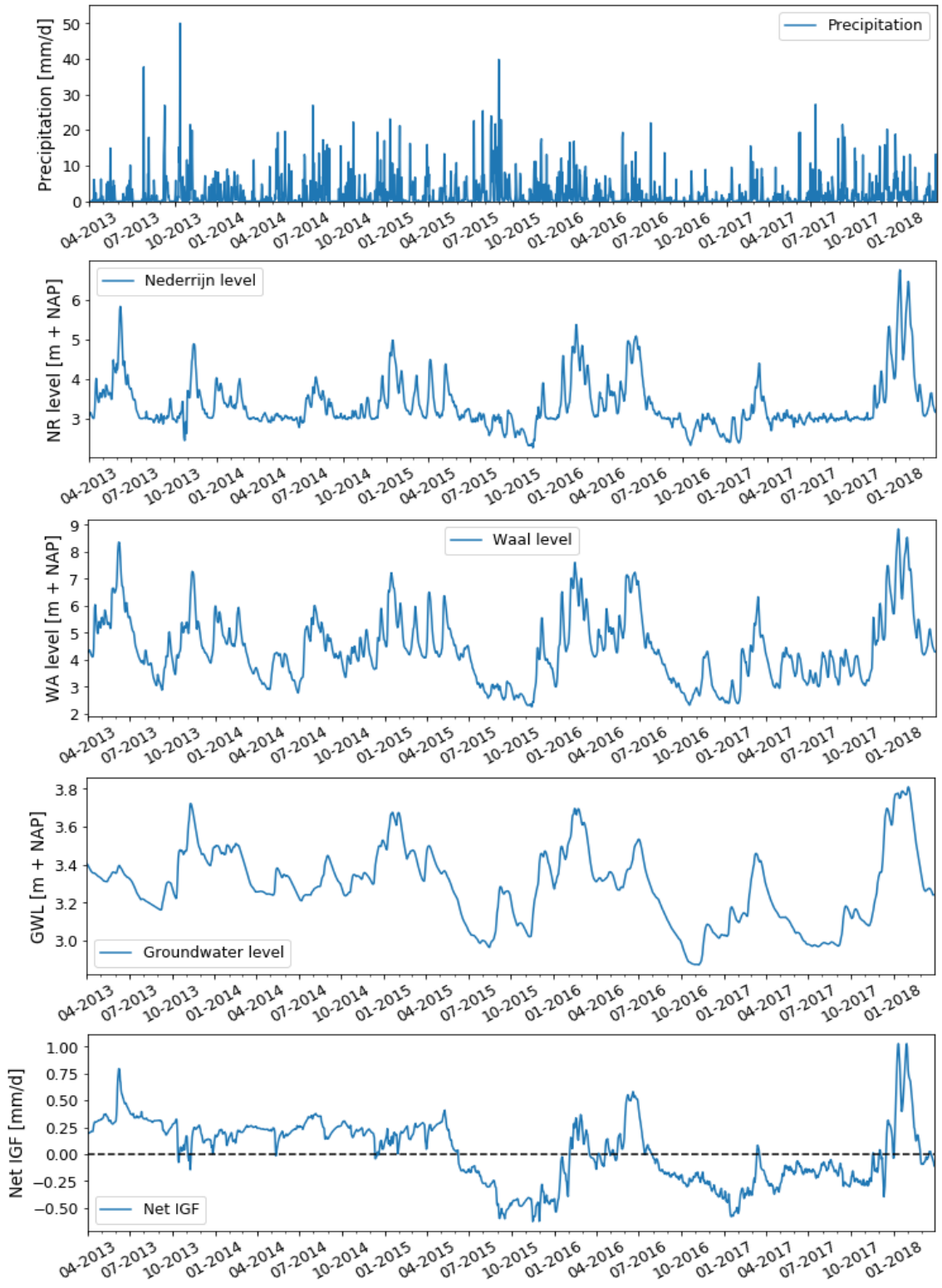


**Figure 4-8, From top to bottom: Precipitation, Nederrijn at Beneden Amerongen, Waal at Tiel, average groundwater head, net IGF flux**

From Figure 4-8 it can be seen that in December 2014 there was a net IGF flux of approximately 0. In May 2015 the water levels in the Nederrijn and Waal were approximately the same, however May 2015 saw less precipitation and more evaporation than December 2014. This caused lower groundwater levels in the catchment for May 2015. As a result, the pressure difference from the main rivers to the Maurikse Wetering catchment increased, causing IGF fluxes to increase to between 20.000 and 30.000 $m^3$/day or 0.25 to 0.35 mm/day.

High rainfall caused groundwater levels to rise, resulting in lower IGF. During the period June 2015 to January 2016 the IGF flux was negative, which can be contributed to low water levels in the Rhine. While the Nederrijn showed some fluctuation, relatively to its respective average the lowest water levels were in the Waal. This caused the IGF flux to drop. October 2015 saw relatively high amounts of precipitation as compared to June to September, and due to this precipitation there was an increase in groundwater head in the catchment. As a result, the IGF flux dropped even more. Whether this means that the groundwater can flow from the Maurikse Wetering catchment to the Nederrijn and Waal, or that the incoming IGF from these sources decreases while at other locations the outgoing IGF increases cannot be determined from this data.

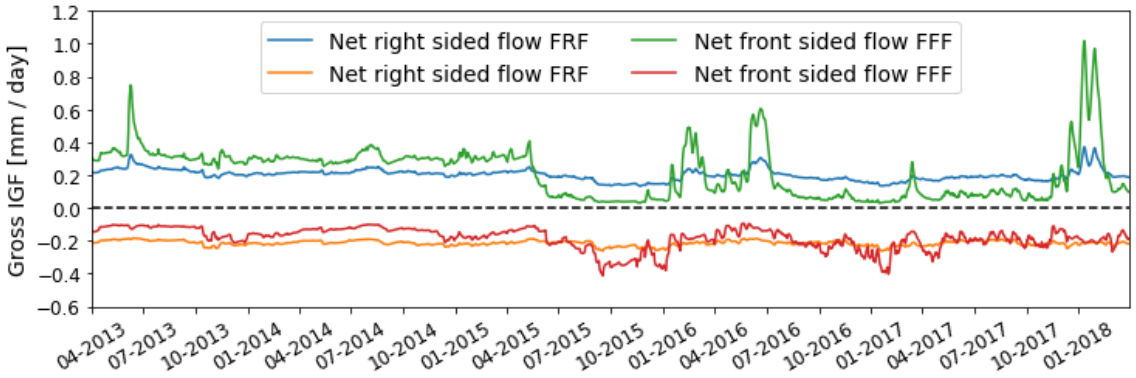


**Figure 4-9, gross incoming and outgoing lateral IGF fluxes. The right sided flow FRF flows in the left-right or east-west direction. The front sided flow FFF flows in the up-down or north-south direction.**

In Figure 4-9 it can be seen that the right sided IGF flux FRF, flow going left to right or vice versa, is relatively constant over the years. The front flux FFF is more variable. This is probably because most FFF enters via the north or south borders whereas the FRF enters on the eastern border and exits on the western border, as can be seen in section 4.3. As the Nederrijn is situated adjacent to the northern border, fluctuations in the Nederrijn level have a more direct effect on the incoming intercatchment groundwater flow. The longer the distances are that the groundwater has to travel the more the variations will dissipate as groundwater moves slowly compared to surface water, which could explain the more constant and less variable nature of the FRF. This also explains the more constant net FRF compared to the net FFF from Figure 4-6.

Looking at Figure 4-8, the water level in the Waal does not appear to have a direct influence on the IGF in the same sense as the water level in the Nederrijn does regarding (short-term) fluctuations. However, from this data, looking at Figure 4-8 and Figure 4-9, the influence of the Waal on the IGF through the interaction of the Waal and Nederrijn can be an explanation for the change in behaviour of the IGF. This can be seen in Figure 4-8, where in March of 2014 the Nederrijn levels and groundwater levels are roughly equal to those in September 2015. However, in September 2015 the Waal had a lower water level than in March 2014. As a result, the net IGF flux was between 40.000 to 60.000 $m^3$/day (or 0.5 to 0.7 mm/day) lower in September 2015 than in March 2014. This is summarised in Table 4-2

| **Month** | **Average Nederrijn level [m + NAP]** | **Average Waal level [m + NAP]** | **Average net IGF [mm / d]** |
|---|---|---|---|
| *March 2014* | 3.1 | 4.0 | + 0.25 |
| *September 2015* | 2.9 | 2.9 | - 0.53 |

**Table 4-2, the possible influence of the Waal on the net IGF shows when comparing two months with similar Nederrijn levels.**

A trend can be seen in Figure 4-9, where around June 2015 there is a significant change in incoming FFF. This trend can also be seen in the net IGF flux in Figure 4-8, but is clearer in Figure 4-9. Around June 2015 the incoming FFF switches from approximately 0.3 mm/day to approximately 0.04 mm/day. This cannot be contributed to the water level in the Nederrijn, as this is constant outside of peak events at 3 m + NAP at Beneden Amerongen throughout this timeseries. The Waal at Tiel however shows an average drop outside peak events from approximately 4 – 4.5 m + NAP to 3.5 m + NAP. As can be seen in Appendix A, all stations in the Nederrijn as well as the Amsterdam Rijnkanaal show no variation during this period. Only the stations in the Waal show this slight trend. As the average groundwater head in the Maurikse Wetering catchment outside peak events drops from 3.3 m + NAP to 3 m + NAP as well, this lowering of the Waal level is likely to be the explanation for the decrease in FFF flux. Otherwise the increase in head difference and resulting pressure difference due to the decreasing groundwater head in the Maurikse Wetering catchment would cause the FFF flux from the Nederrijn to the catchment to increase.

It is unknown if the low water level in the Waal is due to continuous low discharge because of lower-than-average amounts of precipitation in the Rhine catchment, or if the lower average water level in the Waal is due to human intervention. It does not appear that significant dredging has occurred in the Waal or IJssel in 2015. As part of the 'Room for the River' project, groynes in the Waal were lowered around this period. However, this should only affect high water levels (Rijkswaterstaat, 2015). Other measures taken in the Room for the River project appear to only have an effect on high water levels or have local effects that should not result in a decreased discharge around Tiel.

Another reason for this change in incoming IGF can be due to other influences. For this, the origin of the IGF needs to be studied. This is done by looking at the direction of the groundwater flow, the results of which are shown in section 4.3.

## 4.3 Groundwater flow direction

The monthly average groundwater flow direction is plotted and analysed. There are 4 main areas of interest, which are shown in Figure 4-10. The names given to these areas are shown in Table 4-3.

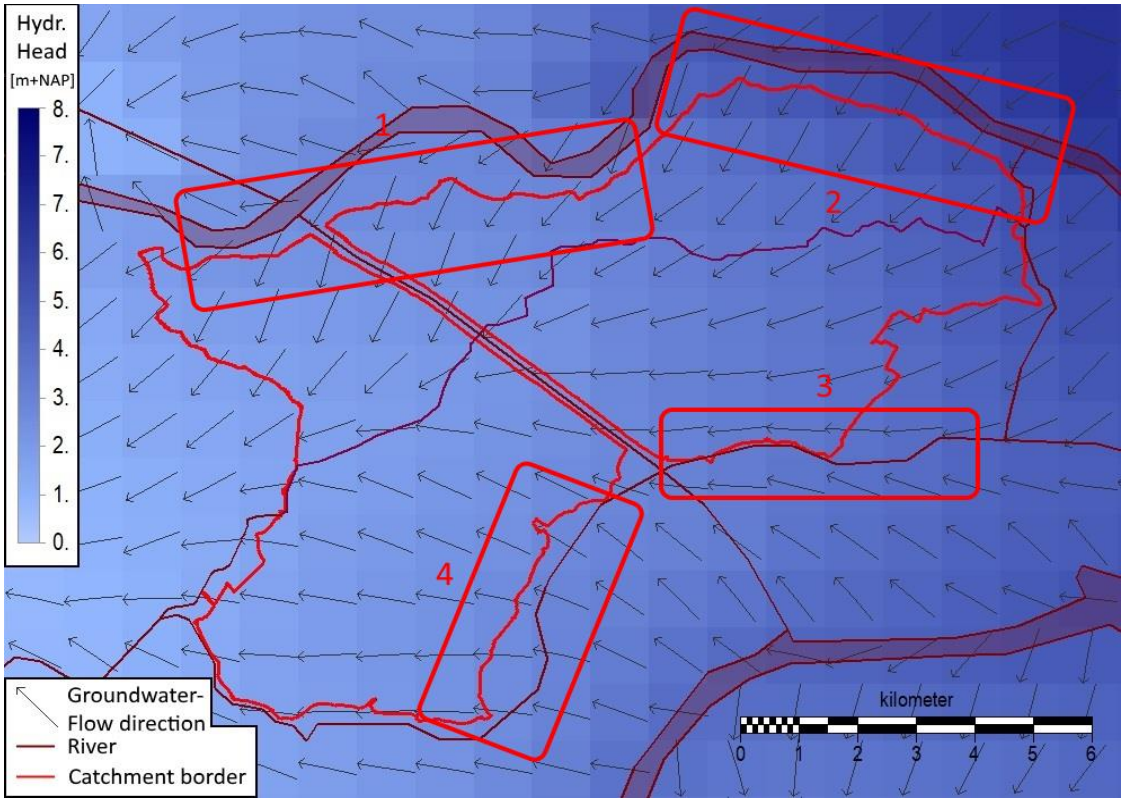


**Figure 4-10, areas of interest in groundwater flow direction plot. The legend shows the hydraulic head in the main aquifer (layer 4) in [m + NAP]. The combination of groundwater level and flow direction will help to determine the origins of the IGF.**

| Area | Description |
|---|---|
| *1* | Lower Amerongen |
| *2* | Upper Amerongen |
| *3* | Upper Linge |
| *4* | Lower Linge |

**Table 4-3, names of areas highlighted in Figure 4-10.**

Between Lower and Upper Amerongen there are differences in groundwater head due to the lock at Amerongen. Upstream of the Amerongen lock, in addition to groundwater from the Utrechtse heuvelrug moraine draining to the Nederrijn and groundwater infiltrating from the Nederrijn and flowing towards the Maurikse Wetering catchment, groundwater from the Utrechtse heuvelrug moraine bypasses the Nederrijn and flows towards the Maurikse Wetering. At the Lower Linge the groundwater coming from the Waal bypasses the Linge river and enters the Maurikse Wetering catchment. At the Upper Linge the groundwater flow direction on the border of the Maurikse Wetering catchment alters between towards the Linge and towards the Maurikse Wetering catchment. When the flow is directed towards the Linge, no groundwater from the Waal enters the Maurikse Wetering catchment here. If directed towards the catchment, groundwater originating in the Waal, in addition to groundwater originating in the Linge, flows to the catchment.

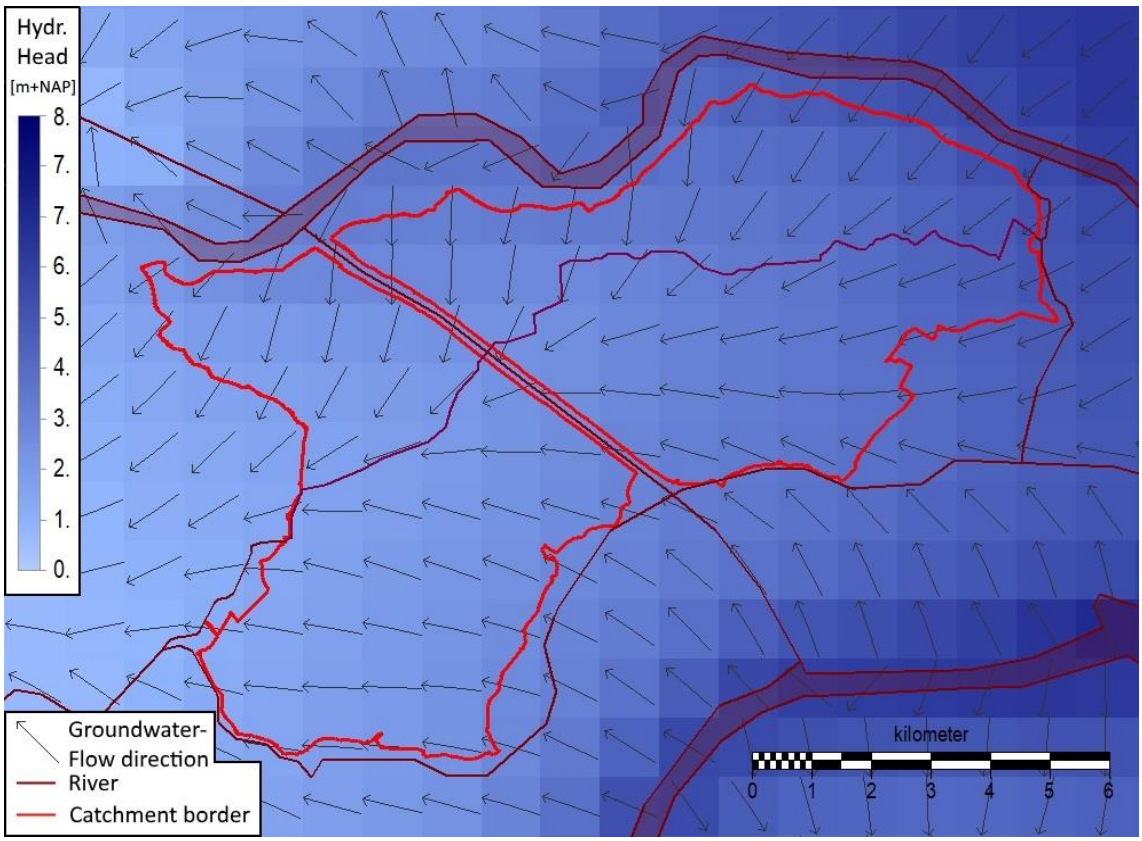


**Figure 4-11, flow direction and spatial groundwater head June 2013**

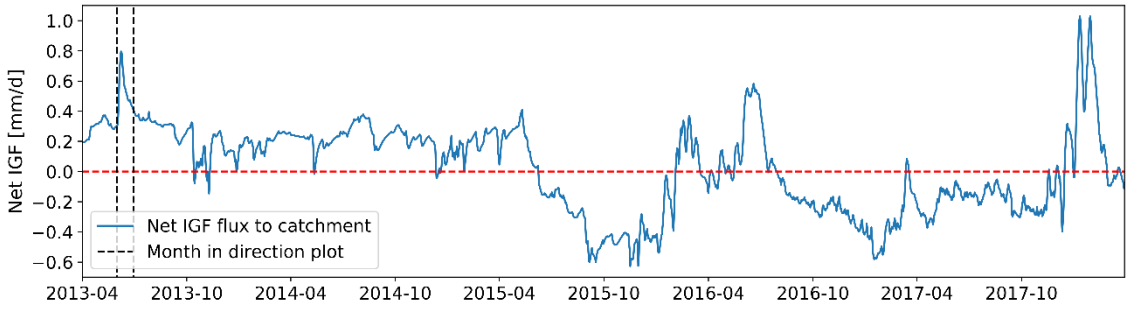


**Figure 4-12, net IGF flux with June 2013 highlighted**

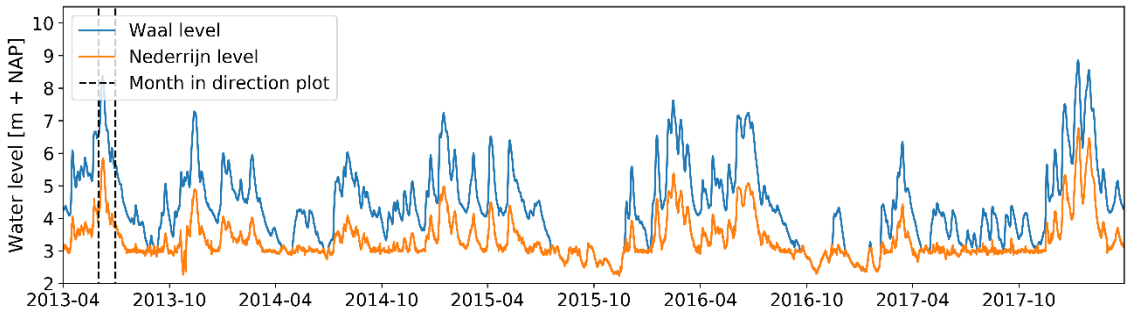


**Figure 4-13, Nederrijn level and Waal level with June 2013 highlighted**

In June 2013, seen in Figure 4-11, Figure 4-12 and Figure 4-13, high water levels in the Waal and Nederrijn see a significant IGF flux all along the catchment borders except the downstream western border. High groundwater levels in the Utrechtse Heuvelrug moraine cause groundwater to bypass the Nederrijn at Upper Amerongen towards the Maurikse Wetering, in addition to groundwater originating in the Nederrijn,

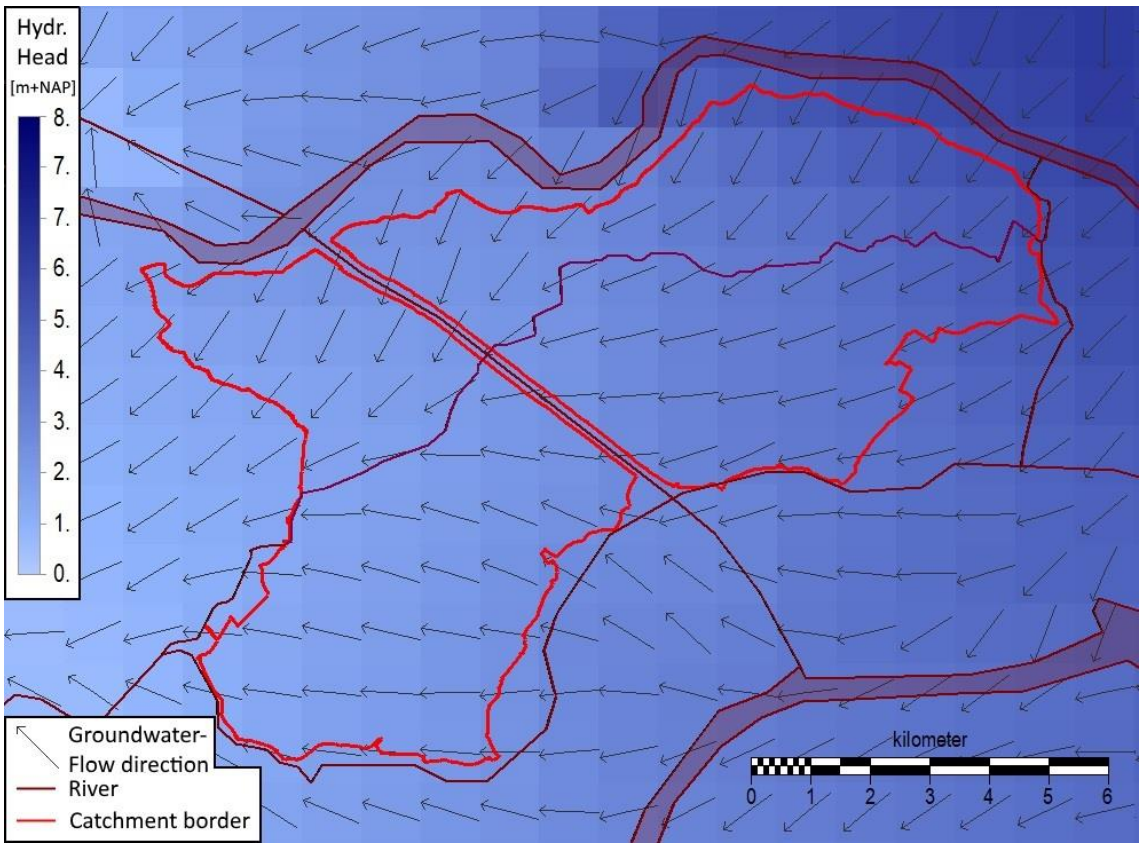


**Figure 4-14, flow direction and spatial groundwater head September 2013**

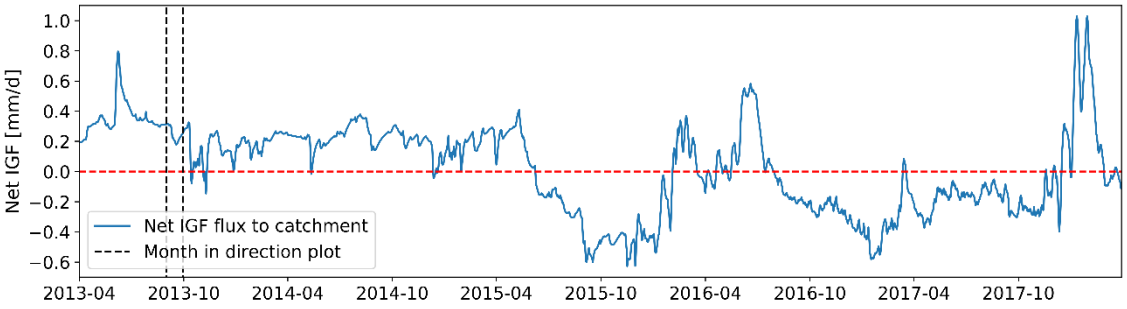


**Figure 4-15, net IGF flux with September 2013 highlighted**

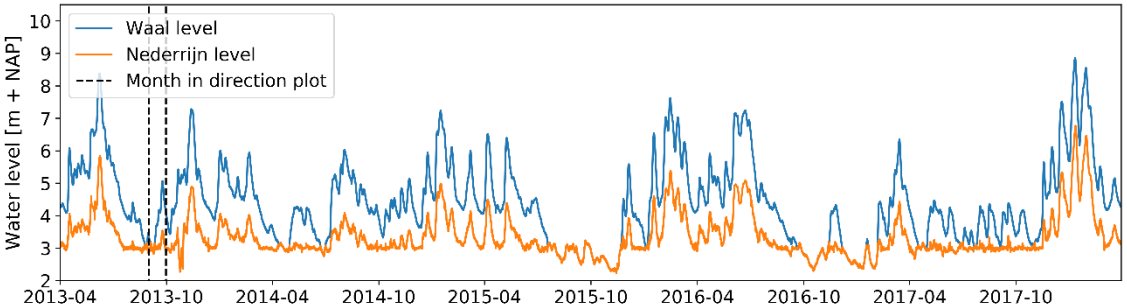


**Figure 4-16, Nederrijn level and Waal level with September 2013 highlighted**

The situation in September 2013, seen in Figure 4-14, Figure 4-15 and Figure 4-16, is representative for the entire period before June 2015. Surface water from the Nederrijn infiltrates to the Maurikse Wetering catchment, groundwater originating in the Waal bypasses the Lower Linge and groundwater from the Utrechtse Heuvelrug moraine bypasses the Upper Amerongen section of the

Nederrijn. Groundwater exits mainly on the western side of the catchment and the groundwater roughly runs parallel to the Linge river in the Upper Linge area.

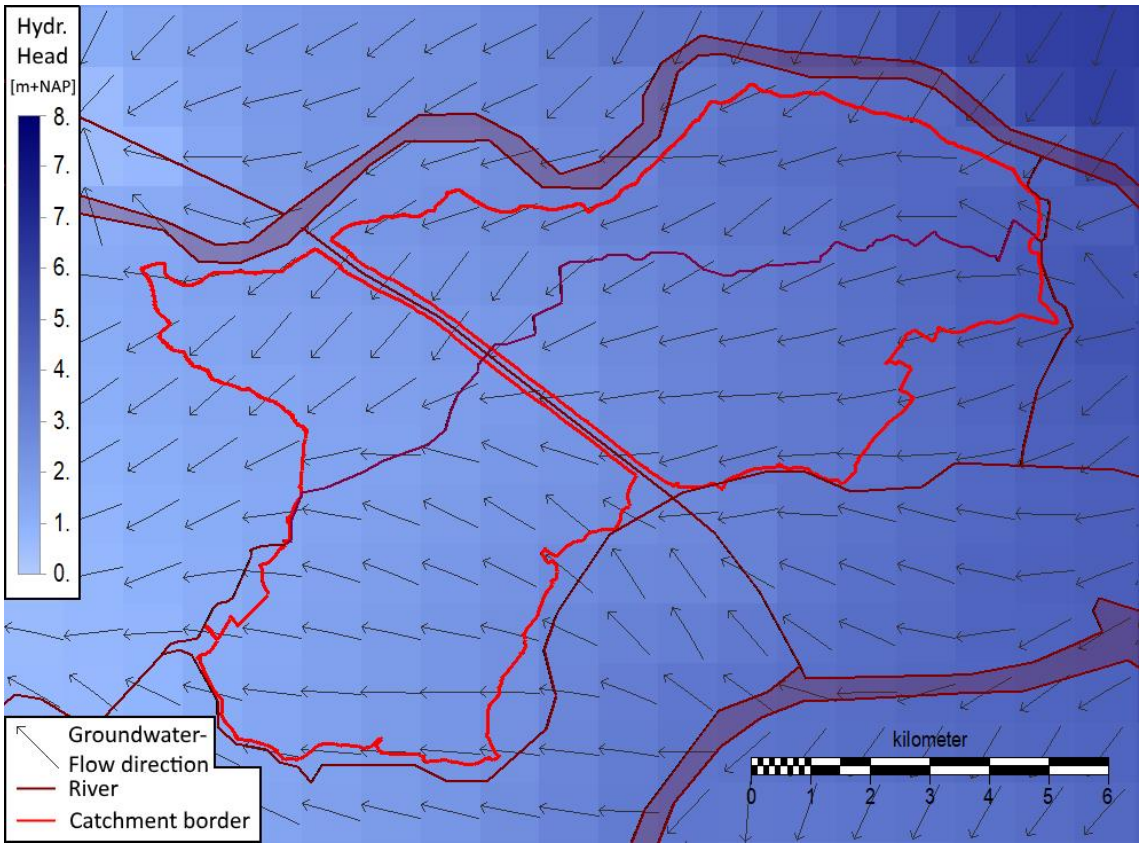


**Figure 4-17, flow direction and spatial groundwater head June 2015**

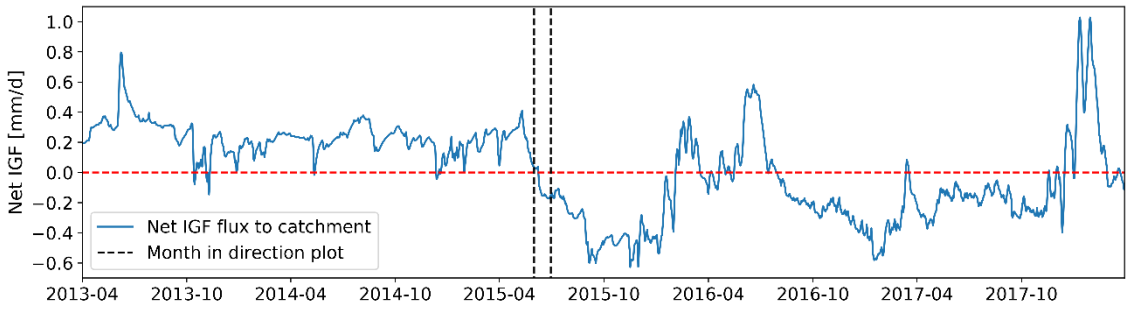


**Figure 4-18, net IGF flux with June 2015 highlighted**

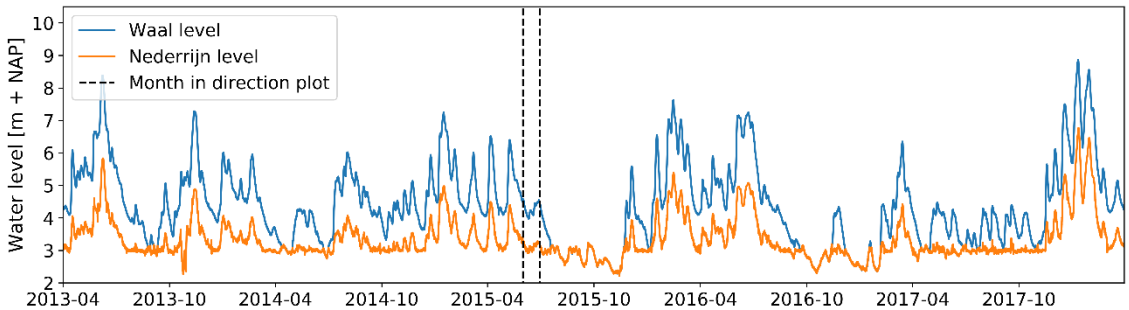


**Figure 4-19, Nederrijn level and Waal level with June 2015 highlighted**

Likely due to decreasing Waal levels (Figure 4-19) and the interaction between the Nederrijn and Waal, as well as decreasing groundwater levels in the Utrechtse Heuvelrug, the incoming IGF flux decreases (Figure 4-18). In Figure 4-17 it can be seen that groundwater from the upstream

catchment to the Maurikse Wetering flows to the Nederrijn to replenish it. Due to lower groundwater levels in the Utrechtse heuvelrug, less groundwater from the Utrechtse heuvelrug flows to the Maurikse Wetering catchment.

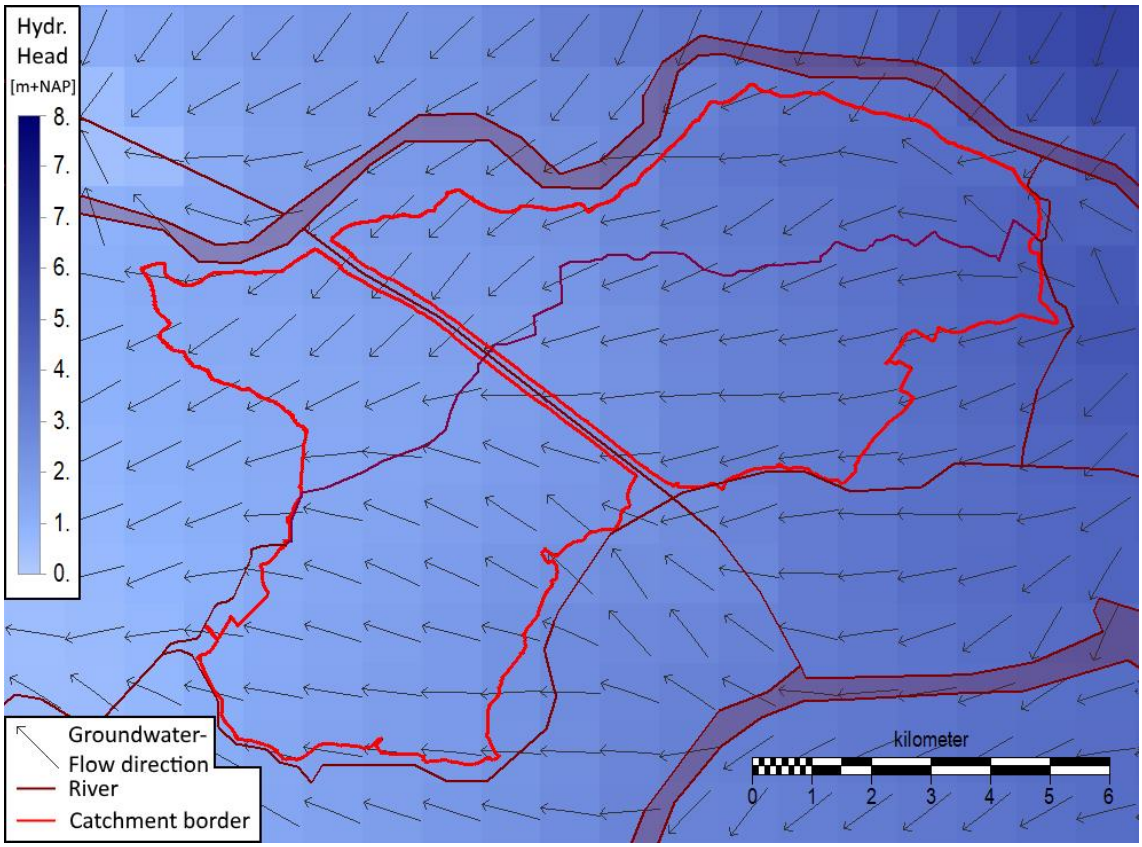


**Figure 4-20, flow direction and spatial groundwater head August 2017**

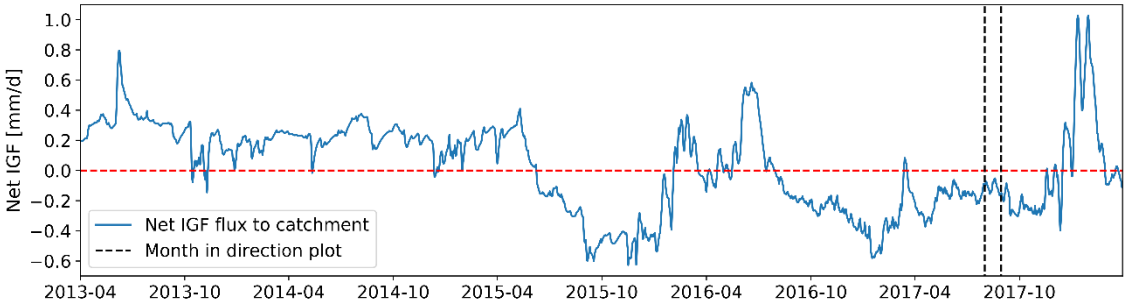


**Figure 4-21, net IGF flux with August 2017 highlighted**

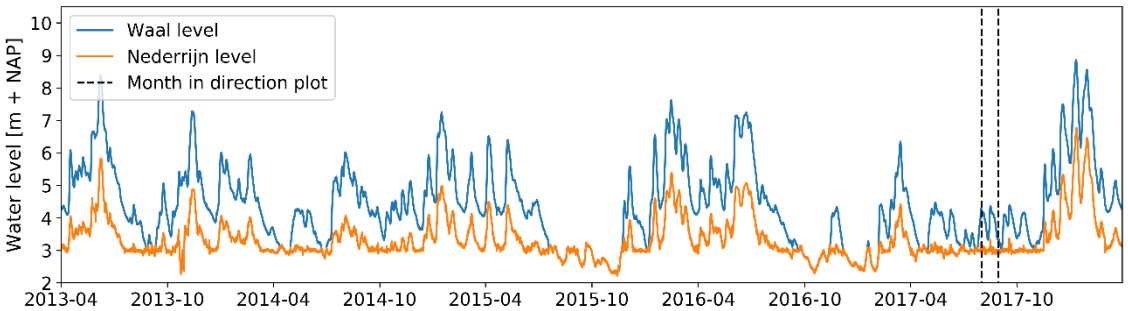


**Figure 4-22, Nederrijn level and Waal level with August 2017 highlighted**

In August 2017 (Figure 4-20, Figure 4-21 and Figure 4-22). less groundwater infiltrates from the Upper Amerongen area due to low Nederrijn levels and low groundwater levels in the Utrechtse

Heuvelrug moraine compared to Figure 4-11 and Figure 4-14. At the Amerongen lock, between areas 1 and 2 in Figure 4-10, groundwater from the Maurikse Wetering flows to the Nederrijn at Lower Amerongen.

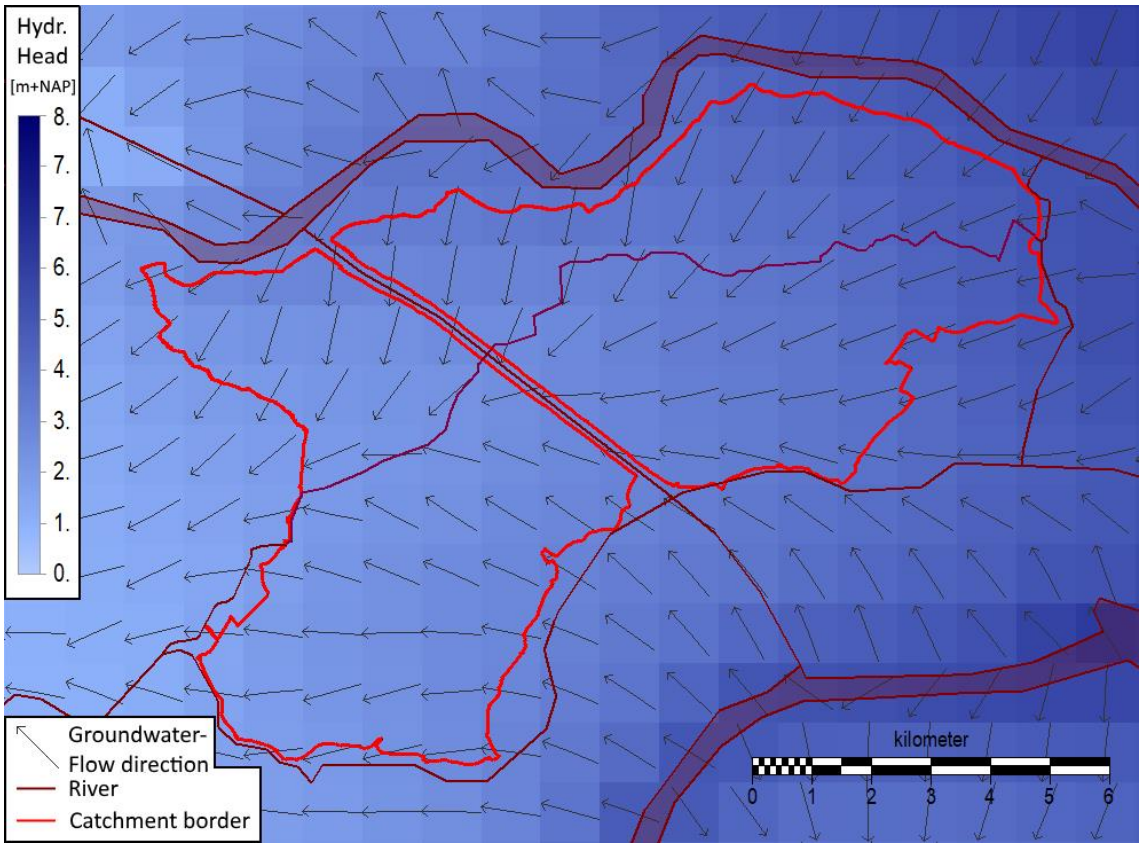


**Figure 4-23, flow direction and spatial groundwater head December 2017**

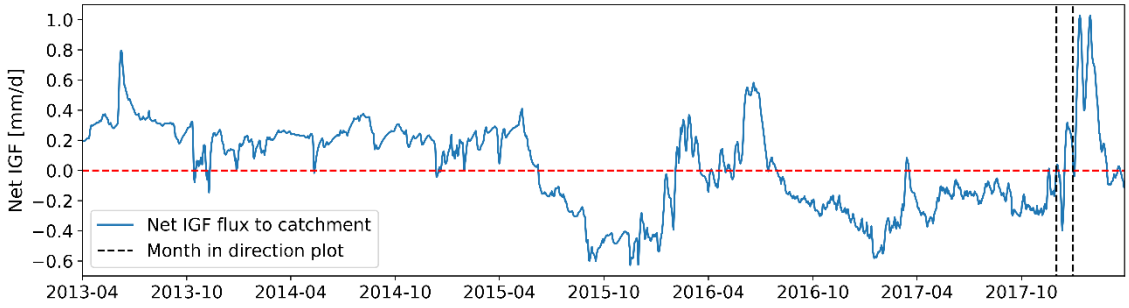


**Figure 4-24, net IGF flux with December 2017 highlighted. The dotted red line marks the zero line**

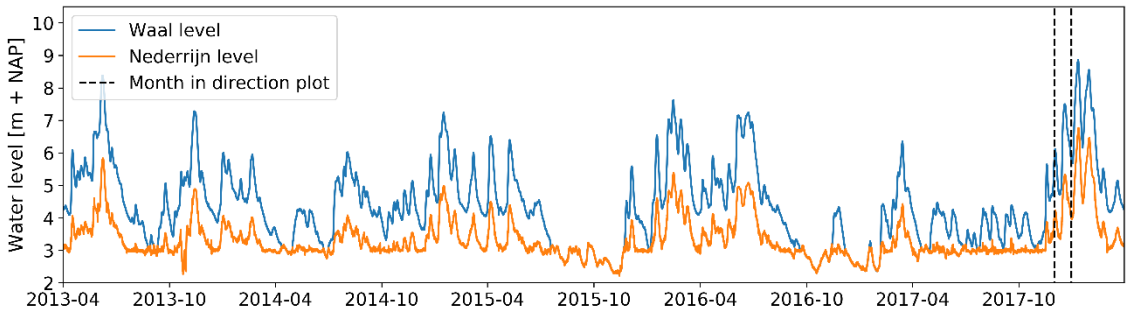


**Figure 4-25, Nederrijn level and Waal level with December 2017 highlighted**

In December 2017 (Figure 4-23, Figure 4-24 and Figure 4-25), high water levels in the Nederrijn and Waal cause an increase in groundwater level This increases the IGF flux to the Maurikse Wetering

catchment. At the Upper Linge, the IGF flux is directed towards the Maurikse Wetering increases due to the high water level in the Waal.

A change in groundwater flow direction indicates water infiltrating or draining, often to the surface water. This can be seen in Figure 4-11, Figure 4-14, Figure 4-17, Figure 4-20 and Figure 4-23, for instance around the Nederrijn and Waal where groundwater flows away from the course of the rivers. Looking at Figure 4-11, Figure 4-14, Figure 4-17, Figure 4-20 and Figure 4-23, it appears that the groundwater in layer 4 is not significantly influenced by the Amsterdam Rijnkanaal. This indicates that no significant seepage occurs from the Amsterdam Rijnkanaal, as this kind of seepage would cause a change in direction of the groundwater flow in the vicinity of the Amsterdam Rijnkanaal on one or both sides of the canal. Here there appear to be no local disturbances and the direction of the groundwater flow appears relatively unphased while running beneath the Amsterdam Rijnkanaal. The hydraulic head of layers 2-11 in Figure 4-3 does not show a peak near the Amsterdam Rijnkanaal, indicating that the Amsterdam Rijnkanaal has little influence on the groundwater in the Maurikse Wetering catchment. This indicates that the Amsterdam Rijnkanaal is not significant for the IGF to the Maurikse Wetering catchment. In Figure 4-26, the groundwater flow around the Amsterdam Rijnkanaal is looked at in more detail to see if any changes occur.

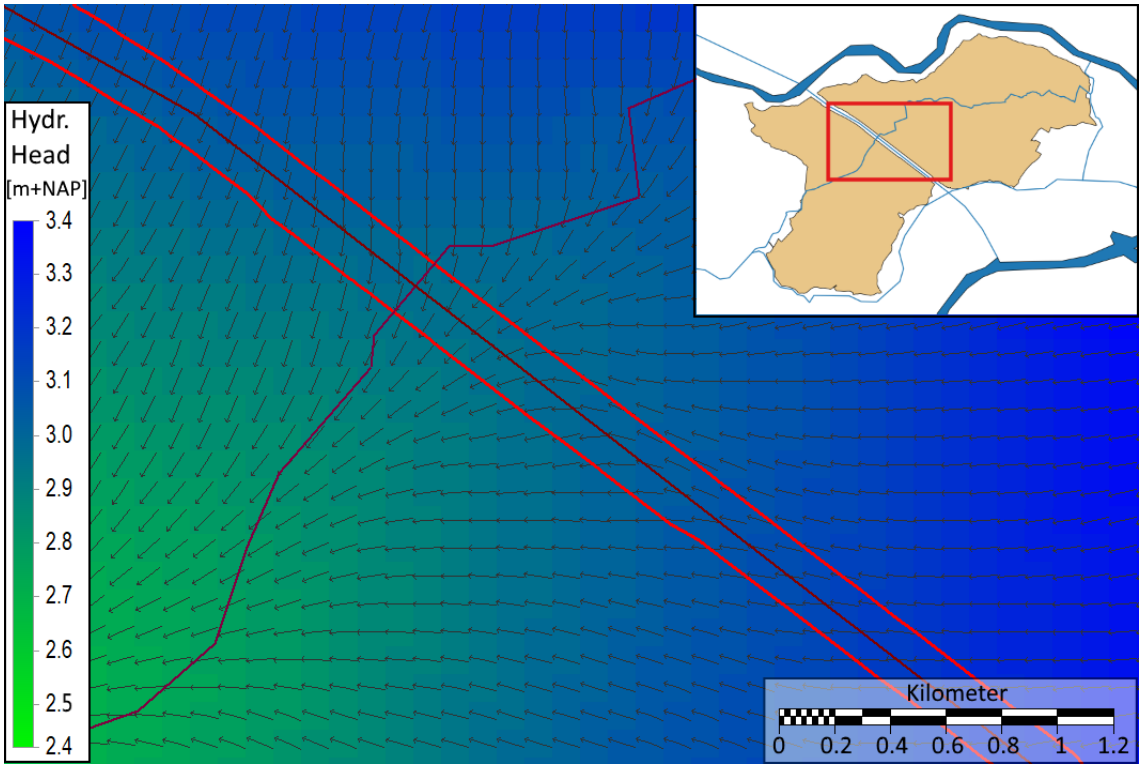


**Figure 4-26, groundwater flow direction showing the influence of the ARK from 1-1-2014 to 28-2-2014, 100 x 100 m resolution. The location of the zoomed area is shown in the top right. The red lines indicate the catchment borders, in between which the Amsterdam Rijnkanaal flows. Perpendicular to the Amsterdam Rijnkanaal runs the Maurikse Wetering. The arrows indicate the groundwater flow direction. Any changes in groundwater flow direction between the upstream and downstream areas indicate groundwater infiltrating from or draining to the Amsterdam Rijnkanaal.**

From the increased detail in Figure 4-26 we can see that, as modelled by MORIA, the Amsterdam Rijnkanaal appears to have little influence on the groundwater flow in the region, meaning that seepage from the Amsterdam Rijnkanaal is likely negligible.

## 4.4 Spatial variation IGF

To see if the water balance of subcatchments are more affected by the effects of IGF on their local water balance, the spatial variation of the IGF is modelled.

### 4.4.1 Spatial variation vertical IGF flux

Figure 4-3 shows a drop in hydraulic head in the second aquifer (layers 12-19) for a distance up to 4000 meters from point A in the cross-section, as opposed to the course of the hydraulic head from 4000 to 12000 meters from point A in the cross-section in Figure 4-3. A local drop in hydraulic head can also be seen in Figure 4-28, which shows the hydraulic head in the second aquifer, when compared to Figure 4-27, which shows the hydraulic head in the upper aquifer. These drops can be attributed to the groundwater extraction by Vitens in this location the second aquifer (Hobbelt et al.,2018). Looking at the difference in hydraulic head between the upper and second aquifer in Figure 4-3, it can be concluded that roughly the eastern and northern parts of the Maurikse Wetering catchment sees more infiltration to the upper aquifer while the western and southern parts see more drainage to the second aquifer, as the head difference and thus pressure difference between the upper and lower aquifer changes from positive to negative at a distance of roughly 4000 meters from the start of the cross-section in Figure 4-3 . This drainage effect will increase closer to the extraction well.

From Figure 4-7, Figure 4-27 and Figure 4-28 it can also be concluded that the second aquifer is most likely influenced further upstream by the same interactions. This conclusion is drawn on the basis that the courses of the vertical and lateral fluxes are the same. That these influences occur upstream (to the east) is because it is less likely that downstream influences propagate upstream in this aquifer.

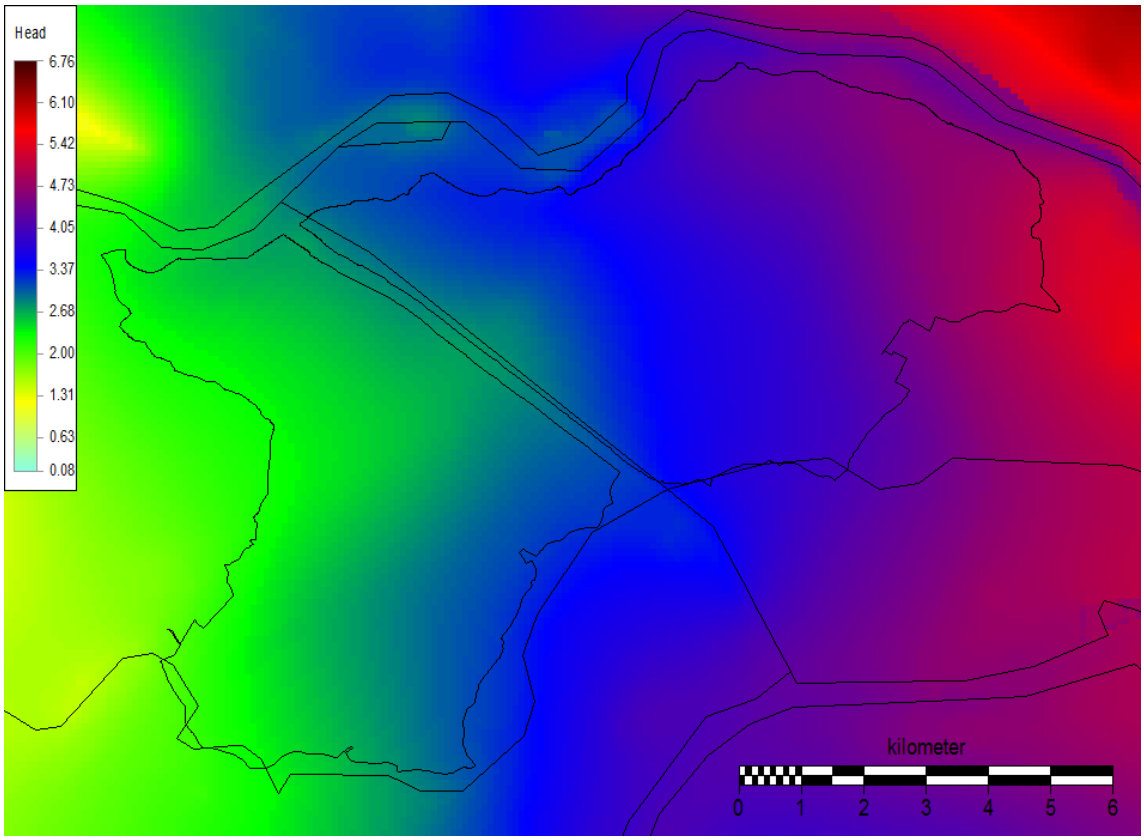


**Figure 4-27, hydraulic head in the upper aquifer on 1-4-2016**

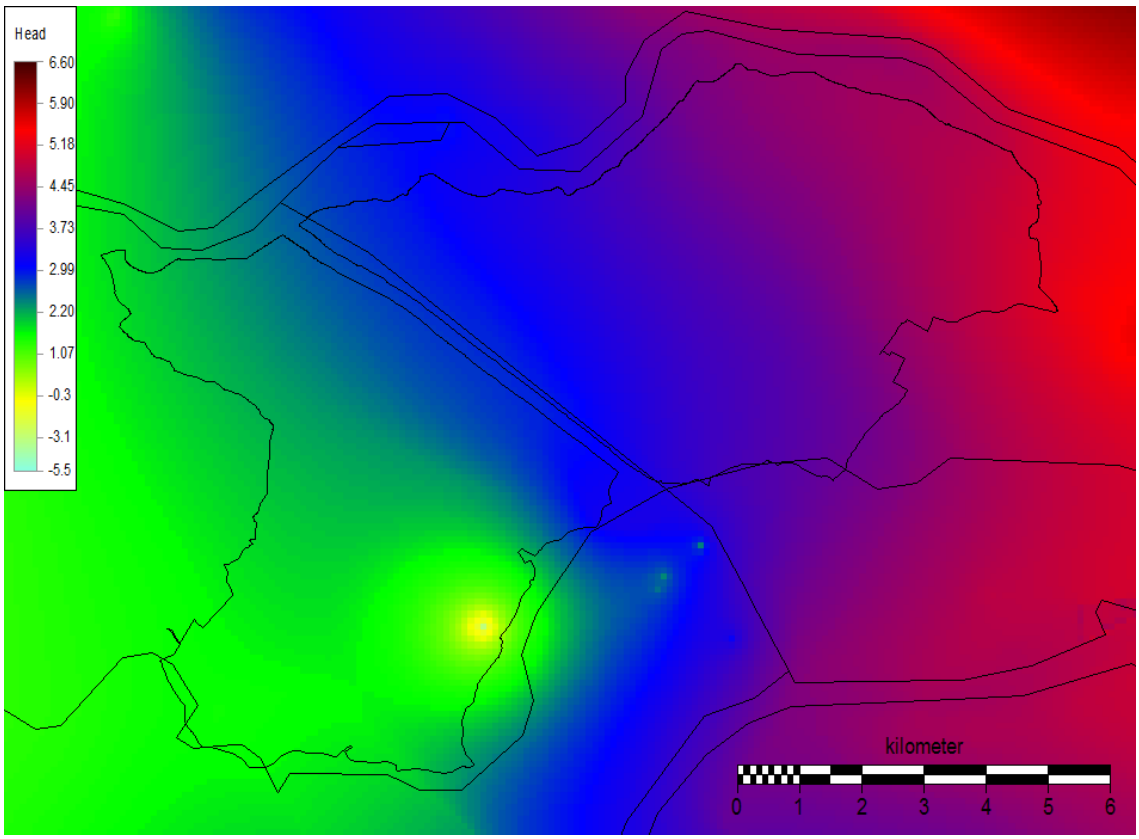


**Figure 4-28, hydraulic head in the second aquifer on 1-4-2016. A clear drop in hydraulic head can be seen in the southern part of the catchment, indicating groundwater extraction. This is the groundwater extraction made by the drinking water company Vitens (Hobbelt et al.,2018).**

### 4.4.2 Spatial variation net IGF flux

The results for June and September 2013 are shown in Figure 4-29 and Figure 4-30 respectively. The results for August and December 2017 are shown in Figure 4-31 and Figure 4-32 respectively. As seen from the legends, the blue cells represent a net surplus of IGF. The red cells represent a net loss. In the case of a positive net IGF flux, the net gain can increase the groundwater level, evaporate in that cell or go to the surface water. A net IGF gain does not mean that the groundwater level must rise, the groundwater level can also decrease or remain stagnant depending on the processes within the cell.

On average the north-eastern half, upstream of the Amsterdam Rijnkanaal, accumulates more water and thus has a net IGF gain while the south-western half, downstream of the Amsterdam Rijnkanaal mainly has a net IGF loss. The southern part is likely influenced by the groundwater withdrawals by Vitens in the second aquifer, causing a drastic drop in water level in that aquifer and thus an increased flux from the upper aquifer to the second aquifer. Even if this flux was not included in the IGF, the vertical flux would cause the groundwater level to drop, resulting in an increase in lateral IGF. This would appear to increase the groundwater level, meaning a larger flux to the surface water and a positive flux to the affected cells. This would be misleading because of the groundwater withdrawal in the second aquifer.

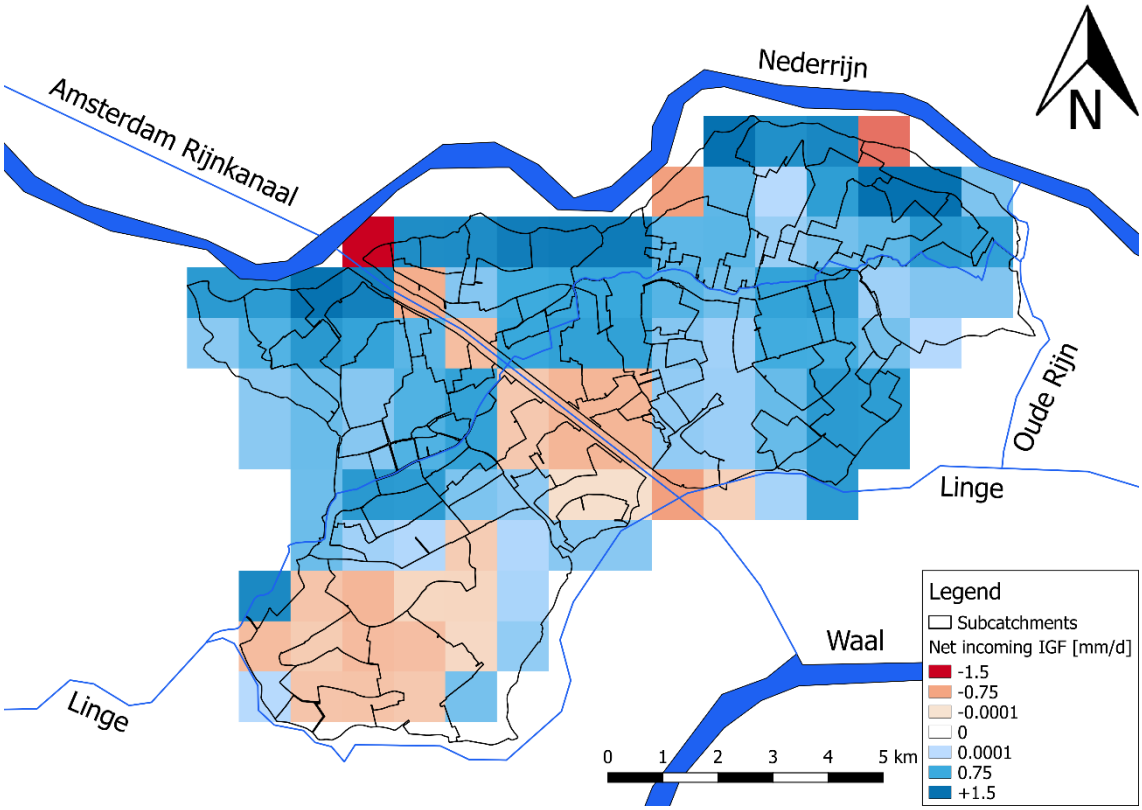


**Figure 4-29, net IGF per square km in June 2013**

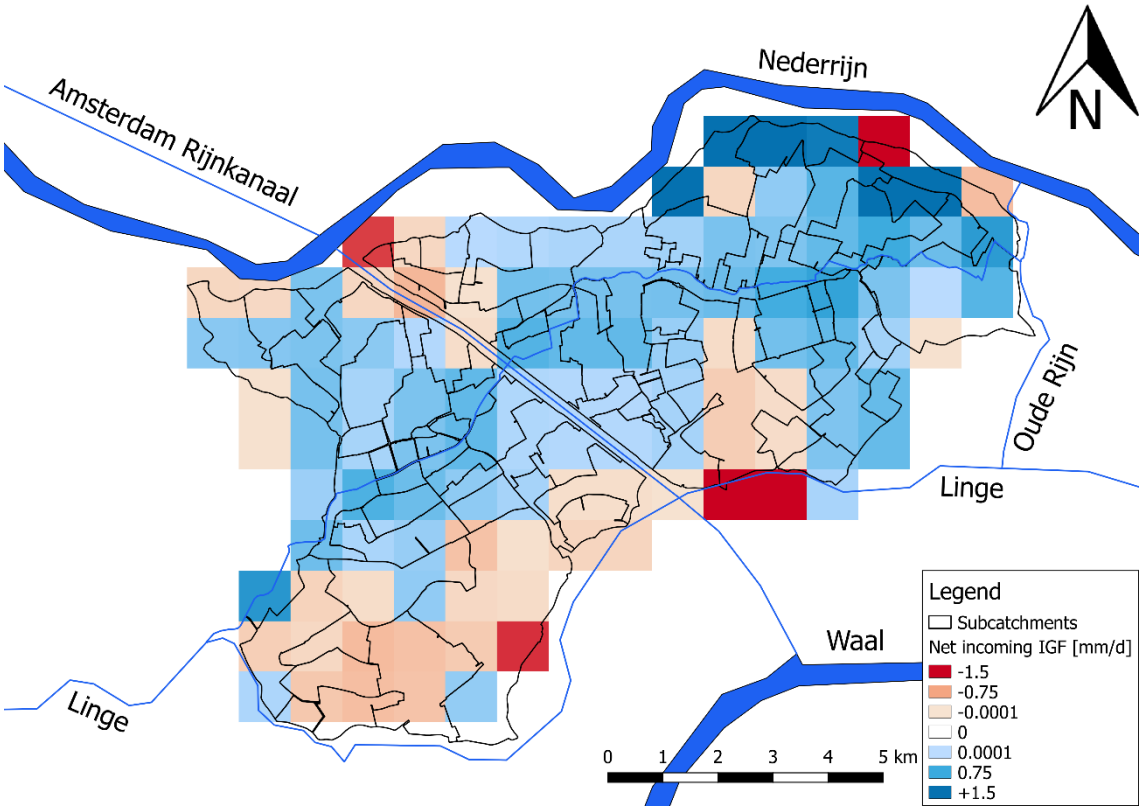


**Figure 4-30, net IGF per square km in September 2013**

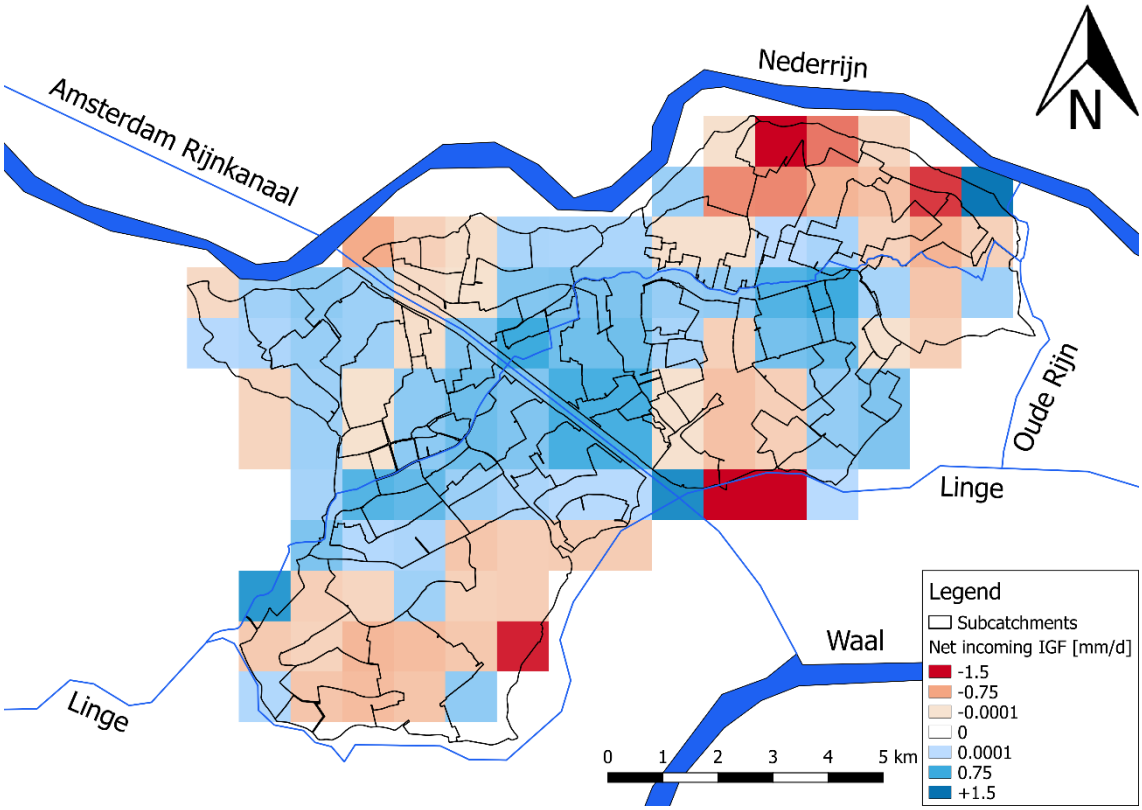


**Figure 4-31, net IGF per square km in August 2017**

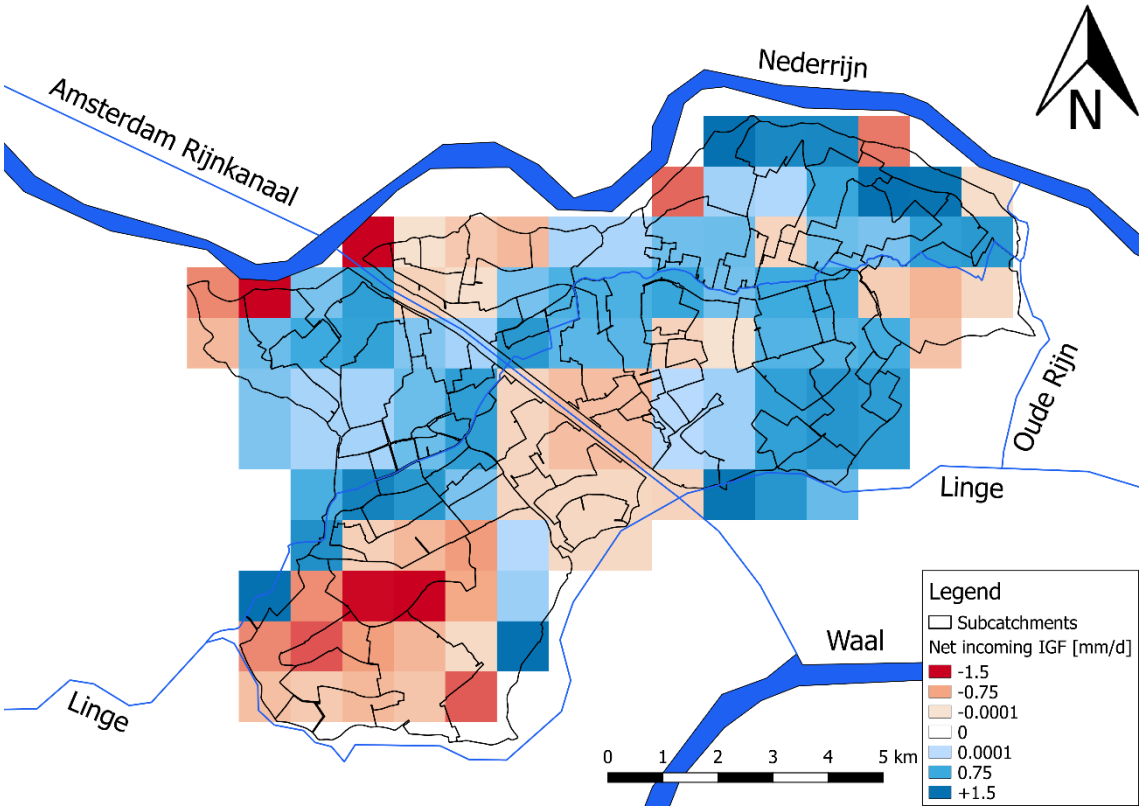


**Figure 4-32, net IGF per square km in December 2017**

June 2013 saw a high net IGF as seen in Figure 4-29. The cells around the Amsterdam Rijnkanaal, which is included in the analyzed area, often show a net IGF loss. This is most visible in Figure 4-29. As the Amsterdam Rijnkanaal is part of the surface water within these cells, a net IGF loss in these cells suggests that there is seepage from the Amsterdam Rijnkanaal to the Maurikse Wetering

catchment as infiltrated (internal) surface water from the Amsterdam Rijnkanaal flows through the soil to an adjacent (external) cell. This effect does not appear to be very pronounced, as this distinction cannot be made in Figure 4-31. If there is seepage from the Amsterdam Rijnkanaal, this likely has mainly local effects, occurring within the 1 x 1 km cells from the analysis.

Most of the incoming net IGF is along the border with the Nederrijn. Towards the center of the catchment the differences are less extreme. This does not mean that there are no gross IGF fluxes, but that the differences between incoming and net IGF are less.

September 2013 has a more even distribution of net gains and losses. It is suspected that at least some of the extremes on the borders are influenced by the Nederrijn or the Linge partially crossing that cell, disturbing the data. Especially the cell in the far north-east with a high loss due to IGF seems uncharacteristic considering the adjacent cells with a high net IGF gain.

August 2017 sees a total net IGF loss, as opposed to the year 2013. This is visible as more red cells are shown. The center of the catchment appears to have a net gain, while the borders have more net loss. This might be because in earlier (wetter) months the borders had a net gain, increasing the groundwater level which now drains to the adjacent cells. This also suggests that the center saw more water going to the surface water, decreasing the groundwater level thus requiring replenishment from adjacent cells.

December 2017 is not the height of the peak in the winter of 2017. Figure 4-32 does show how an increase in IGF progresses, with most of the IGF flux entering upstream of the ARK along the borders of the catchment. Downstream the IGF still often results in a net loss.

From all figures we can see that the IGF is more variable closer to the catchment borders, especially the catchment border with the Nederrijn. This means that for the subcatchments in these areas, Over the location with groundwater withdrawals in the second aquifer there is a net loss due to IGF.

## 4.5 Chapter summary

In this chapter, the IGF is modelled using the detailed groundwater model MORIA. The modelled MORIA data is analysed using the program iMOD. The IGF is quantified, resulting in both the gross and net IGF fluxes from or to the catchment. There are two distinct periods in IGF quantity, a more stable net gain before June 2015 and a variable period after June 2015. From the available data, this appears to be caused by the interaction between the Nederrijn and Waal, as the mean Waal level drops during this period.

To get a deeper understanding of the workings and origins of the IGF in the Maurikse Wetering catchment, the direction of the groundwater flow in the region is plotted. This shows that the majority of the groundwater exits the catchment on the western border. The direction groundwater flow is influenced by the water level in the Nederrijn and Waal rivers. It appears that part of the groundwater originating in the Utrechtse Heuvelrug moraine passes underneath the Nederrijn into the Maurikse Wetering catchment. As the groundwater level of the Utrechtse Heuvelrug was higher before June 2015, this can be the cause of the change in IGF behaviour. As the Utrechtse Heuvelrug is outside the study area for this thesis, this cannot be analysed further.

According to MORIA, the Amsterdam Rijnkanaal does not appear to significantly influence the direction of the groundwater flow. As it is assumed that a significant seepage flux would be noticeable in the groundwater flow direction, it is assumed that the Amsterdam Rijnkanaal does not play a significant role in the water balance of the Maurikse Wetering.

# 5 IGF RELATION

The flux from intercatchment groundwater flow (IGF) is among the hardest fluxes to quantify in a hydrological model as it cannot be measured directly and requires a program like MORIA to estimate. This has several practical drawbacks: Running MORIA is time consuming and requires additional expertise. But most importantly, without knowing the causes of IGF it is very difficult to use in predictive conceptual hydrological modelling. It would therefore be preferable if a relation can be found between the IGF flux and a different variable, preferably a surface variable that is easy to monitor like the water level. Showing that the IGF can be related to variables that can be measured directly will be useful in research into the IGF in catchments without a detailed groundwater model like MORIA, as such a model requires plentiful data concerning the subsurface.

It quickly became clear that in the data there are two distinct periods, which correspond with the shift in incoming IGF flux as shown by the vertical dotted line in Figure 5-1. These periods are April 2013 to June 2015 and July 2015 to March 2018. It was attempted to find a relation between several input variables and the IGF flux. To see if a relation is present, the data is plotted with the variable data on the x-axis and the modelled IGF data from MORIA on the y-axis. A perfect relation would show for instance a linear relation without any deviation. This way, every value for that variable would correspond to a specific IGF value. However, for a lumped model this would be unrealistic.

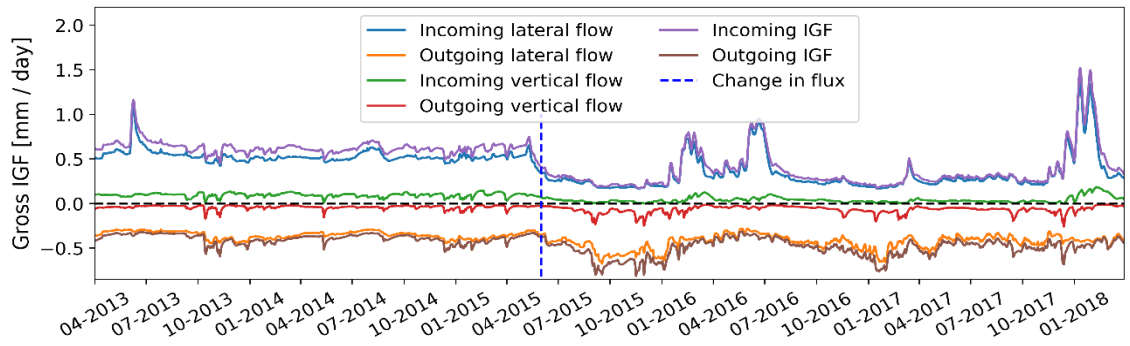


**Figure 5-1, gross incoming/outgoing IGF fluxes to the Maurikse Wetering catchment, with the change in behaviour marked by a blue dotted line. Before this, the IGF is rather constant and with a net gain. Afterwards, the IGF is more variable and often sees a net loss.**

The IGF as modelled by MORIA, to which the relations from the SLR and MLR analyses are compared to in this chapter are compared to, is plotted in Figure 5-2.

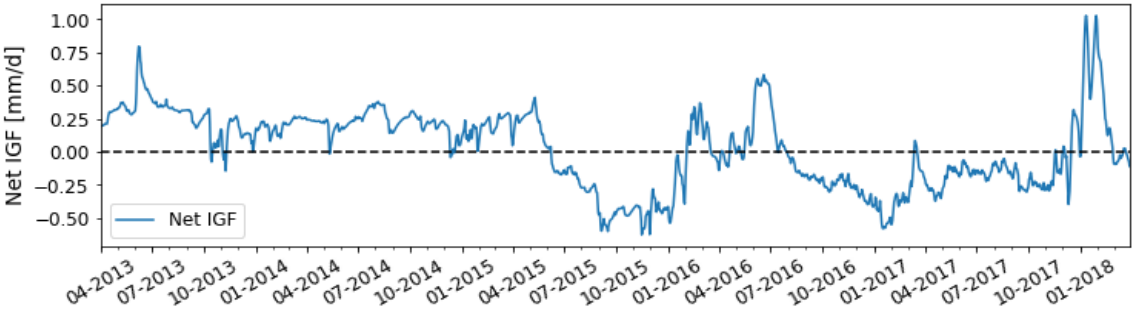


**Figure 5-2, net IGF to the Maurikse Wetering catchment as modelled by MORIA**

## 5.1 Relation between water levels

The water levels in the Nederrijn and Waal are plotted against each other and the IGF, the average groundwater level and the storage deficit to see how these variables relate to each other. The storage deficit is chosen to represent the soil moisture in the unsaturated zone, to see if this influences the IGF. Before analysing the relation between variables using simple- and multiple linear regression analyses, the water level in the Nederrijn and Waal is plotted against each other, the net IGF, the groundwater level and the saturation of the unsaturated zone (top soil layer). This is done to see if the relations between these variables are linear, and if notable conclusions can be drawn from a visual inspection before turning to SLR and MLR analyses.

In Figure 5-3 the groundwater level is given in mm below ground level. A high value therefore means a low groundwater table. From Figure 5-3 it can be seen that the groundwater level increases as the Waal and Nederrijn levels increase. However, logically this would be more of a correlation rather than a direct effect. It follows that if there is a lot of precipitation in the area for a longer period, the groundwater levels rise. At the same time, if the entire Rhine basin experiences a period of high precipitation, as is often the case the Rhine level rises.

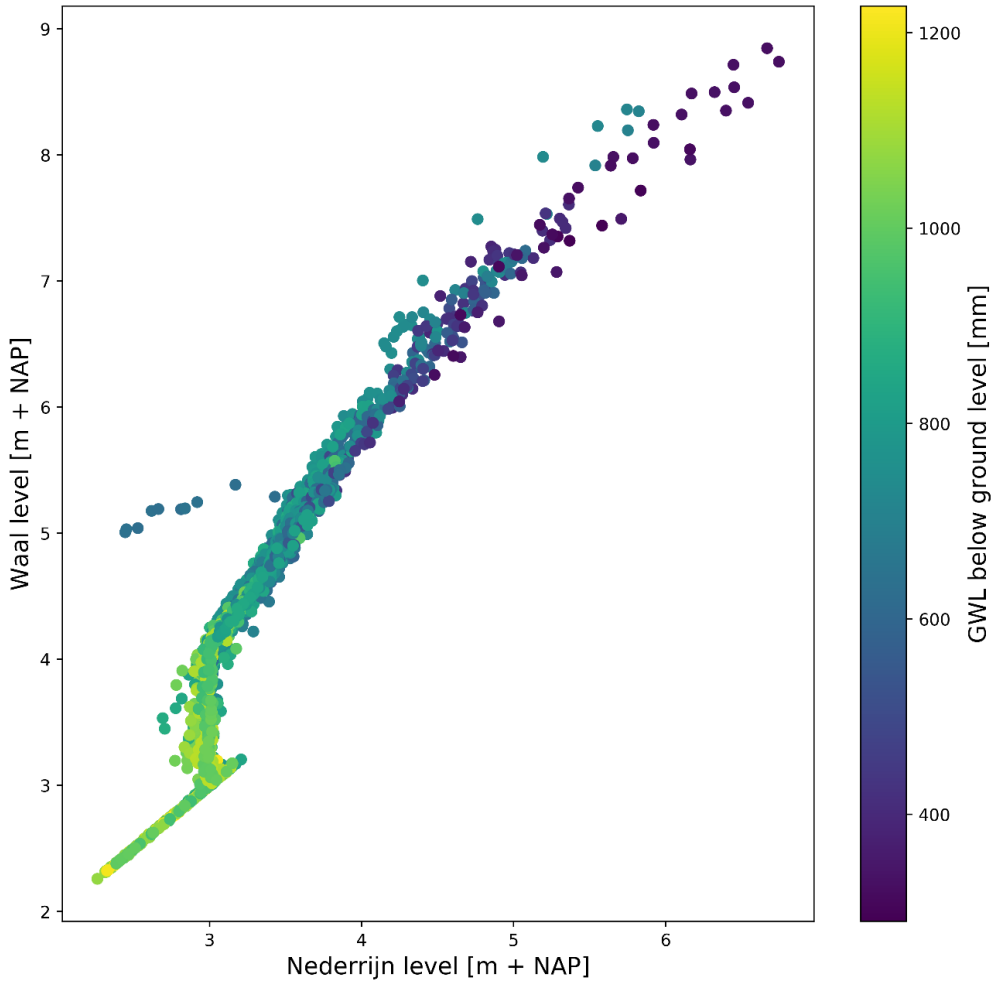


**Figure 5-3, Nederrijn level plotted against Waal level and groundwater level GWL**

From Figure 5-3 it shows that the Waal and Nederrijn have a discontinuous relation, likely due to the lock(s) in the Nederrijn river. There is a one-to-one linear relation for Waal levels between 2 and 3 m + NAP. Then when the Waal is between 3 and 4 m + NAP, the Nederrijn level stays around 3 m + NAP. This is due to the lock at Amerongen. From the Waal level around 4 m + NAP the Nederrijn level increases again, with the Waal level rising faster than the Nederrijn level.

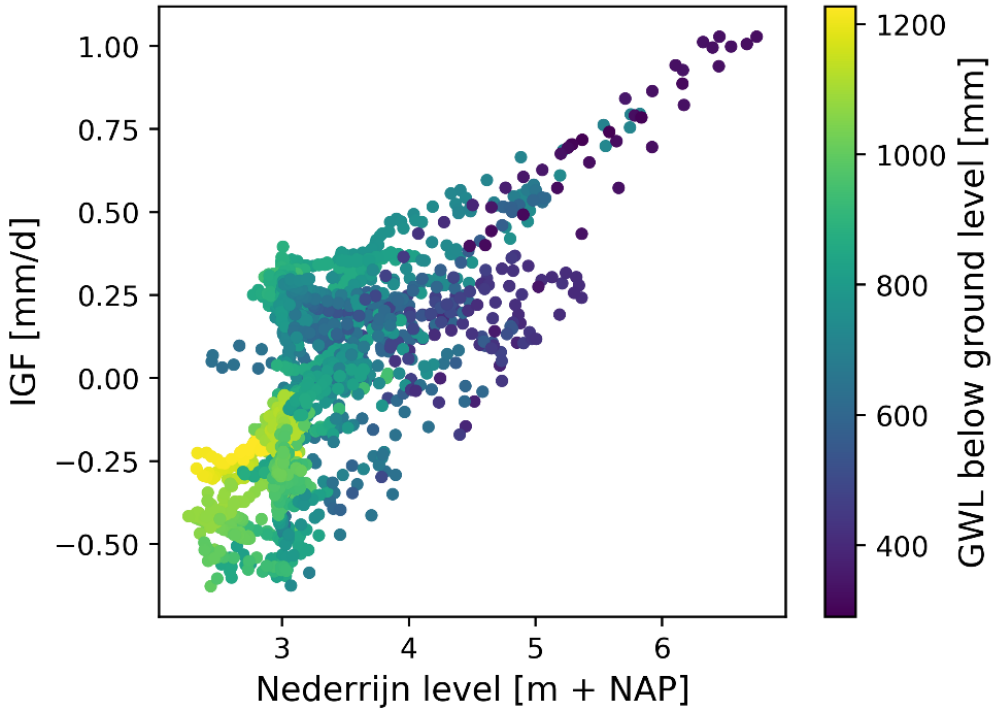


**Figure 5-4, Nederrijn level plotted against IGF and groundwater level GWL**

From Figure 5-4 we see that generally as the Nederrijn level increases, the IGF and groundwater level increase as well. However, looking at a single IGF value, say where the IGF is -0.25 mm/day, we see that when the Nederrijn level increases, the groundwater level increases as well. This means that changes in the groundwater level have a negative effect on the IGF to the catchment. This agrees with the formula of Darcy. The same is true for the Waal level, as can be seen in Figure 5-5.

This suggests that the IGF is influenced by the water level difference between the groundwater in the catchment of the Maurikse Wetering and the Nederrijn level. The formula of Darcy states that an increase in water level difference increases the flow. As the fluctuation in the Nederrijn level ΔNR is between 3 to 4 meters as seen in Figure 5-4 while the groundwater level fluctuation ΔdG is less than 1 meter, the net change during wet conditions is in favour of the Nederrijn level and thus the lower groundwater levels are found during low IGF conditions.

Looking at section 4.3, the downstream groundwater level will be important too, as that would be a major influence on the outgoing IGF.

The difference between the major rivers and the IGF doesn't provide a clearer picture, as can be seen in Figure 5-6. This is likely because of the discontinuous function between the Waal and Nederrijn as shown in Figure 5-3.

The storage deficit dV, representing the moisture of the unsaturated zone, does not give as clear of a picture as the groundwater level. This shows in Figure 5-8, Figure 5-9 and Figure 5-10. This is possibly because the moisture in the unsaturated zone does not influence horizontal pressure on the catchment scale, which influence groundwater flow. This is visible in Figure 5-7, where the storage deficit does not have a clear relation with the Nederrijn and Waal levels. The same is true for the relation between the Maurikse Wetering level and the major rivers, as seen in Figure 5-11, Figure 5-12, Figure 5-13 and Figure 5-14. This is likely in part due to the the Maurikse Wetering level being artificially maintained through the tilting weirs in the Maurikse Wetering and the relatively small difference in water level in the Maurikse Wetering compared to the Nederrijn and Waal.

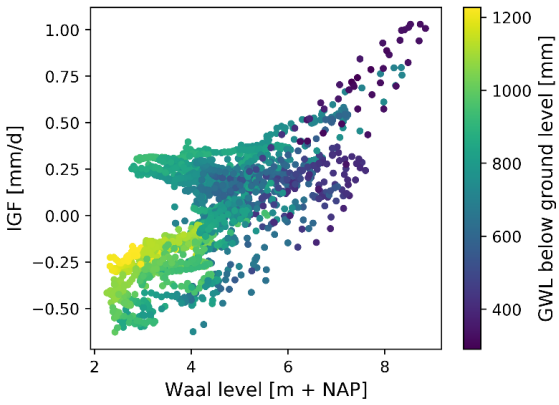


**Figure 5-5, Waal level plotted against the IGF and the groundwater level GWL**

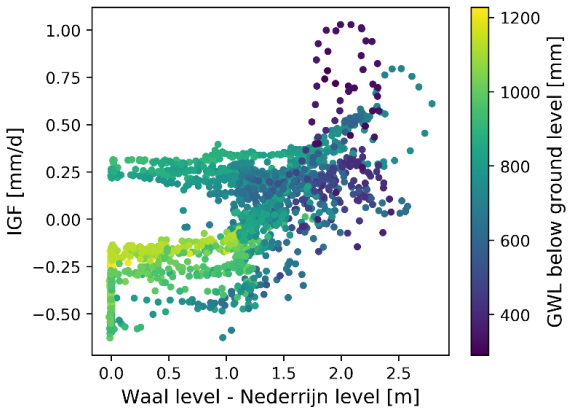


**Figure 5-6, Waal minus Nederrijn level plotted against the IGF and groundwater level GWL**

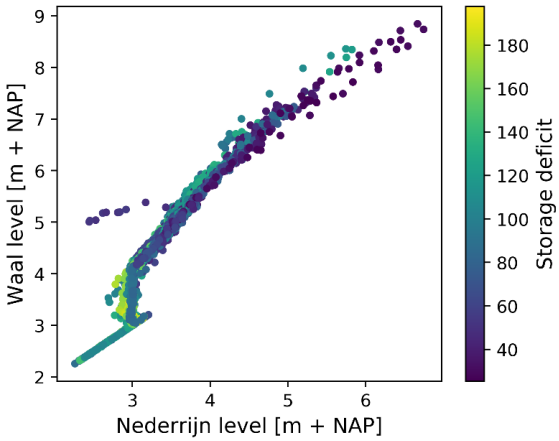


**Figure 5-7, Nederrijn level plotted against the Waal level and the storage deficit**

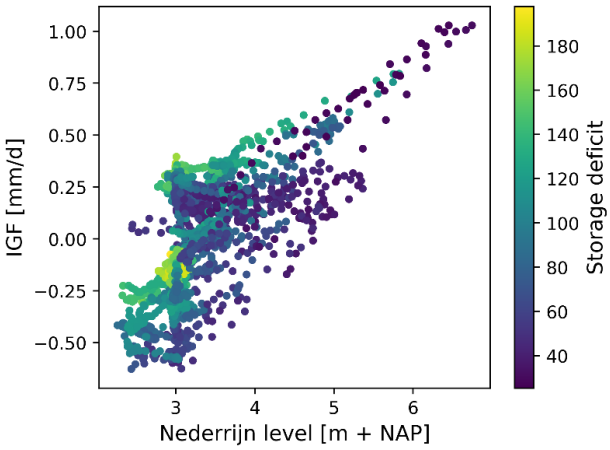


**Figure 5-8, Nederrijn level plotted against the IGF and the storage deficit**

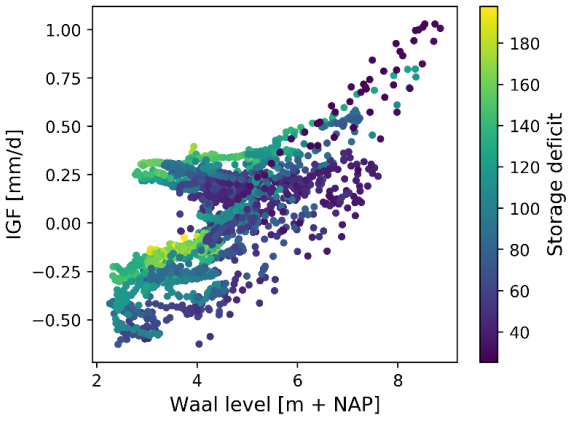


**Figure 5-9, Waal level plotted against IGF and the storage deficit**

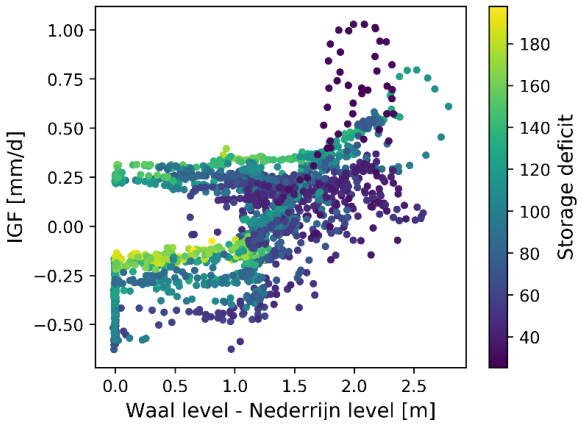


**Figure 5-10, Waal minus Nederrijn level plotted against IGF and the storage deficit**

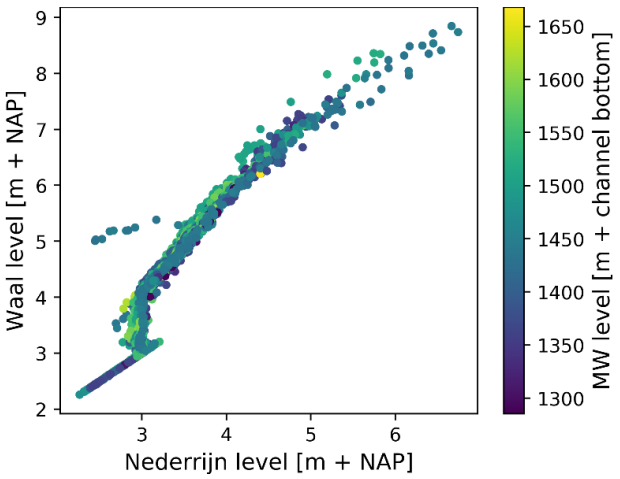


**Figure 5-11, Nederrijn level plotted against the Waal level and water level in the Maurikse Wetering**

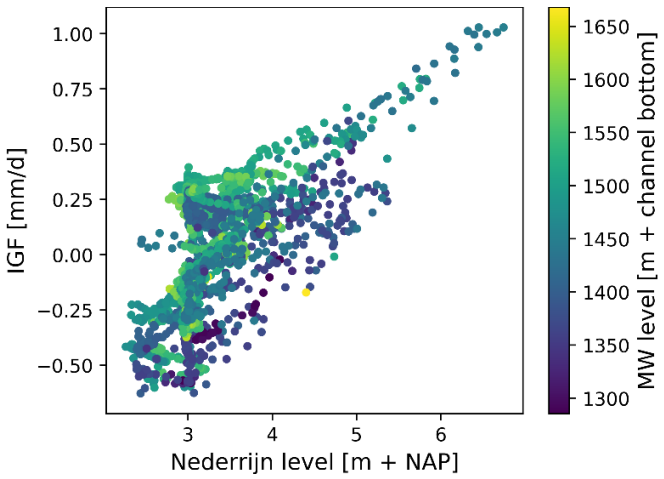


**Figure 5-12, Nederrijn level plotted against the IGF and the water level in the Maurikse Wetering**

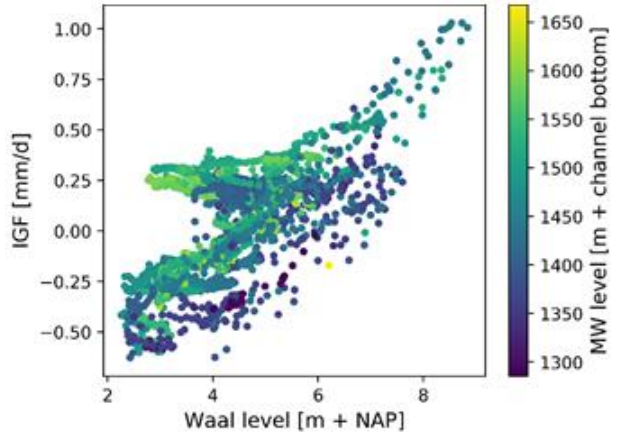


**Figure 5-13, Waal level plotted against the IGF and the water level in the Maurikse Wetering**

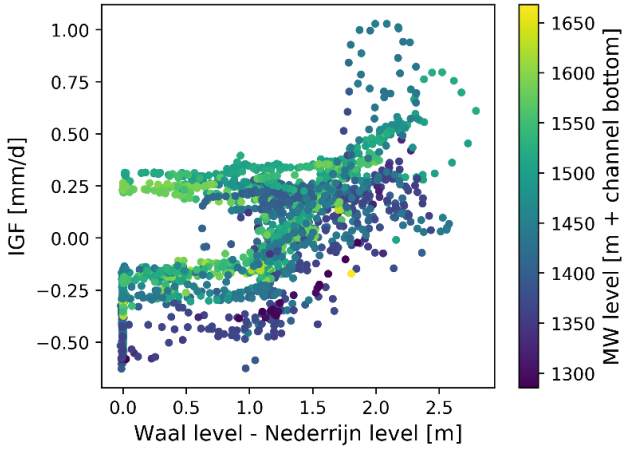


**Figure 5-14, Waal minus Nederrijn level plotted against the IGF and the Maurikse Wetering level**

## 5.2 Simple linear regression

The IGF is plotted against the Nederrijn level NR, the Waal level WA, the average groundwater level in layer 4 GWL (also named dG), the precipitation P, potential evaporation $ET_{pot}$ and the average water level in the Maurikse Wetering catchment MW. The average water level in the Maurikse Wetering is the average of the river and the secondary waterways present in the provided SOBEK2 model. The resulting regressions are shown in Figure 5-17 through Figure 5-28. Figure 5-17 through Figure 5-22 show the SLR for April 2013 to July 2015, whereas Figure **5-23** through Figure 5-28 show the SLR for July 2015 to April 2018.

### 5.2.1 Relation between IGF and Nederrijn level 2015 – 2018

The independent variables are plotted against the IGF in Figure 5-17 through Figure 5-28. As can be seen, the clearest linear relations appear in Figure 5-23 and Figure 5-24. These concern the Nederrijn level and the Waal level for 2015 – 2018. Some relation appears in the groundwater level in Figure 5-25, however this conflicts with the formula of Darcy as increasing the groundwater level within the catchment should decrease the pressure difference and thus work against groundwater flow crossing the topographic border into the catchment. Looking at the relation between the IGF and the water level in the major rivers Nederrijn and Waal, it appears that during high water levels the IGF increases. This is seen in section 5.1. This would mainly occur during wet periods, which would increase the groundwater level through the increased precipitation.

Using linear regression, a relation is drawn up, starting with the relation between the Nederrijn level and the IGF as modelled by MORIA.

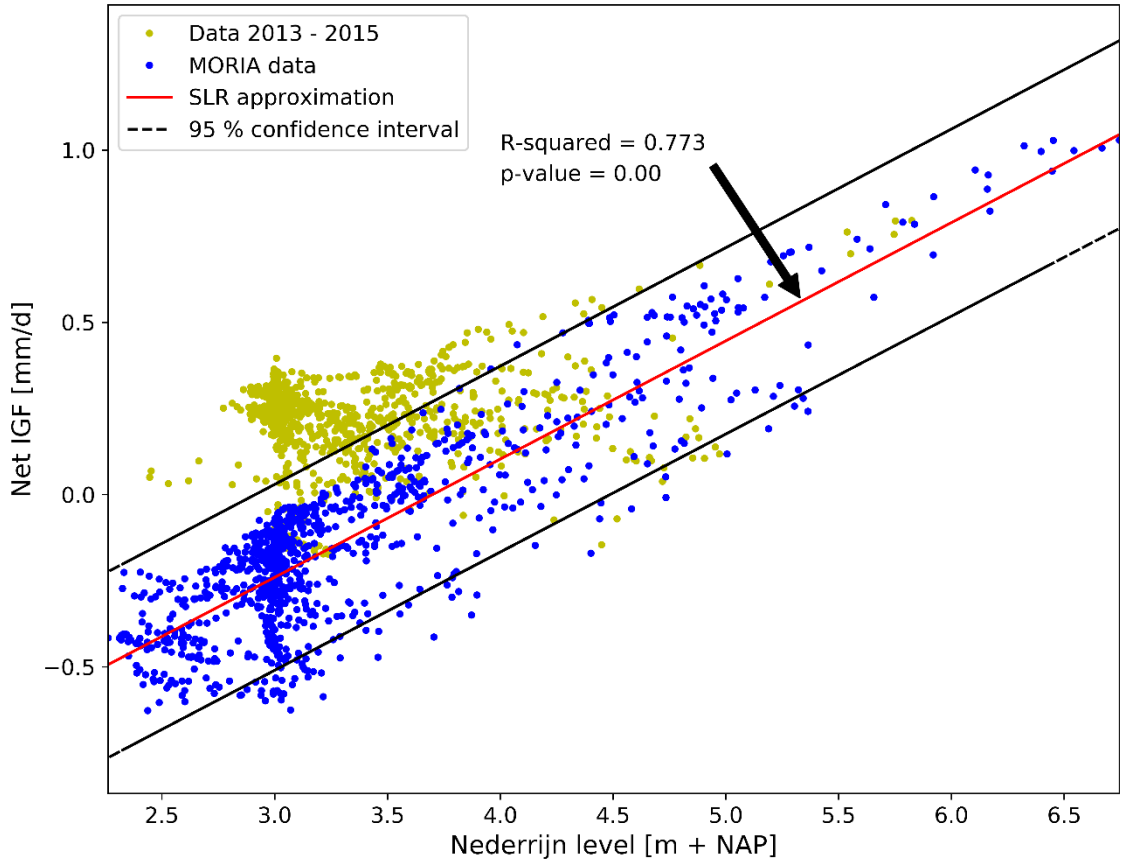


**Figure 5-15, IGF data vs Nederrijn data for July 2015 – 4-2018 with SLR approximation**

The resulting curve fit Is a linear relation. With the IGF flux in mm/d and the Nederrijn level at m + NAP, the relation has the following formula:

$$\boldsymbol{IGF = 0.343 * [Nederrijn\ level] - 1.27} \qquad \textbf{(5.1)}$$

This relation has an adjusted R-squared of 0.773, as can be seen in Figure **5-23**.

There is still some noise around this curve fit, as can be seen in Figure 5-15. The spread of this noise is shown in Figure 5-16. The limits in which 95% of the datapoints are present are given in Table 5-1.

| | **2.5 %** | **97.5 %** |
|---|---|---|
| *Constant* | -1.31 | -1.23 |
| *Nederrijn level* | 0.332 | 0.355 |

**Table 5-1, values 95 % confidence interval Nederrijn**

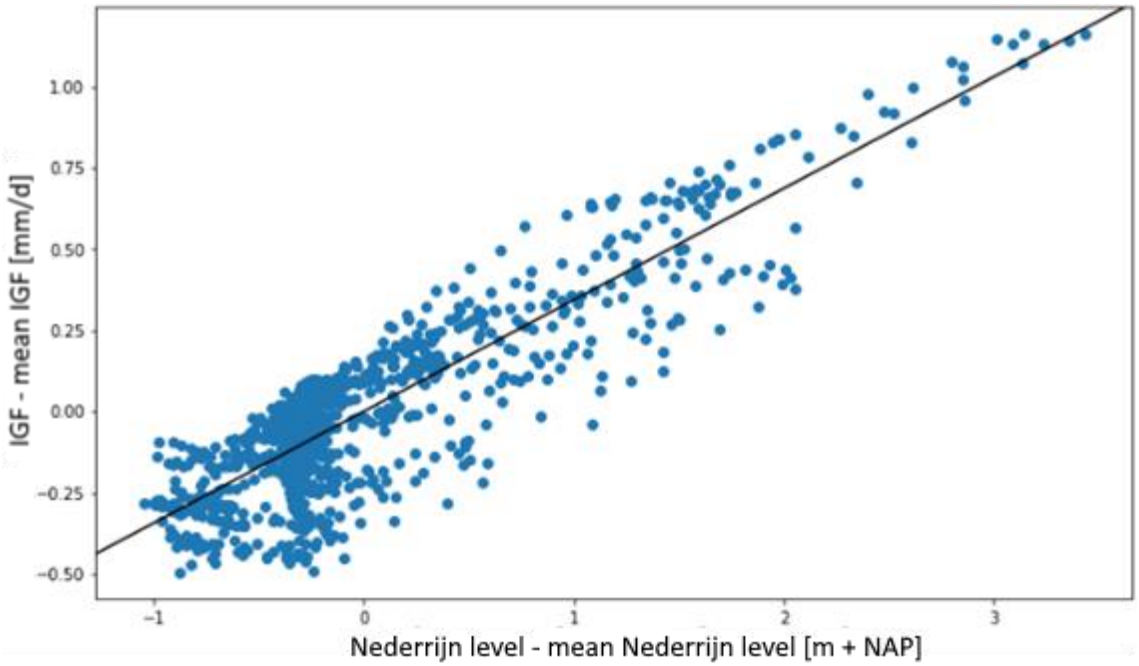


**Figure 5-16, regression plot Nederrijn level 2015 – 2018**

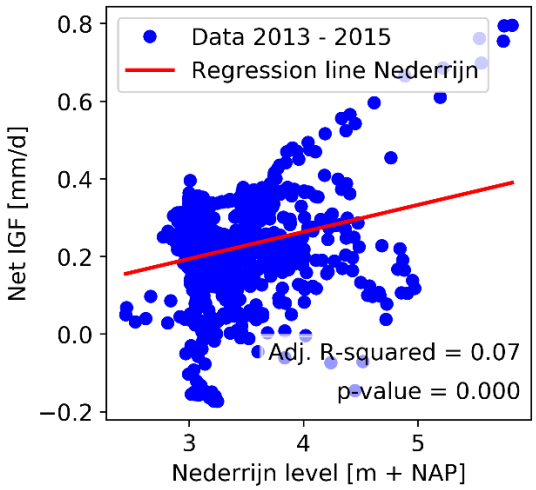


Figure 5-17, IGF vs Nederrijn, 4-2013 – 4-2015

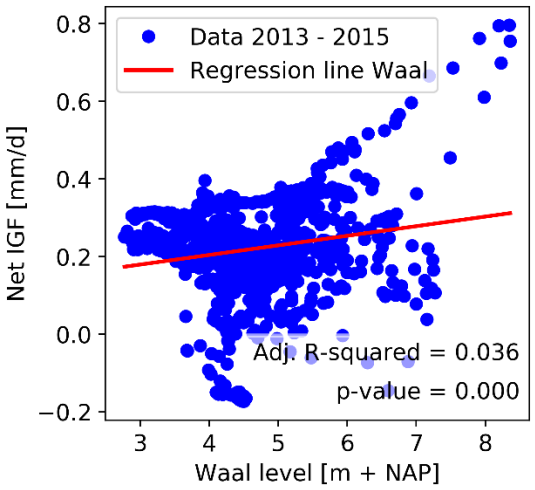


Figure 5-18, IGF vs Waal level, 4-2013 – 4-2015

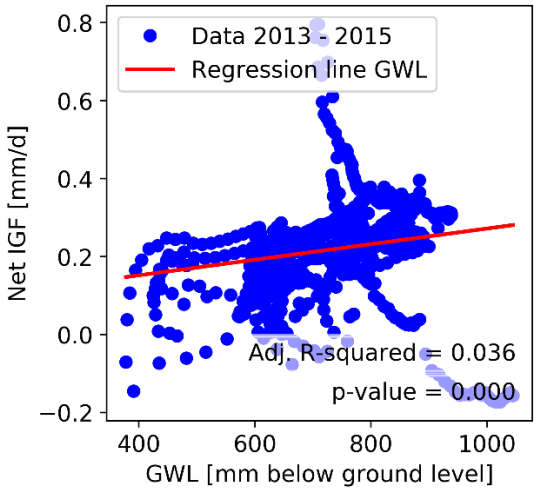


Figure 5-19, IGF data vs GWL, 4-2013 – 4-2015

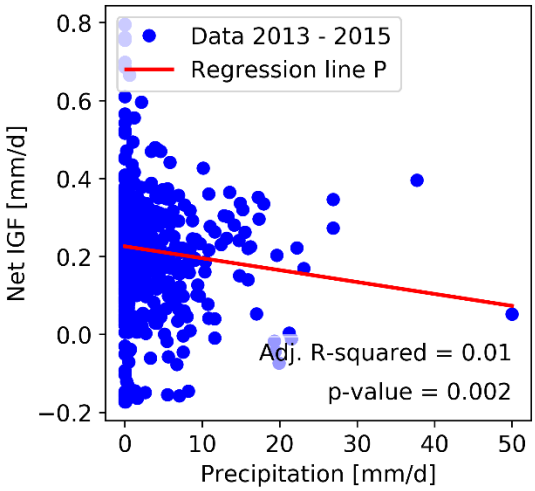


Figure 5-20, Precipitation vs IGF, 4-2013 –2015

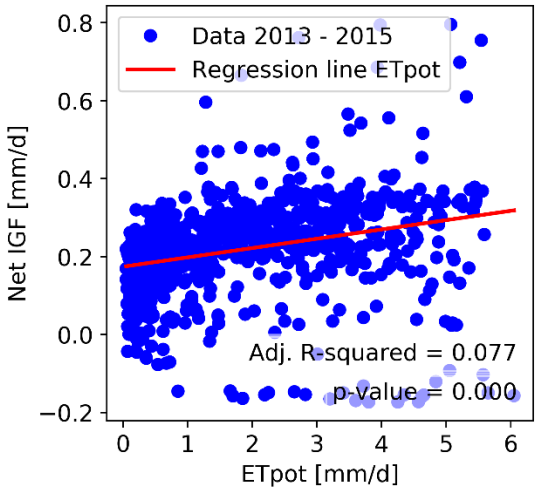


Figure 5-21, ETpot vs IGF, 4-2013 – 4-2015

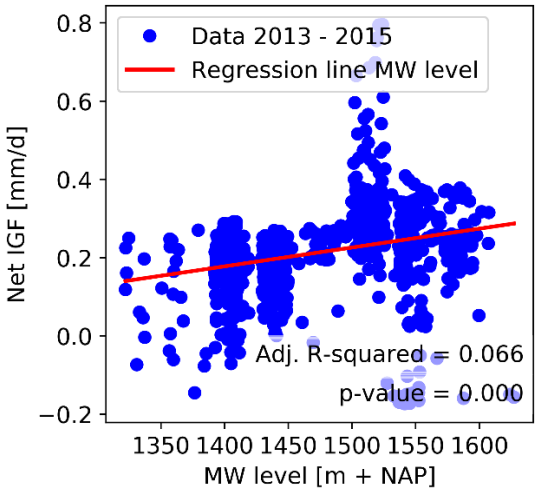


Figure 5-22, MW level vs IGF, 4-2013 – 4-2015

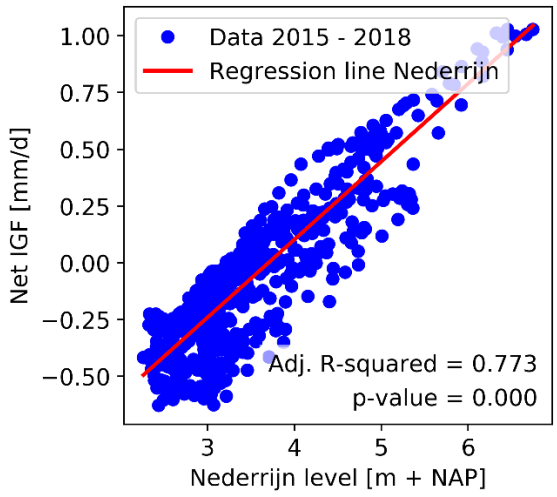


**Figure 5-23, IGF vs Nederrijn, 7-2015 – 4-2018**

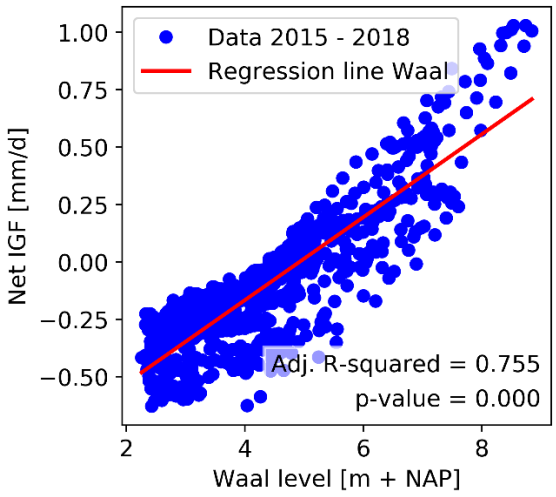


**Figure 5-24, IGF vs Waal level, 7-2015 – 4-2018**

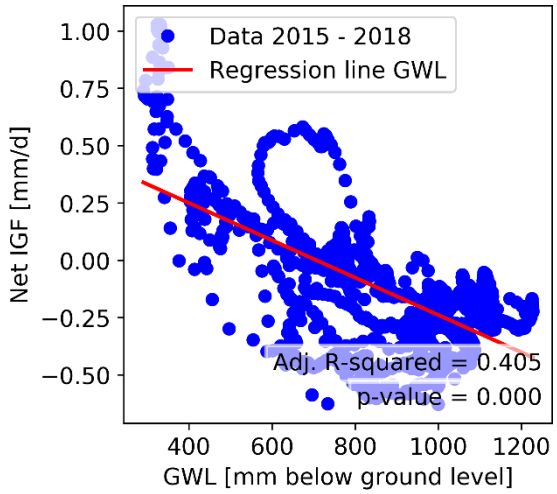


**Figure 5-25, IGF data vs GWL, 7-2015 – 4-2018**

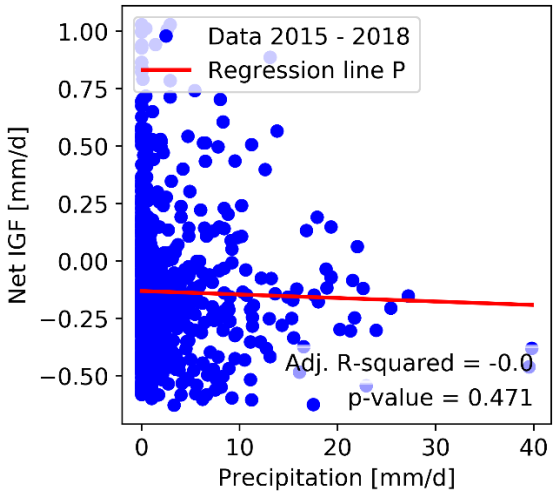


**Figure 5-26, Precipitation data vs IGF data**

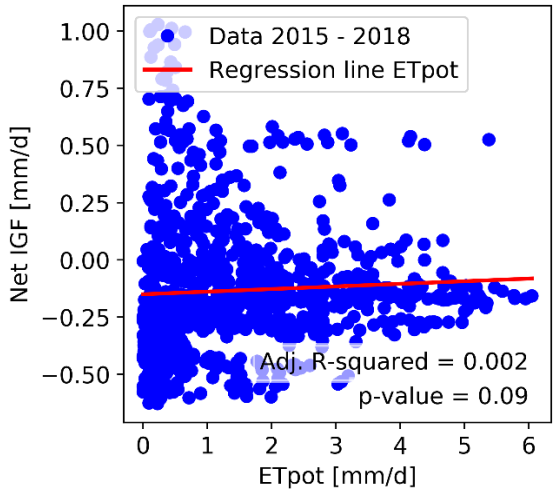


**Figure 5-27, ETpot vs IGF, 7-2015 – 4-2018**

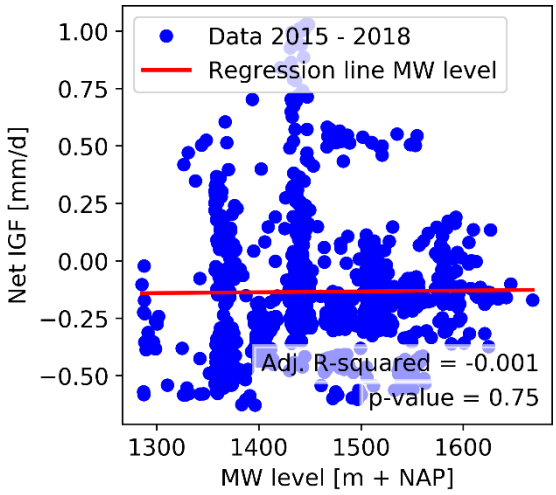


**Figure 5-28, MW data vs IGF, 7-2015 – 4-2018**

### 5.2.2 Relation between IGF and Waal level 2015 – 2018

The relation between the Waal level and the IGF is drawn up using linear regression.

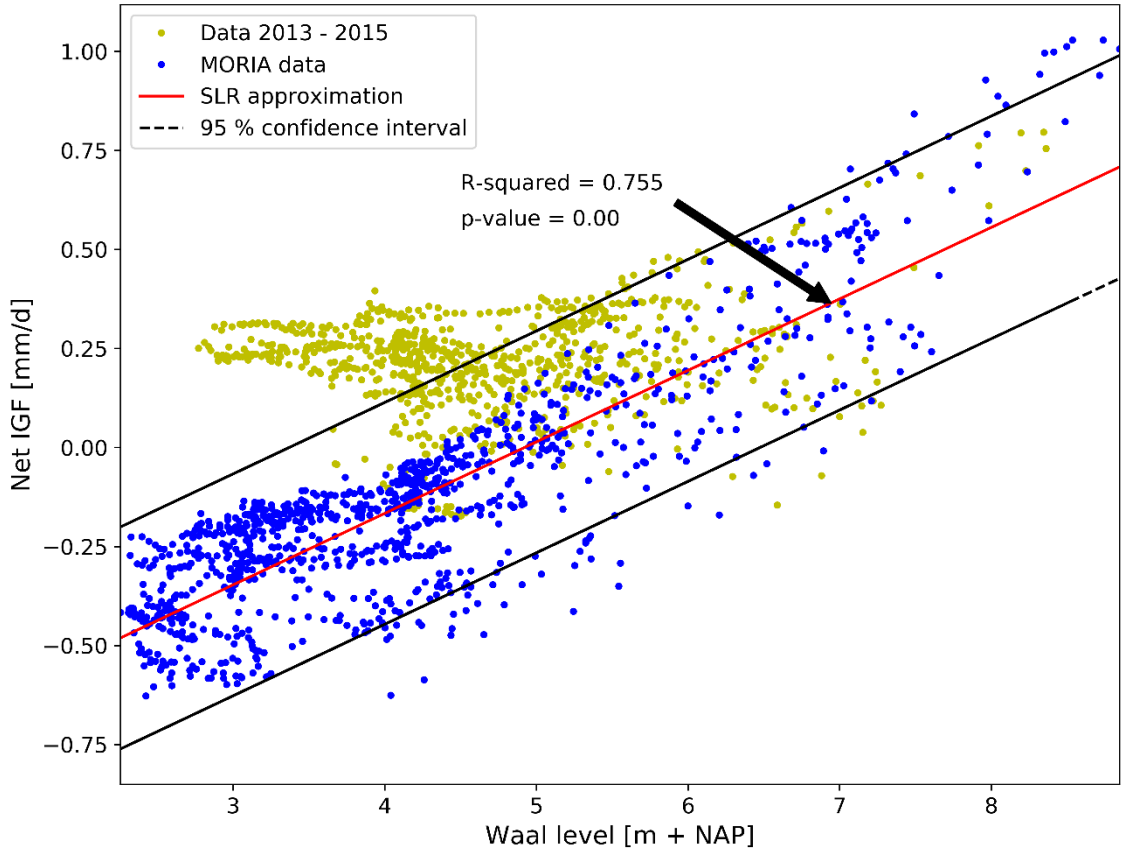


**Figure 5-29, IGF data vs Waal data for July 2015 – 4-2018 with SLR approximation**

The relation between the IGF as modelled by MORIA and the Waal is the following:

$$IGF = 0.1805 * [Waal\ level] - 0.888 \qquad (5.2)$$

The limits in which 95% of the datapoints are present are given in Table 5-2.

| | **2.5 %** | **97.5 %** |
|---|---|---|
| *Constant* | -0.916 | -0.860 |
| *Waal level* | 0.174 | 0.187 |

**Table 5-2, values 95 % confidence interval Waal**

This relation has a R-squared of 0.755. This is a value which is comparable to that of the Nederrijn relation, however when comparing the partial regression plots from Figure 5-16 and Figure 5-30 it shows that the partial regression plot for the Waal has more bias. This bias shows around e(WA|X) = 0 in Figure 5-30 as resembling an U-shape, and in the top right having all points above the regression line.

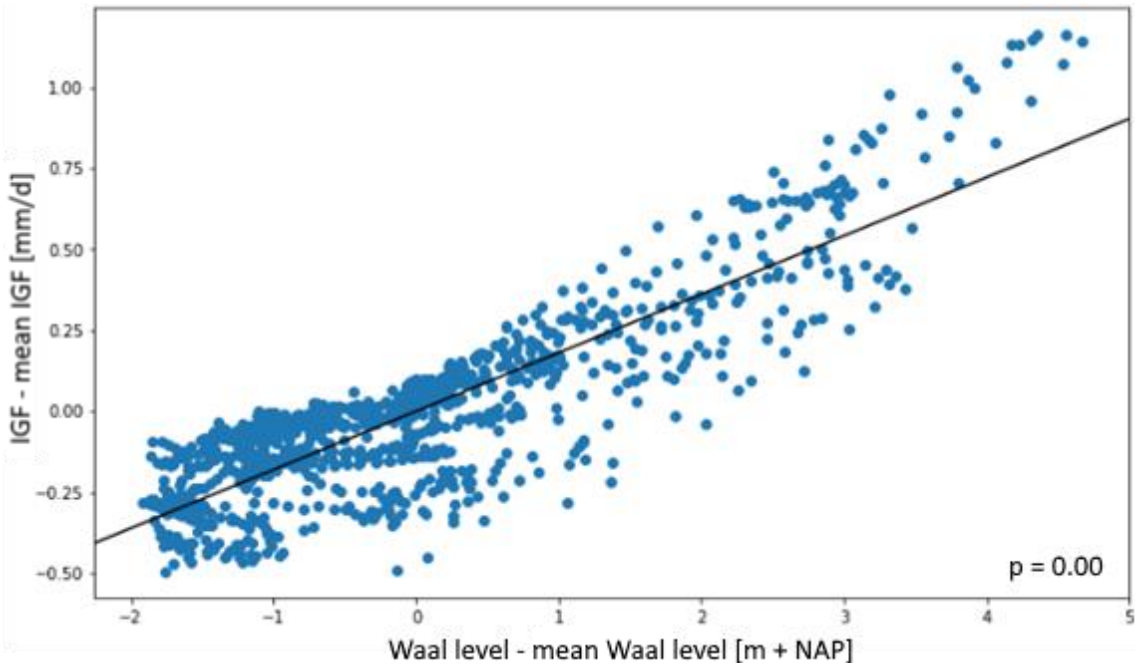


**Figure 5-30, regression plot Waal level 2015 – 2018**

Both the Waal and Nederrijn relations are plotted in Figure 5-31, where it can be seen that the courses are similar.

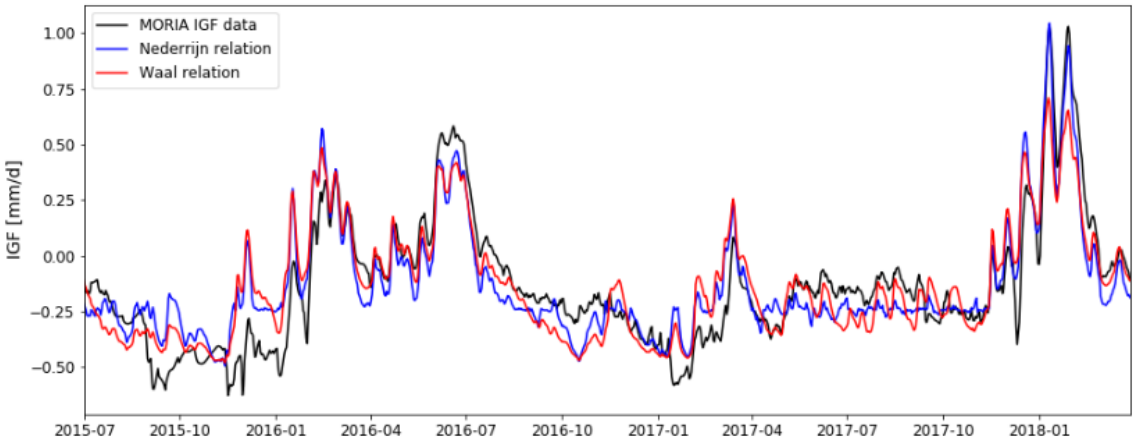


**Figure 5-31, Waal and Nederrijn relation overlaid with IGF data**

Since both relations provide almost the same result, neither is objectively better than the other. The relation for the Nederrijn will be used in the WALRUS analysis. It is assumed that due to the Nederrijn's proximity to the catchment compared to the Waal, any variations in its level will have a more immediate response on the catchment. The correlation between the two relations can in part be explained by both rivers being connected not too far upstream. They thus roughly share the same course, although the Nederrijn contains locks like the one in Amerongen which causes a constant water level in the Nederrijn during periods of relatively low to medium discharge in the Rhine.

## 5.3 Multiple linear regression analysis

To see if the outcome of the SLR analysis can be improved with the addition of more variables, and to see which variables influence the IGF, a multiple linear regression (MLR) analysis is performed.

### 5.3.1 Entire range of data (2013 – 2018)

For the period 2013 – 2018, the resulting coefficients of the MLR are given in Table 5-3. Table 5-3 also gives the standard error, t-value, p-value and the lower and upper boundaries for the 95 % confidence interval.

| | coef | std err | t | P>\|t\| | [0.025 | 0.975] |
|---|---|---|---|---|---|---|
| const | -1.3806 | 0.123 | -11.179 | 0.000 | -1.623 | -1.138 |
| NR | -0.0166 | 0.019 | -0.868 | 0.385 | -0.054 | 0.021 |
| WA | 0.0952 | 0.011 | 8.574 | 0.000 | 0.073 | 0.117 |
| dG | -0.0011 | 5.57e-05 | -18.962 | 0.000 | -0.001 | -0.001 |
| P | -0.0026 | 0.001 | -2.641 | 0.008 | -0.004 | -0.001 |
| ETpot | -0.0040 | 0.004 | -0.941 | 0.347 | -0.012 | 0.004 |
| dV | 0.0030 | 0.000 | 12.667 | 0.000 | 0.003 | 0.004 |
| MW | 0.0011 | 7.54e-05 | 14.691 | 0.000 | 0.001 | 0.001 |

**Table 5-3, MLR results with all variables. R-squared: 0.633. Adjusted R-squared: 0.632.**

These coefficients give an R-squared of 0.633 and an adjusted R-squared of 0.632. Surprisingly, the Nederrijn level NR in Table 5-3 has a p-value of 0.385. This is much higher than the threshold of 0.05. This might be due to the Waal having a similar course and the Nederrijn having a constant level between peaks. The potential evaporation ETpot has a p-value above 0.05 as well and will therefore be removed from the MLR.

| | coef | std err | t | P>\|t\| | [0.025 | 0.975] |
|---|---|---|---|---|---|---|
| const | -1.3648 | 0.117 | -11.654 | 0.000 | -1.595 | -1.135 |
| WA | 0.0869 | 0.006 | 14.918 | 0.000 | 0.075 | 0.098 |
| dG | -0.0010 | 5.4e-05 | -19.345 | 0.000 | -0.001 | -0.001 |
| P | -0.0024 | 0.001 | -2.522 | 0.012 | -0.004 | -0.001 |
| dV | 0.0029 | 0.000 | 13.813 | 0.000 | 0.003 | 0.003 |
| MW | 0.0011 | 6.93e-05 | 15.581 | 0.000 | 0.001 | 0.001 |

**Table 5-4, MLR coefficients after selection. R-squared: 0.633. Adjusted R-squared: 0.632.**

The remaining variables with the coefficients as given in Table 5-4 give an R-squared of 0.633 and an adjusted R-squared of 0.632, the same rounded value as the MLR analysis gives before the removal of parameters, indicating a negligible difference with the coefficients in Table 5-3. Removing the variables increased the f-value for this MLR analysis from 448 to 627, with a Prob > F of 0.00, meaning that the null hypothesis can be rejected. Acquiring the best fit by means of determining the highest adjusted R-squared value also results in rejecting the NR and ETpot variables. From all parameter combinations, the combination shown in Table 5-4 has the highest adjusted R-squared value. This means that manual selection according to the p-values of the variables has the same outcome as looking at the adjusted R-squared value.

From the partial regression plots in Figure 5-32 we can see that the regression plot for the water level in the Maurikse Wetering (MW) is somewhat biased to the left side of the graph. This bias

was deemed not enough to discard the variable. There is also some bias in the Waal, groundwater level and storage deficit above the regression line. This can suggest a nonlinear or discontinuous relation.

According to the MLR, the IGF depends on the Waal level, groundwater level, precipitation, storage deficit in the unsaturated zone and the water level in the Maurikse Wetering.

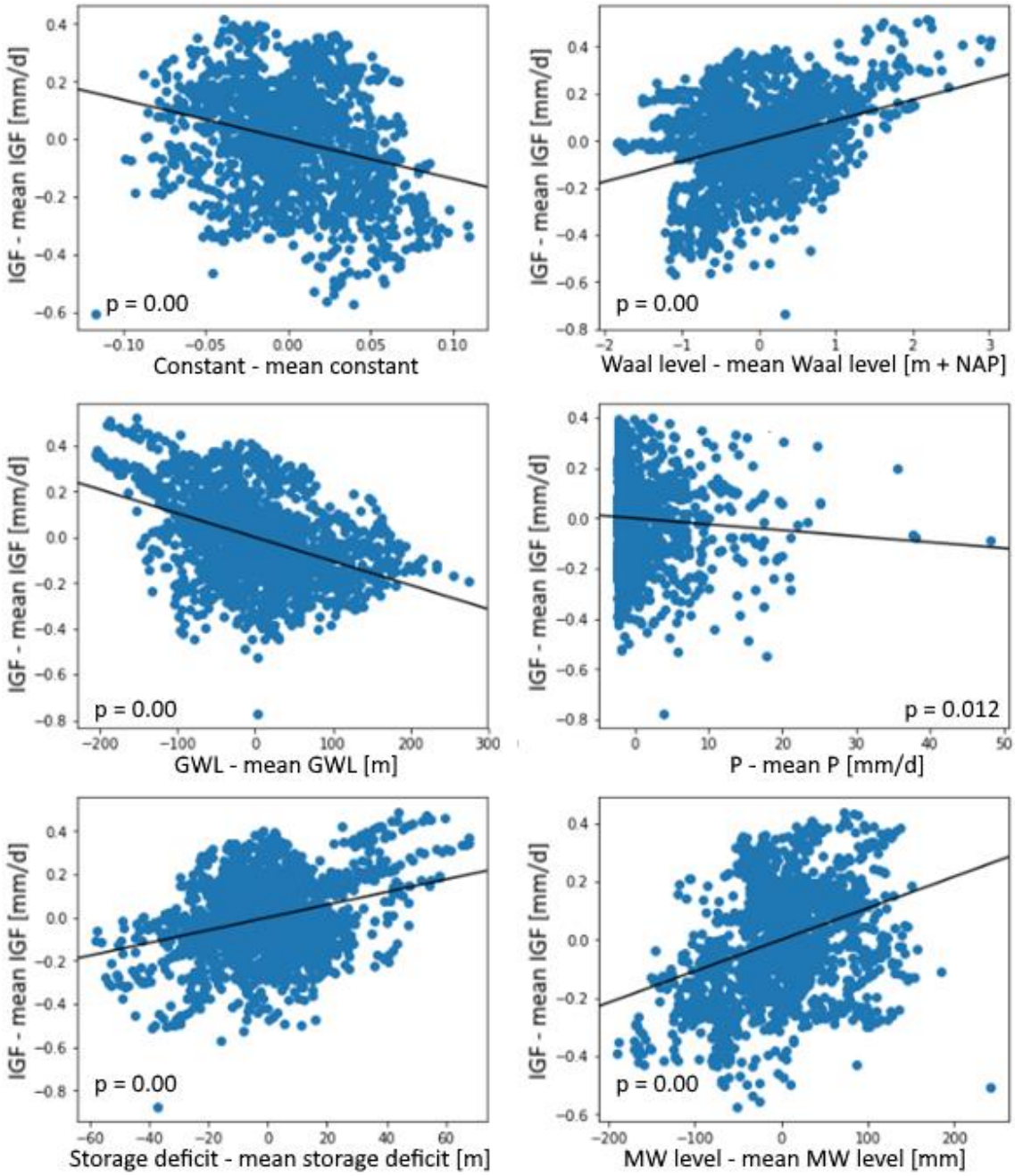


**Figure 5-32, partial regression plots for the MLR for 2013 – 2018**

The graph with the found MLR over time compared to the IGF as modelled by MORIA is shown in Figure 5-33.

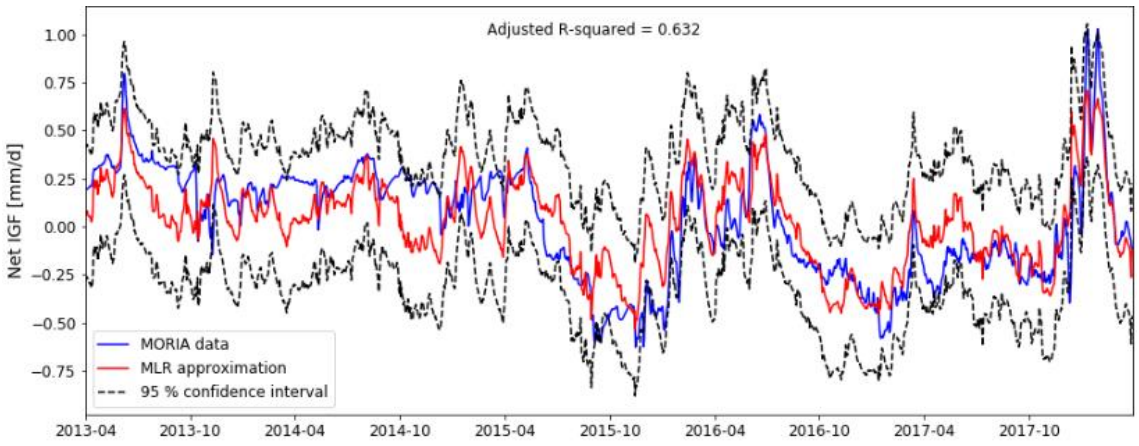


**Figure 5-33, the resulting MLR from Table 5-4 compared to the IGF data as modelled by MORIA for 2013 – 2018, with 95% confidence interval**

## 5.3.2 MLR 2013 – 2015

To get a clear idea of the difference between the two periods defined in Figure 5-1, the multilinear regression analysis was done for the two periods. The first period in Figure 5-1, from April 2013 to July 2015, will be analysed first.

| | coef | std err | t | P>\|t\| | [0.025 | 0.975] |
|---|---|---|---|---|---|---|
| const | -0.5397 | 0.142 | -3.798 | 0.000 | -0.819 | -0.261 |
| NR | 0.1266 | 0.022 | 5.680 | 0.000 | 0.083 | 0.170 |
| WA | -0.0113 | 0.011 | -1.019 | 0.309 | -0.033 | 0.011 |
| MW | 0.0002 | 9.19e-05 | 1.786 | 0.074 | -1.62e-05 | 0.000 |
| dG | 6.298e-05 | 7.46e-05 | 0.845 | 0.399 | -8.34e-05 | 0.000 |
| dV | 0.0014 | 0.000 | 5.344 | 0.000 | 0.001 | 0.002 |
| P | -0.0036 | 0.001 | -3.888 | 0.000 | -0.005 | -0.002 |
| ETpot | -0.0098 | 0.004 | -2.287 | 0.022 | -0.018 | -0.001 |

**Table 5-5, MLR results 2013 – 2015 with all variables. R-squared: 0.271. Adjusted R-squared: 0.265.**

From Table 5-5 it shows that the p-values for the variables Waal level WA and the groundwater level dG are significantly above the p-value threshold of 0.05. The Maurikse Wetering level MW was only slightly above this threshold, after removing variables WA and dG it was below 0.05. Removing these variables increases the f-value from 43.2 to 60.1. the Prob > F is $5.7 * 10^{-52}$, which is practically zero. This means that the null hypothesis can be rejected.

The resulting selection was run again, with the results of this selection being shown in Table 5-6.

| | coef | std err | t | P>\|t\| | [0.025 | 0.975] |
|---|---|---|---|---|---|---|
| const | -0.5074 | 0.134 | -3.774 | 0.000 | -0.771 | -0.243 |
| NR | 0.1006 | 0.008 | 12.099 | 0.000 | 0.084 | 0.117 |
| MW | 0.0002 | 9.03e-05 | 2.084 | 0.037 | 1.09e-05 | 0.000 |
| dV | 0.0016 | 0.000 | 8.825 | 0.000 | 0.001 | 0.002 |
| P | -0.0037 | 0.001 | -4.041 | 0.000 | -0.005 | -0.002 |
| ETpot | -0.0108 | 0.004 | -2.581 | 0.010 | -0.019 | -0.003 |

**Table 5-6, MLR results 2013 – 2015 after selection. R-squared: 0.269. Adjusted R-squared: 0.265.**

The MLR of Table 5-6 has a R-squared of 0.269. This is rather poor. This can be in part due to the fact that the first period has a much smaller variation in net IGF than the second period, because of which the differences of the mean value have a more significant effect.

The regression plot for the constant shows towards the top left, the regression plot for the Nederrijn level NR shows bias towards the top right. All partial regression plots show bias in the bottom, as there is a gap between the data cluster around the regression line and the cluster at the bottom. An unbiased regression should show one cluster, distributed around the regression line. All plots do appear homoscedastic.

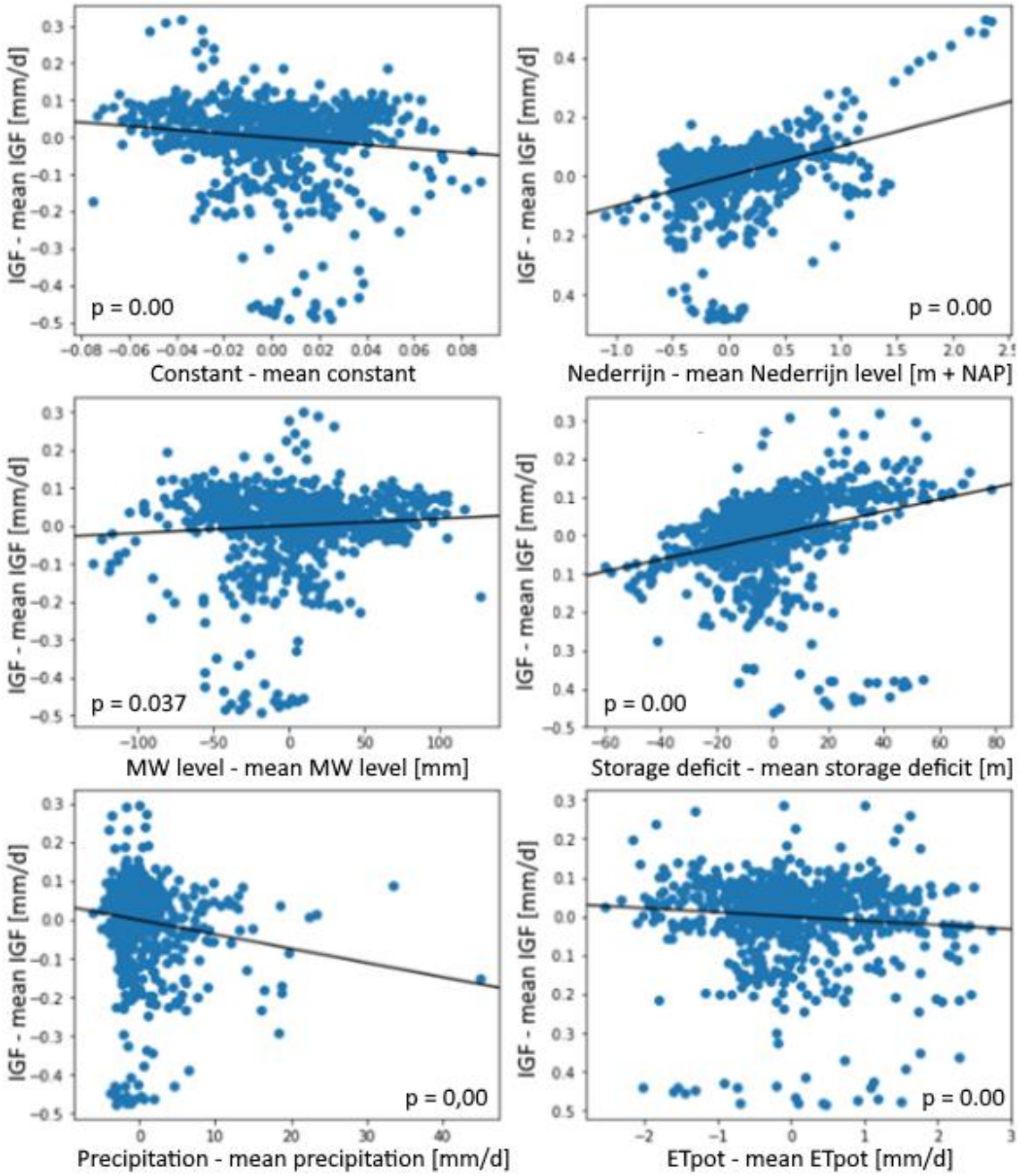


**Figure 5-34, partial regression plots for the MLR for 2013 – 2015**

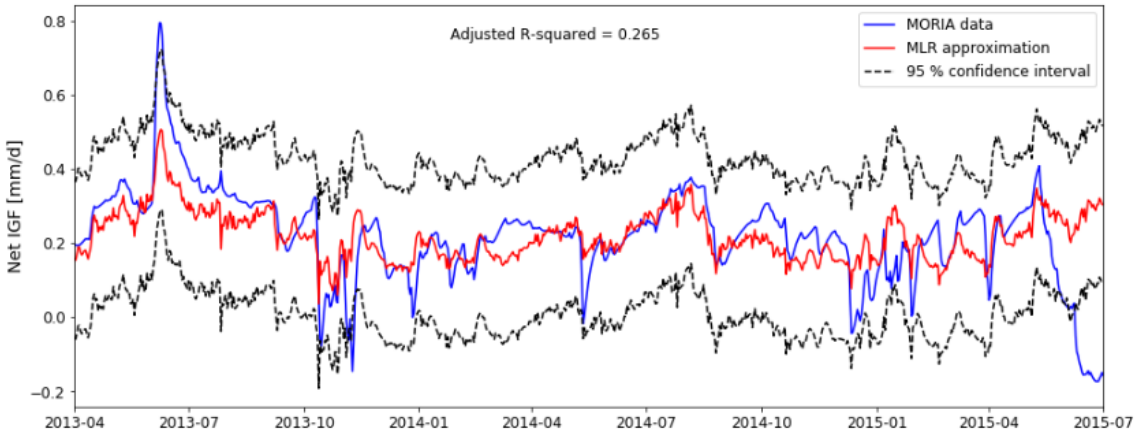


**Figure 5-35, the resulting MLR from Table 5-6 compared to the IGF data as modelled by MORIA for 2013 – 2015, with 95% confidence interval**

## 5.3.3 MLR 2015 – 2018

The multiple linear regression analysis was done for the second period as defined in Figure 5-1, from July 2015 to the end of March 2018. The results of this MLR for all variables are shown in Table 5-7.

| | coef | std err | t | P>\|t\| | [0.025 | 0.975] |
|---|---|---|---|---|---|---|
| const | -2.2618 | 0.093 | -24.423 | 0.000 | -2.444 | -2.080 |
| NR | 0.2214 | 0.016 | 13.648 | 0.000 | 0.190 | 0.253 |
| WA | 0.1067 | 0.010 | 11.106 | 0.000 | 0.088 | 0.126 |
| MW | 0.0005 | 5.74e-05 | 9.154 | 0.000 | 0.000 | 0.001 |
| dG | 6.083e-05 | 4.93e-05 | 1.234 | 0.217 | -3.59e-05 | 0.000 |
| dV | 0.0014 | 0.000 | 7.355 | 0.000 | 0.001 | 0.002 |
| P | -0.0020 | 0.001 | -2.479 | 0.013 | -0.004 | -0.000 |
| ETpot | -0.0051 | 0.003 | -1.450 | 0.147 | -0.012 | 0.002 |

**Table 5-7, MLR results 2015 – 2018 with all variables. R-squared: 0.857. Adjusted R-squared: 0.856.**

The groundwater level dG and the potential evaporation ETpot show a p-value significantly above the threshold of 0.05. After rerunning the MLR analysis, the precipitation P showed a p-value above 0.05 as well and was subsequently removed from the MLR analysis. The resulting selection is shown in Table 5-8. This increases the f-value from 851 to 1476, with a Prob > F of 0.00. This means that the null hypothesis can be rejected.

| | coef | std err | t | P>\|t\| | [0.025 | 0.975] |
|---|---|---|---|---|---|---|
| const | -2.1555 | 0.075 | -28.738 | 0.000 | -2.303 | -2.008 |
| NR | 0.2219 | 0.016 | 13.786 | 0.000 | 0.190 | 0.253 |
| WA | 0.0997 | 0.009 | 11.579 | 0.000 | 0.083 | 0.117 |
| MW | 0.0005 | 5.32e-05 | 9.279 | 0.000 | 0.000 | 0.001 |
| dV | 0.0015 | 0.000 | 13.216 | 0.000 | 0.001 | 0.002 |

**Table 5-8, MLR results 2015 – 2018 after selection. R-squared: 0.855. Adjusted R-squared: 0.855.**

The resulting MLR shown in Table 5-8 has an R-squared of 0.855 and an adjusted R-squared of 0.855. Acquiring the best fit by means of determining the maximum adjusted R-squared value results in none of the variables being rejected, with a maximum adjusted R-squared value of 0.856. As this is a difference of only 0.1 % and the f-statistic for the MLR with all predictor variables being

851 compared to the f statistic of 1476 for the MLR with the variables in Table 5-8, the MLR with the variables in Table 5-8 is taken as the best relation.

Looking at the partial regression plots in Figure 5-36, the regression plot for the Nederrijn shows some bias towards the top left, with all residuals being above the regression line. This bias only contains 4 % of the datapoints (20 out of 822 observations), so this is not deemed significant. It can mean that a discontinuous relation exists.

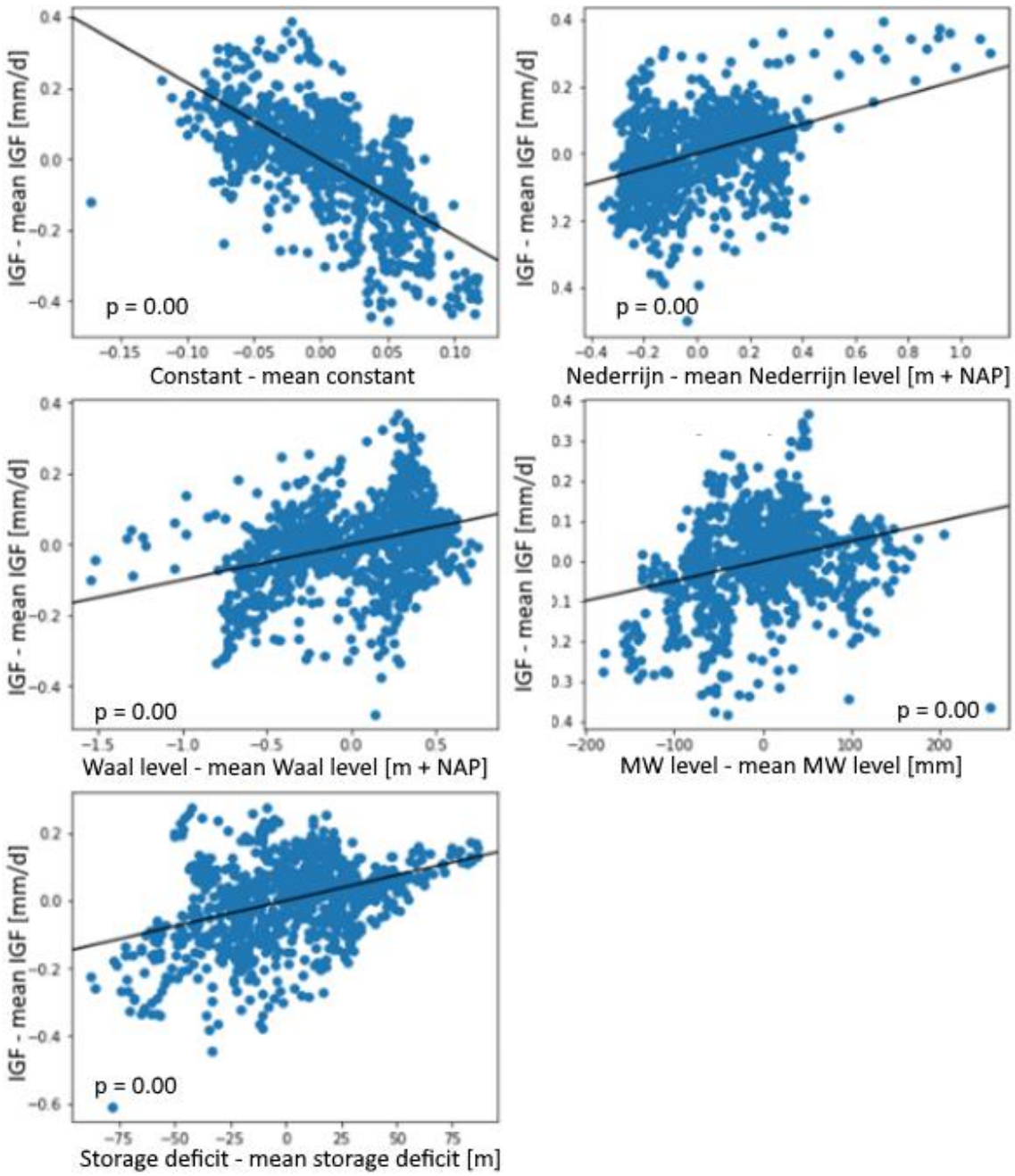


**Figure 5-36, partial regression plots for the MLR for 2015 – 2018**

Figure 5-37 shows the resulting plot from the MLR analysis. Comparing the R-squared value of this second period of 0.855 to the value of 0.269 resulting from the MLR from section 5.3.2 and comparing the fit from Figure 5-37 with the fit from Figure 5-35 as well as the partial regression plots from Figure 5-36 and Figure 5-34 for the second and first period respectively and it shows that the IGF for this second period can be more accurately modelled with the used variables than the first period.

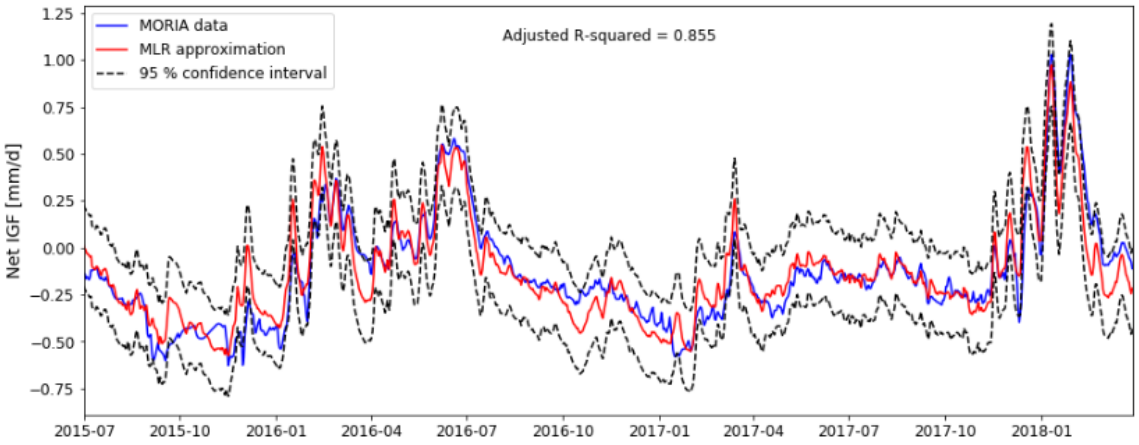


**Figure 5-37, the resulting MLR from Table 5-8 compared to the IGF data as modelled by MORIA for 2015 – 2018, with 95% confidence interval**

In all MLR analysis results, of the two separate periods and the entire dataset, one or both of the major rivers Nederrijn and Waal are important variables. The storage deficit and the water level in the Maurikse Wetering are relevant variables as well. This suggests that the storage deficit, being the dryness of the unsaturated zone (Brauer et al., 2014a) (Brauer et al., 2014b) is more important than the groundwater level of the main aquifer.

## 5.4 Chapter summary

In this chapter, it was researched if the net IGF flux can be expressed in terms of variables within the catchment and the water levels of the Nederrijn and Waal rivers. First the water levels of the Nederrijn and Waal were plotted against eachother and other variables for a better understanding of the relations between these variables. Then the data is subjected to simple- and multiple linear analyses. Using the simple linear regression (SLR) analysis, a relation was found for the period of July 2015 to March 2018 between the net IGF and the water level in the Nederrijn. For the entire time frame, this relation does not hold and a multiple linear regression (MLR) analysis is performed. The MLR shows that the net IGF can be expressed as a function of the Waal level, the groundwater level, the precipitation, the storage deficit in the unsaturated zone and the water level in the Maurikse Wetering. During periods of high water levels in the Waal and Nederrijn for the period 2015 - 2018, the IGF increases. This is in accordance with the findings in chapter 4. As discussed in chapter 4, it was suspected that the interaction between the Waal and Nederrijn would cause the change in IGF quantity around June 2015. This does not show from the MLR analysis, which omits the Nederrijn level.

The SLR relation can be seen as more robust for the period 2015 – 2018, as this only requires a single parameter and has a high efficiency for the time it was calibrated to. The MLR analysis is better applicable for the entire range of data however. The inability of the Nederrijn relation to estimate the IGF for the period 2013 – 2015 can be due to IGF sources outside the studied variables, as section 4.3 shows that the Utrechtse Heuvelrug is a possible source of IGF. Because the Utrechtse Heuvelrug lies outside the study area, this can not be analysed further.

# 6 WALRUS MODEL

In this chapter the acquired data and insights will be combined to make a WALRUS model of the Maurikse Wetering catchment. The code for WALRUS needs to be altered to meet the desired output, then the model will be calibrated. The adaptation of the default WALRUS discharge formula as well as the channel depth will be discussed in section 6.1. The calibration in section 6.2 provides the best fit parameter set as the result of a Monte Carlo analysis for a model with IGF data, whereas the calibration in section 6.3 provides the best fit parameter set as the result of a Monte Carlo analysis for a model without IGF data. Section 6.4 shows the resulting best fit WALRUS models, with section 6.5 expanding on this by showing the results above a certain efficiency. In section 6.6 the models are validated, and the models are compared in section 6.7.

This will result in a conceptual hydrological model for the Maurikse Wetering.

## 6.1 Building a WALRUS model

Creating a WALRUS model for the Maurikse Wetering catchment requires some adaptation of the code in WALRUS.

### 6.1.1 Channel depth and discharge formula

The average channel depth of all waterways in the Maurikse Wetering catchment was determined to be 2.34 m. The channel depth at Buren, where the discharge formula was calibrated to, is 4.05 m. This is elaborated on in Appendix C.

The conversion factors account for changing the input values to the same unit as the output. The original weir formula resulted in the desired output of discharge Q in $m^3/s$. As the desired output for WALRUS is mm/d, the conversion factor is introduced:

$$[\boldsymbol{Conversion\ factors}] = \frac{\left[\frac{\boldsymbol{mm}}{\boldsymbol{d}}\right]}{\left[\frac{\boldsymbol{m^3}}{\boldsymbol{s}}\right]} = \frac{\boldsymbol{1000 * 86400}}{\boldsymbol{Area}} = \frac{\boldsymbol{1000 * 86400}}{\boldsymbol{84.5 * 10^6}} = \boldsymbol{1.022}\ [-] \tag{6.1}$$

In this formula the water depth h is a variable, computed by WALRUS, not necessarily a data point with the same value as in the original weir formula. Filling in the constants results in the following discharge formula:

$$\boldsymbol{Q = 55.36 * \left(\max\left(\frac{h}{1000} - 0.47 * \frac{h_s}{1000}\right)\right)^{\frac{3}{2}}} \tag{6.2}$$

## 6.2 Calibration model with IGF

The model is calibrated using the Monte Carlo method to the groundwater depth and the discharge as modelled by MORIA. To acquire the best parameter set, the resulting Nash-Sutcliffe efficiencies will be multiplied. The highest value of this product will be the best model. As this will not result in a perfect model, all parameter sets with a resulting efficiency above a certain threshold will be used to plot the uncertainty range in which the actual discharge/groundwater level is very likely to be.

### 6.2.1 Calibration to groundwater level

The model is first calibrated to the groundwater depth. The resulting parameter sets are plotted against their corresponding NS value in Figure 6-1. In Figure 6-1 the parameter value with the highest possible NS efficiency is also plotted.

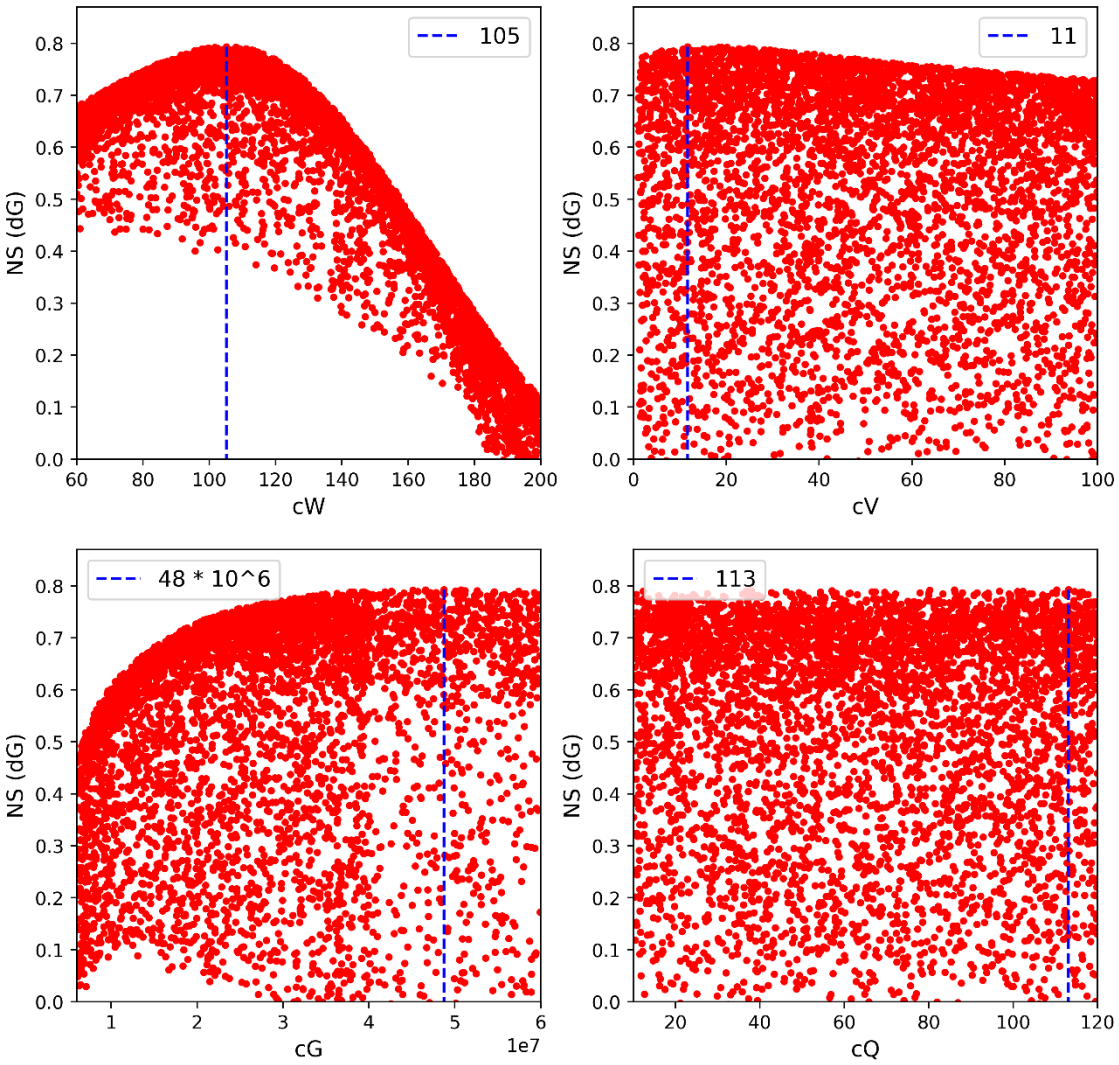


**Figure 6-1, results calibration of the 4 WALRUS parameters to groundwater depth $d_G$, with the location of the optimal (maximum) value in blue**

As can be seen Figure 6-1, the model is insensitive to $c_Q$ when calibrated to the groundwater level as modelled by MORIA. This makes sense, because $c_Q$ concerns the time it takes to empty the quickflow reservoir which does not affect the groundwater table. There would be some influence from $c_Q$ if the exchange between the groundwater and surface water was a function of (among

others) the modelled surface water level, but this was changed to the water level data as described in section 6.1.1.

The model seems to be most sensitive to the parameter $c_W$, as this parameter has the most pronounced maximum. A 10 % change in either direction will have the most consequences in terms of change in NS value (and thus curve fit) of all parameters. The parameter $c_G$ appears rather stable in the 30 * $10^6$ to 60 * $10^6$ range, but the NS efficiency quickly drops for lower values.

### 6.2.2 Calibration to discharge as modelled by MORIA

MORIA modelled the daily exchange between groundwater and surface water as well as quickflow through the soil, for instance via drainage, macropores and cracks. Except for saturation or hortonian overland flow, where water flows overland because the soil is fully saturated or where the infiltration capacity is reached respectively, these two fluxes account for the discharge generated on land. The precipitation and evaporation directly on the surface water are taken into account by WALRUS, but this will likely not play a large role as only 1 % of the catchment area is assumed to consist of surface water. This combined flux from MORIA is therefore taken as the discharge Q. The primary reason for using this modelled discharge data is to determine the quickflow parameter $c_Q$, as section 6.2.1 shows that the model is insensitive to parameter $c_Q$ when calibrating the WALRUS model to the groundwater level.

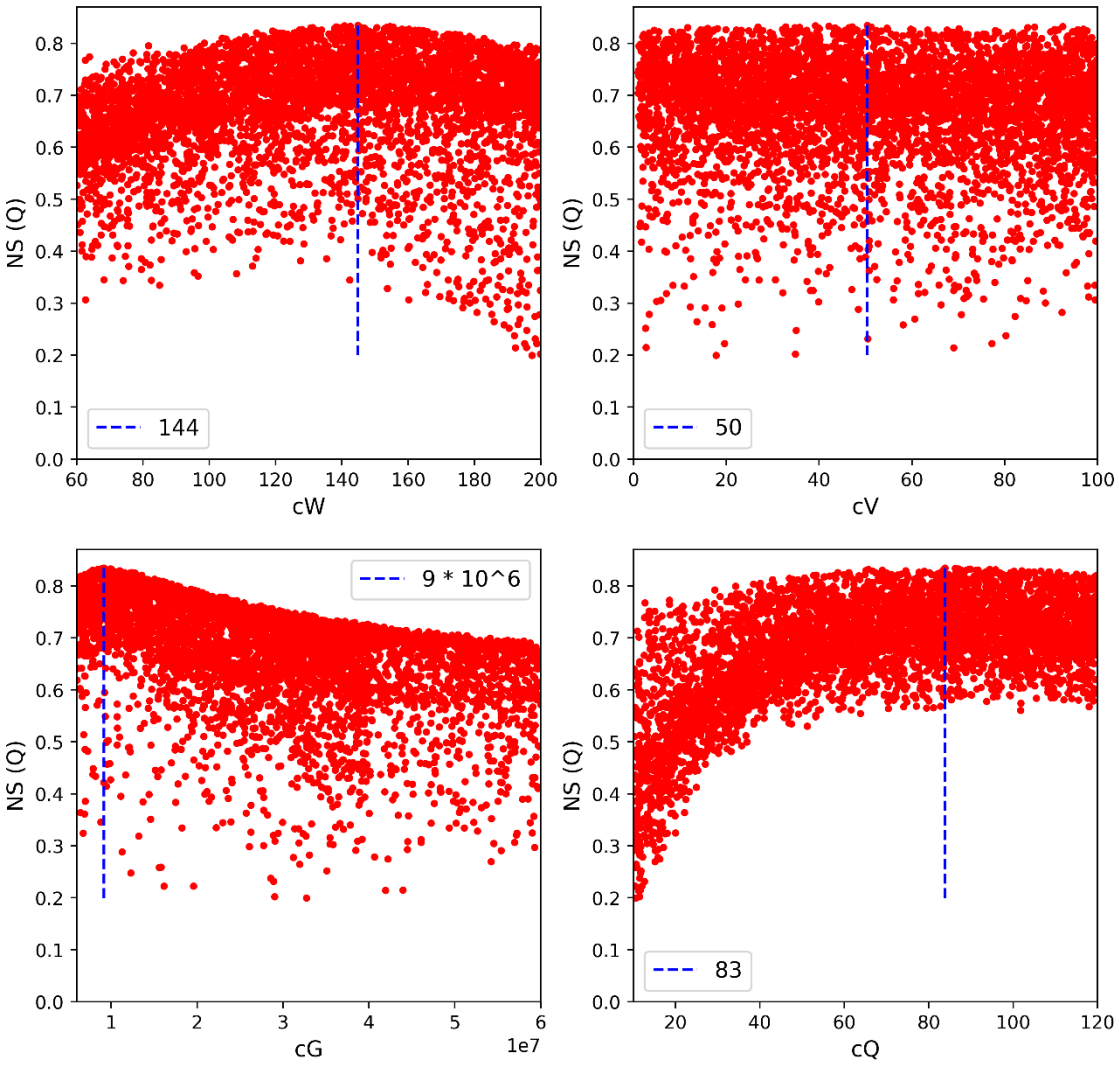


**Figure 6-2, results calibration of the 4 WALRUS parameters to discharge modelled by MORIA, with the location of the optimal (maximum) value in blue**

From Figure 6-2 it can be seen that the model is rather insensitive to parameter $c_V$. When $c_V >> 100$, the resulting NS values begin to drop. For the set boundaries the optimum for $c_V$ for the calibration to groundwater is a lot more pronounced and as there is no optimum outside these boundaries for calibration to groundwater no expansion of boundaries is needed. Unlike the calibration to groundwater level the model is sensitive to parameter $c_Q$. This was expected as the emptying of the quickflow reservoir is important in determining the discharge.

### 6.2.3 Calibration to both groundwater level and discharge as modelled by MORIA

For the best representative model, the results of the calibration to both groundwater level and discharge should be combined. Multiplying the respective NS values for the product of said NS values gives the optimal combination of parameter values to fit both processes well.

The product of the NS values was chosen, not the sum. A very good fit for one process and a bad fit for the other process would be inferior to an average fit for both processes with the same summed NS values, as the poor performance for one process would mean an unrealistic model and would likely not hold up in later predictions.

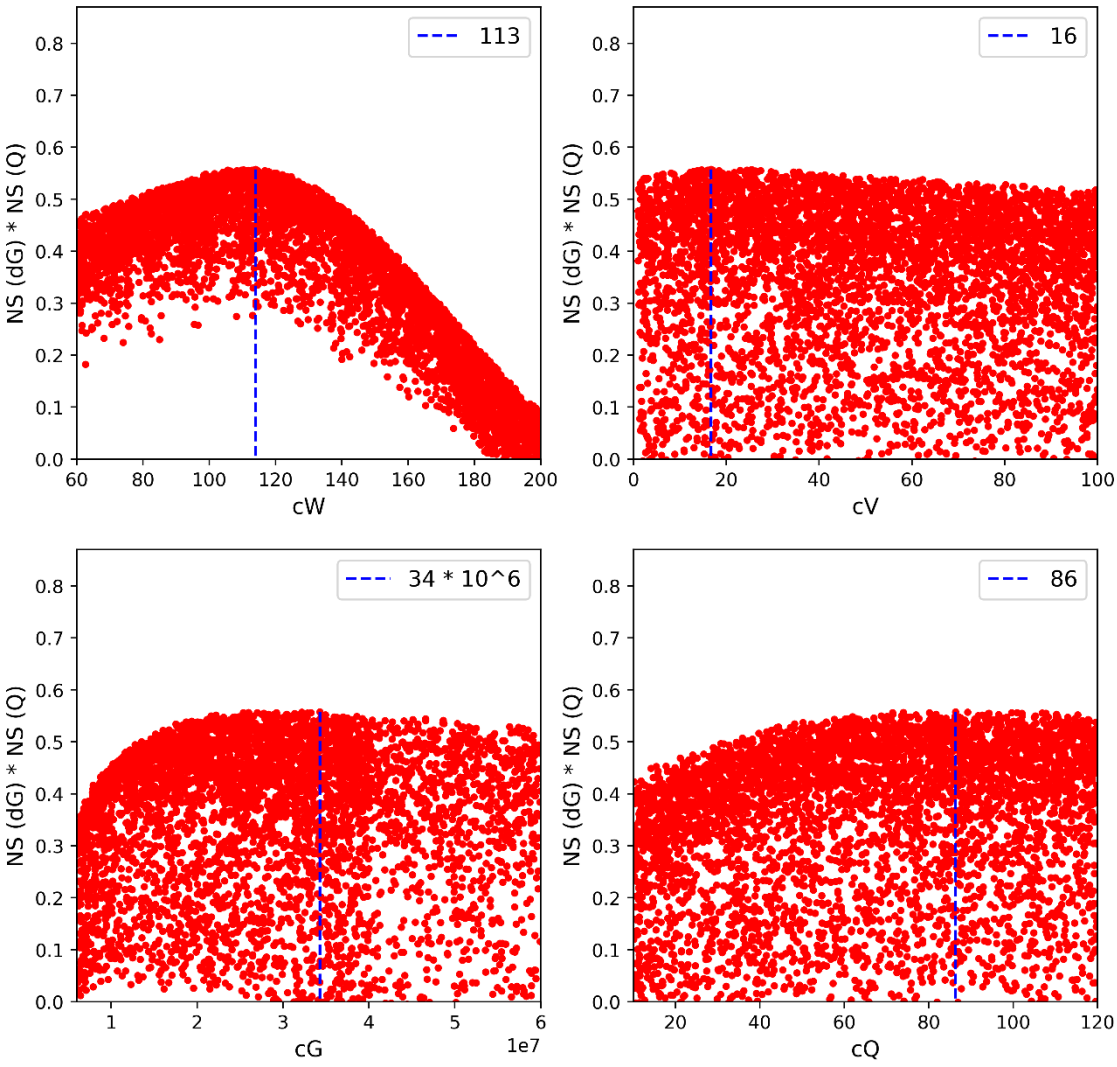


**Figure 6-3, results plotted against the product of Nash-Sutcliffe of calibrations of the 4 WALRUS parameters to groundwater depth and discharge as modelled by MORIA, with the location of the optimal (maximum) value in blue**

| Process | NS best fit dG | NS best fit Q | NS best fit product |
|---|---|---|---|
| *Groundwater level* | 0.79 | 0.40 | 0.77 |
| *Discharge* | 0.68 | 0.83 | 0.72 |
| *Product NS ($d_G$) * NS(Q)* | 0.54 | 0.33 | 0.56 |

**Table 6-1, NS values best fit for both groundwater level dG and discharge Q and their product**

More parameter sets in Monte Carlo analysis would likely bring product results for $c_V$ closer to the $c_V$ value for the optimal fit of groundwater level $c_Q$ closer to the $c_Q$ value for the calibration to discharge.

It can be argued that the discharge modelled by MORIA is less accurate than the groundwater level as modelled by MORIA. As MORIA is a groundwater model, any water that does not enter the soil will not be considered without additional (Vermeulen, 2018). Therefore, saturation- or hortonian overland flow will not be considered by MORIA. These flows will only noticeably occur during heavy storms, so this will not affect the overall model efficiency that much. But it can mean that MORIA can underestimate the peak discharges.

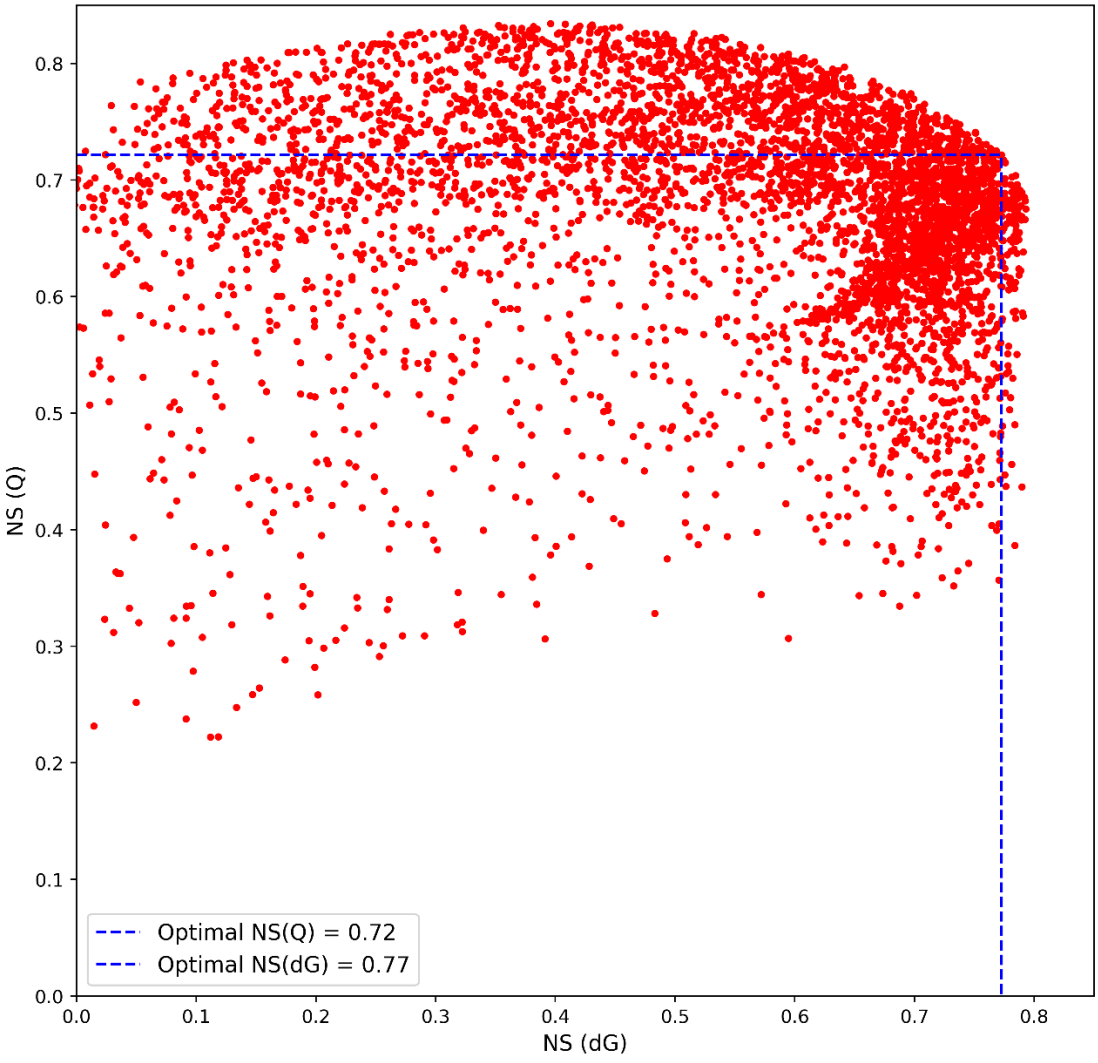


**Figure 6-4, Nash-Sutcliffe groundwater depth to Nash-Sutcliffe discharge as modelled by MORIA**

It can be seen from Figure 6-4 that results for discharge tend to have a good fit over a wider range of outcomes for results for groundwater level than vice versa.

## 6.3 Calibration model without IGF

To see if incorporation of intercatchment groundwater flow changes the WALRUS model for the Maurikse Wetering, and if so in what way, the model is calibrated using a Monte Carlo analysis again. This time the IGF data is omitted/set to null. If the incorporation of IGF is relevant, the model parameters of the best fit should differ from the previous outcome.

### 6.3.1 Calibration to groundwater level

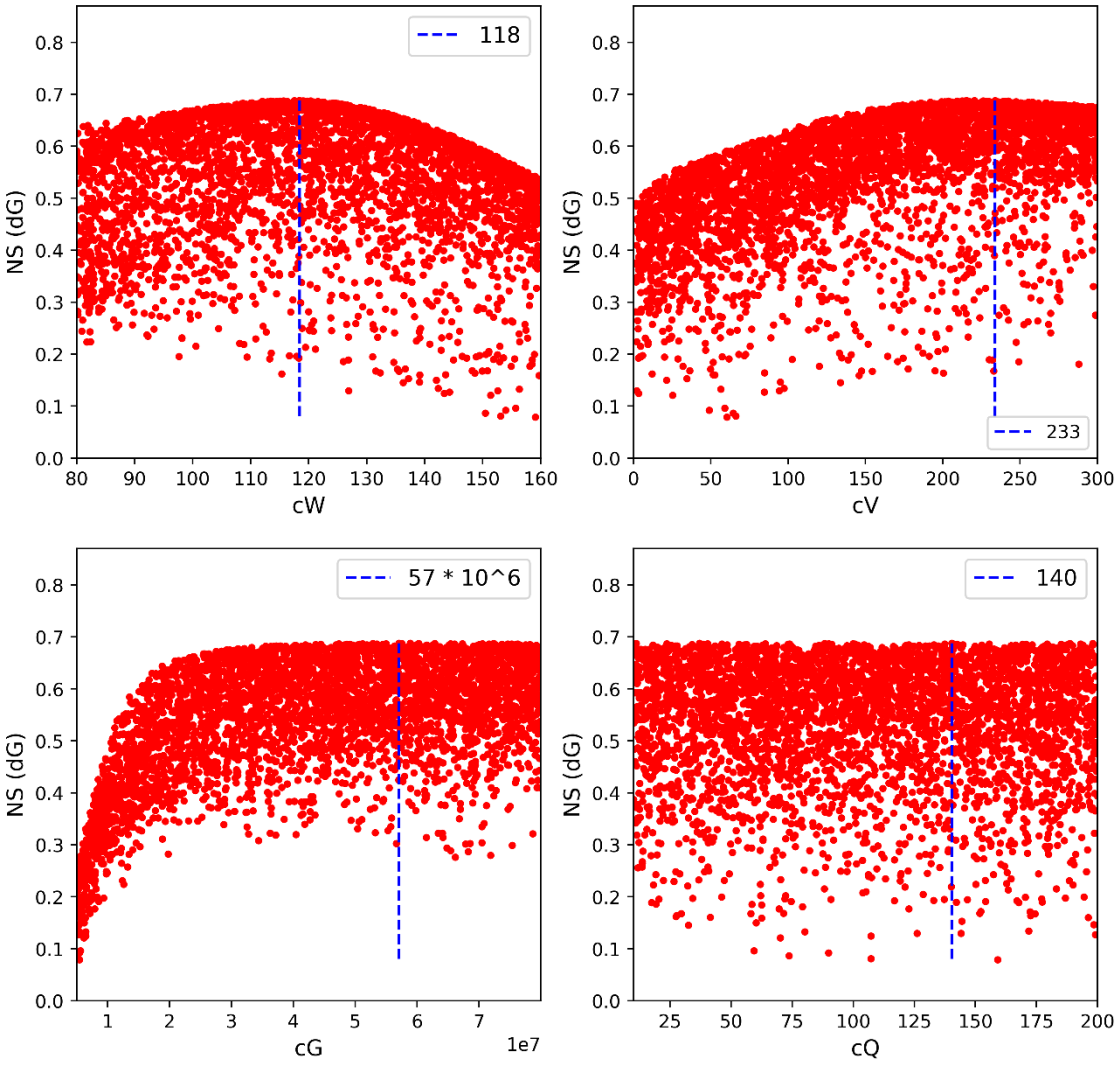


**Figure 6-5, calibration of the 4 WALRUS parameters to groundwater level for model without IGF, with the location of the optimal (maximum) value in blue**

Figure 6-5 shows the calibration to the groundwater level. Comparing this to Figure 6-1, the calibration to the groundwater level with IGF data, several differences are noticeable.

Table 6-2 shows the parameter sets that form the best fit with and without IGF. The values for $c_V$ differ by more than a full order of magnitude. Unlike parameter $c_Q$, which has no clear optimum in either calibration, in both situations the parameter $c_V$ has a clear optimum. This shows a significant effect that the inclusion of IGF has. Parameters $c_W$ and $c_G$ both differ by 12 % and 16 % respectively. These changes are not as significant as the difference in $c_V$, but nonetheless not negligible.

| Parameter | Best fit dG with IGF | Best fit dG without IGF | Difference to "with IGF" |
|---|---|---|---|
| $c_W$ | 105 | 118 | + 12 % |
| $c_V$ | 17 | 233 | + 1271 % |
| $c_G$ | 49 * $10^6$ | 57 * $10^6$ | + 16 % |
| $c_Q$ | 113 | 140 | + 24 % |

**Table 6-2, comparing parameter sets for best fit to GWL with and without IGF**

The curve that the plot for $c_W$ makes is gentler for the calibration without IGF data. This implies that the model with IGF data is more sensitive to the parameter $c_W$. The plot for $c_G$ is steeper for lower values of $c_G$. The best fit with IGF data from MORIA has an NS efficiency of 0.79. The best fit without IGF data has an NS efficiency of 0.69. The curve fit with IGF data is thus considered "very good", whereas the curve fit without IGF is considered "good" according to Moriasi et al. (2007).

### 6.3.2 Calibration to discharge as modelled by MORIA

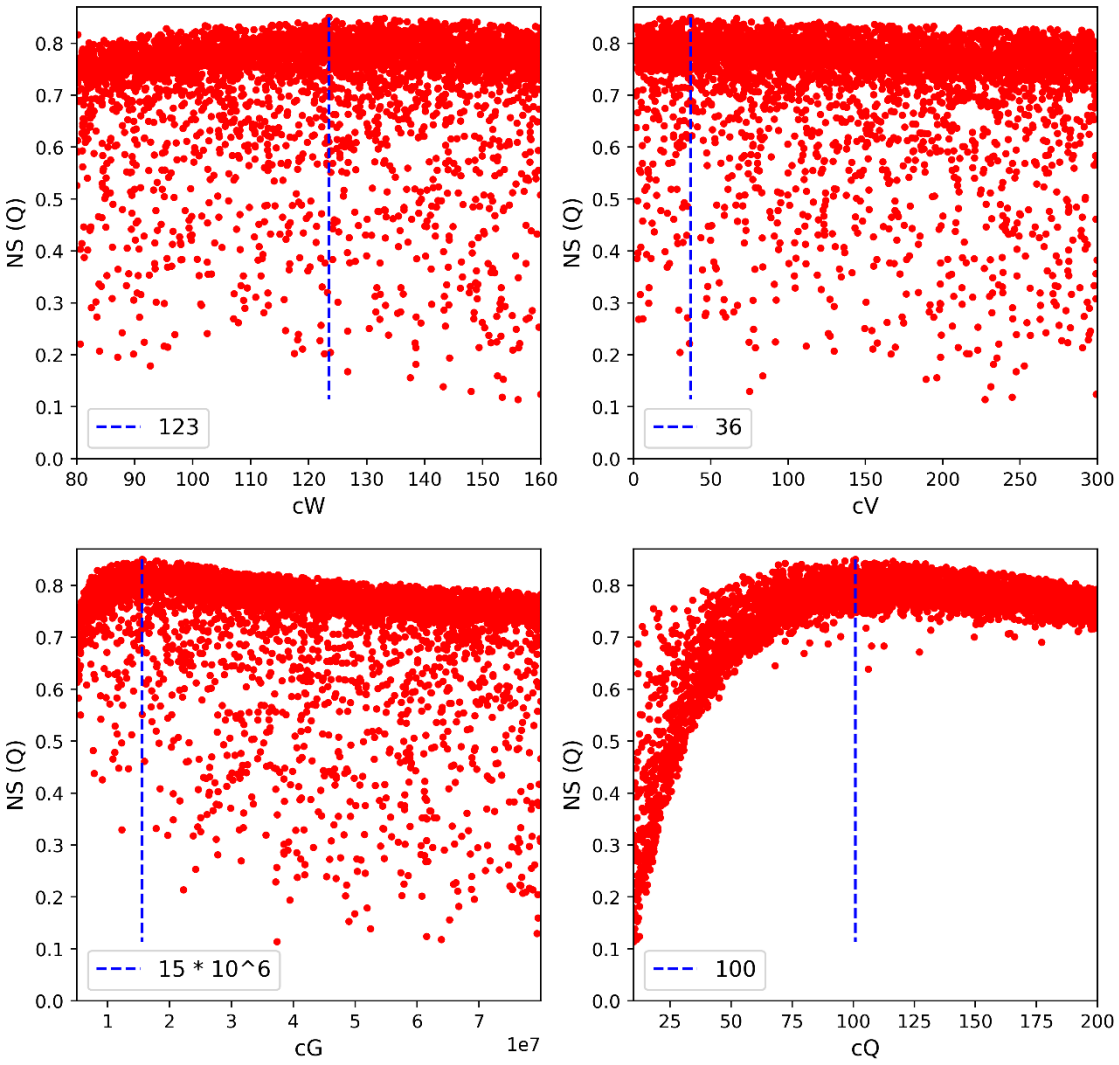


**Figure 6-6, calibration of the 4 WALRUS parameters to discharge for model without IGF, with the optimal (maximum) value in blue**

Looking at Figure 6-6, the course of $c_W$ is gentler for the model without IGF data as with IGF data. The same is true for $c_G$.

### 6.3.3 Calibration to both groundwater level and discharge as modelled by MORIA

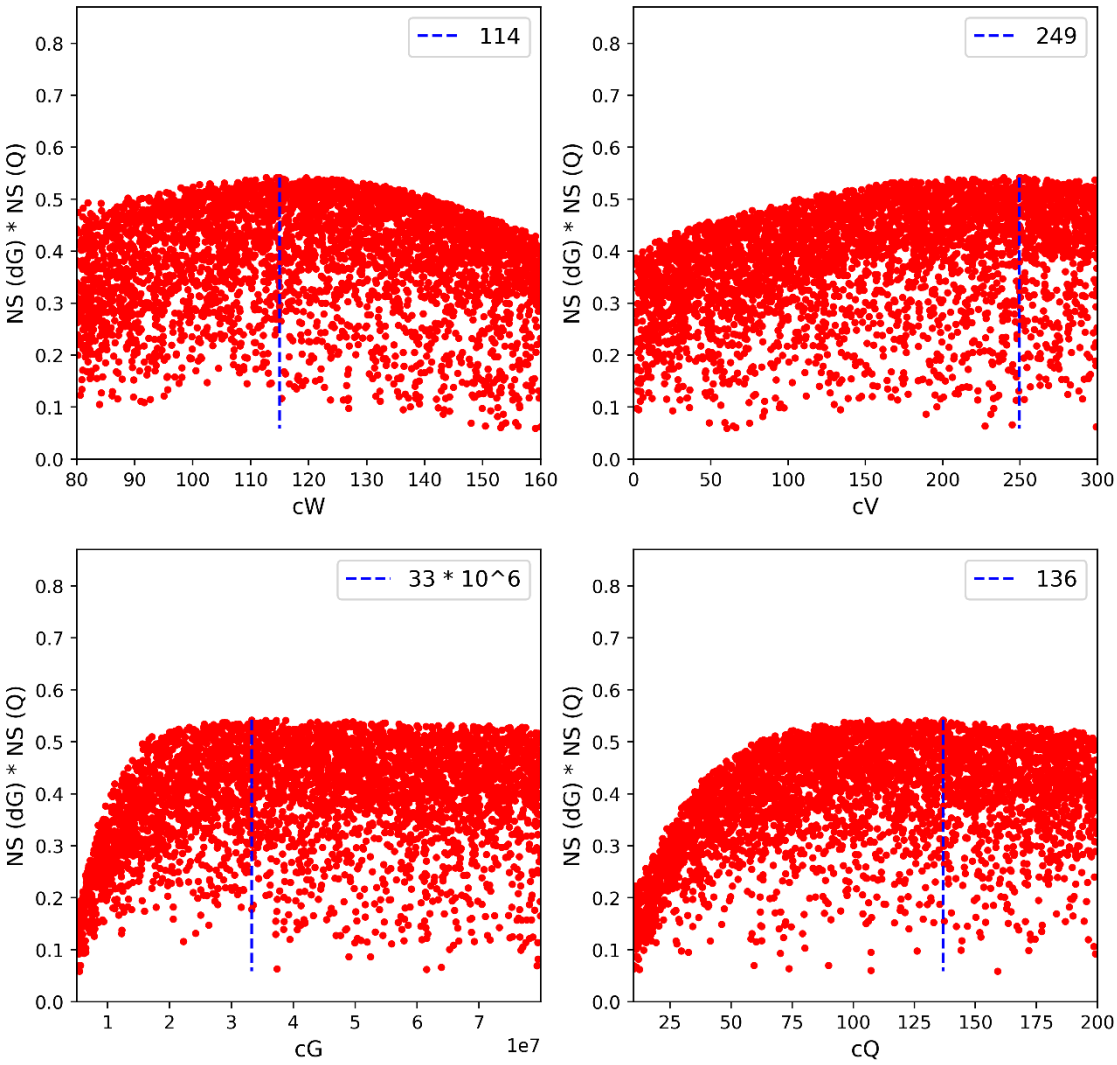


**Figure 6-7, calibration of the 4 WALRUS parameters to the product of groundwater level and discharge for model without IGF, with the location of the optimal (maximum) value in blue**

For the combination of discharge and groundwater level the parameters $c_W$, $c_V$ and $c_Q$ have clear optimum values as seen in Figure 6-7. For low values, the NS efficiency related to parameter $c_G$ drops sharply. For larger values the slope is more gentle, almost horizontal.

| Parameter | Best fit product with IGF | Best fit product without IGF | Difference to "with IGF" |
|---|---|---|---|
| $c_W$ | 114 | 115 | + 1 % |
| $c_V$ | 17 | 250 | + 1371 % |
| $c_G$ | $34 * 10^6$ | $33 * 10^6$ | + 3 % |
| $c_Q$ | 86 | 137 | + 59 % |

**Table 6-3, comparing parameter sets for best fit to the product of GWL and discharge with and without IGF**

In Table 6-3 the best fit parameter values for the combination of discharge and groundwater level are put next to each other. it can be seen that the values for $c_W$ and $c_G$ are almost equal, which suggests that these parameters are not affected by IGF. The values for $c_Q$ and especially $c_G$ differ from one scenario to the other.

| Process | NS best fit dG | NS best fit Q | NS best fit product |
|---|---|---|---|
| *Groundwater level* | 0.69 | 0.41 | 0.68 |
| *Discharge* | 0.77 | 0.85 | 0.79 |
| *Product NS ($d_G$) * NS(Q)* | 0.53 | 0.35 | 0.54 |

**Table 6-4, comparing NS efficiencies for the best fit for the WALRUS model without IGF**

The NS efficiencies for the model without IGF are shown in Table 6-4. The best fit to the groundwater level models the discharge well, but the best fit for the discharge models the groundwater level poorly. The NS efficiencies of the best fit for both discharge and groundwater level is close to the NS efficiencies of the best fit to the groundwater level.

| Parameter | Best fit dG | Best fit Q | Best fit product |
|---|---|---|---|
| $c_W$ | 118 | 123 | 115 |
| $c_V$ | 234 | 37 | 250 |
| $C_G$ | $57 * 10^6$ | $16 * 10^6$ | $33 * 10^6$ |
| $C_Q$ | 140 | 101 | 137 |

**Table 6-5, parameter sets for the best fit for the WALRUS model without IGF**

Looking at Table 6-5, the largest difference between parameter values for the different scenarios is found in the value for $c_V$.

## 6.4 Resulting WALRUS model

The parameters with the highest NS efficiency to both the average groundwater level and discharge as modelled by MORIA from the calibration will be entered in WALRUS. The NS efficiency for the groundwater level will be displayed as "NS (GWL)" in the third graph of the WALRUS output, and the NS efficiency for the discharge will be shown as "NS (Q)" in the fourth graph.

### 6.4.1 WALRUS model with IGF relation

To test the quality of the WALRUS model with the IGF relations, the model is first run with the IGF data as modelled by MORIA for the calibration period 9-2015 – 4-2017. The outcome of this model is shown in Figure 6-8.

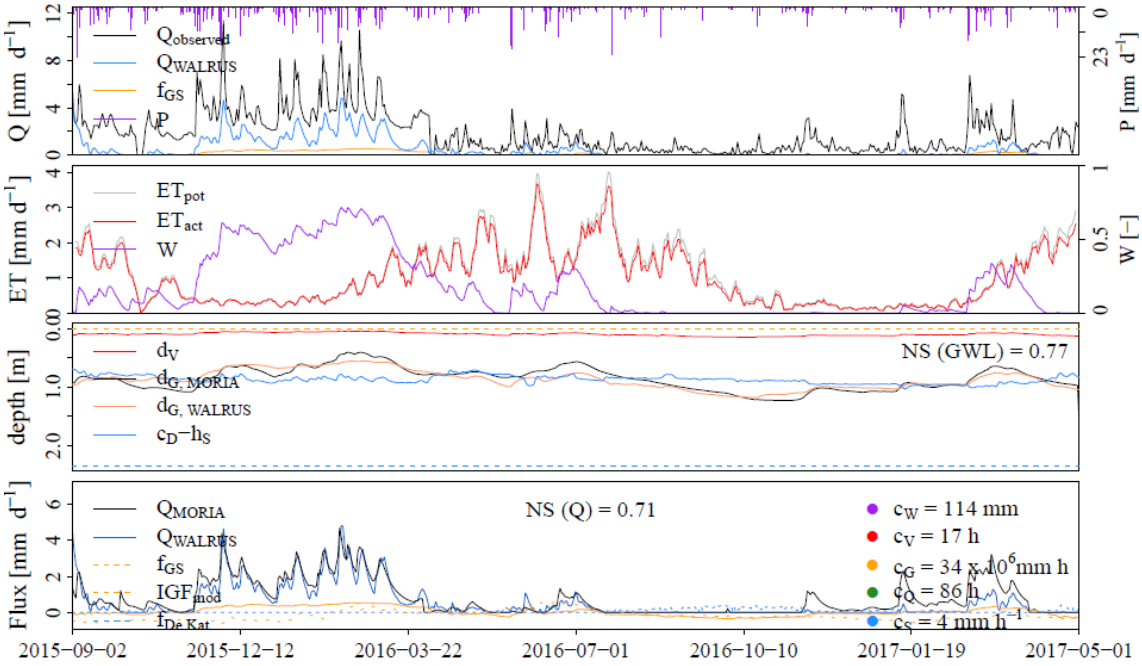


**Figure 6-8, output WALRUS model for the period 9-2015 – 4-2017 with IGF data as modelled by MORIA.**

In Figure 6-8, the top figure shows the discharge data from the stuw at Buren as given by the Rivierenland Water Board as the black line ($Q_{original}$) and the modelled data by WALRUS in blue ($Q_{mod}$). This was plotted to give an indication of the error in the discharge data from Rivierenland, assuming that the discharge as modelled by MORIA and WALRUS are a realistic approximation of reality. As the courses of both graphs are roughly the same, it can be concluded that the problem with the data from Rivierenland only lies in an offset of the weir level, either a linear offset (due to for instance the weir data being multiplied by an unknown factor introduced in data conversion) or an added constant (due to an erroneous reference level). The bottom figure in Figure 6-8 shows the discharge as modelled by MORIA in black ($Q_{obs}$), which is the discharge data the model is calibrated to.

The IGF relation established between the intercatchment groundwater flow and the Nederrijn level in chapter 5 will now be entered in WALRUS. As the model is already calibrated to the IGF data it will not be calibrated to the modelled data from this relation. Calibrating the model to this would divert the WALRUS model from reality.

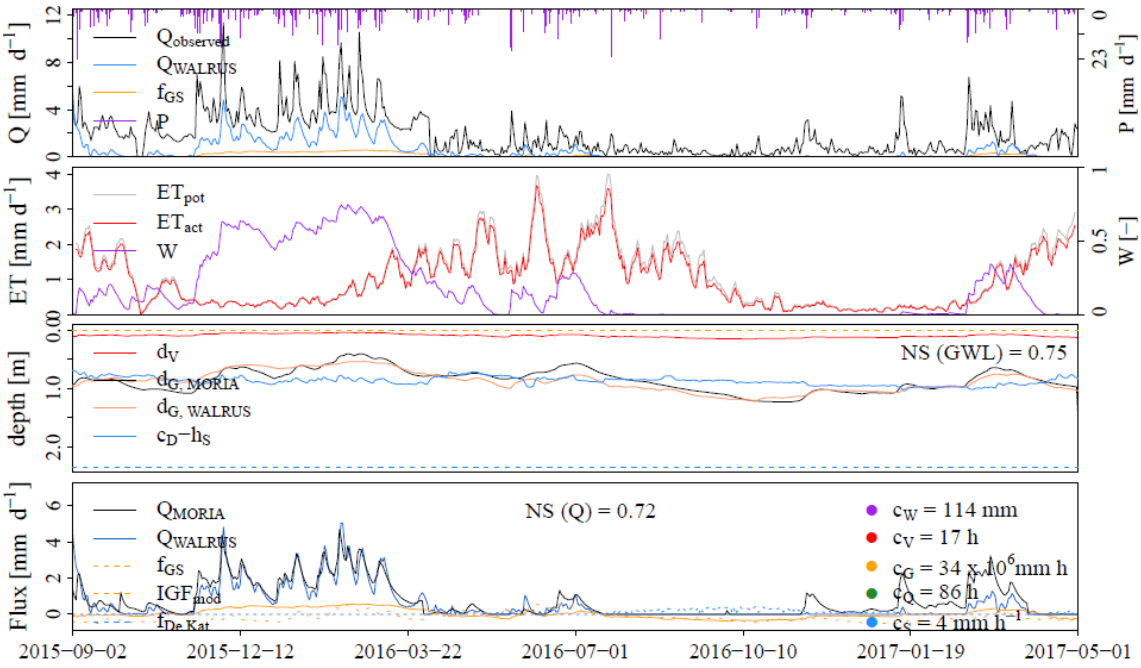


**Figure 6-9, output WALRUS model for the period 9-2015 – 4-2017 with the IGF relation from the MLR.**

The input IGF data as modelled by MORIA is replaced by the IGF data resulting from the IGF relation from the MLR analysis from 2015 - 2018 in 5.3.3. The best fit parameter set to both discharge and groundwater level from Table 6-1 is used as input parameter set. The resulting WALRUS output is shown in Figure 6-9.

To see the effects of the IGF relation with the Nederrijn, the best outcome of the SLR analysis, are comparable with the relation from the MLR, WALRUS is run with the IGF from the Nederrijn relation. The result is shown in Figure 6-10.

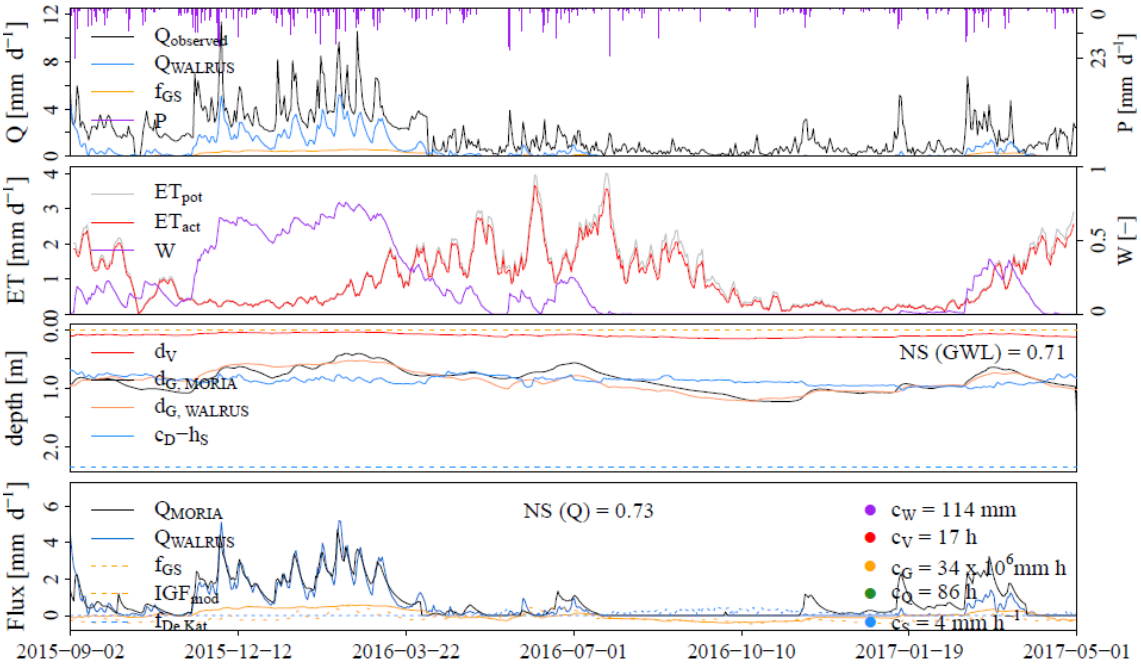


**Figure 6-10, output of the WALRUS model for the period 9-2015 – 4-2017 using the IGF relation to the Nederrijn.**

Comparing Figure 6-9 with Figure 6-10 shows similar results, with the Nash-Sutcliffe efficiency to the groundwater level being better for the MLR analysis. This is expected, as the MLR analysis models the IGF better than the relation with just the Nederrijn.

For both WALRUS outcomes in Figure 6-9 and Figure 6-10, the course of the groundwater level is followed well, both over months as well as over shorter periods. However, the slope is often a bit less for the data modelled by WALRUS. The discharge is modelled quite well, except for just after the dry period. The dry period occurs when the discharge as modelled by MORIA is negative, meaning surface water infiltrates to the groundwater reservoir. To stop the water level from lowering, water is being let into the system (as would be the case in reality via the inlet at De Kat). After this period where the wetness W is zero, the WALRUS model takes longer to model discharge again.

This is likely because the modelled average groundwater level is below the surface water level, meaning water infiltrates to the groundwater reservoir. The unsaturated zone needs to be replenished by precipitation for the wetness to increase, which would result in quickflow. I do not know why this does not occur for instance during November 2016 in Figure 6-10, where it appears that enough precipitation occurs. Perhaps the storage deficit $d_V$ requires a certain threshold, but this is not clear from the formulas or the literature.

| **Process** | **NS MORIA data** | **NS MLR** | **NS Nederrijn relation** |
|---|---|---|---|
| *Groundwater level* | 0.77 | 0.75 | 0.71 |
| *Discharge* | 0.71 | 0.72 | 0.74 |
| *Product NS ($d_G$) * NS(Q)* | 0.56 | 0.54 | 0.53 |

**Table 6-6, comparing NS values of the WALRUS model with MORIA data as seen in Figure 6-8, the model with the IGF modelled by the MLR analysis as seen in Figure 6-9 and the WALRUS model with the IGF modelled by the relation with Nederrijn level as seen in Figure 6-10.**

In Table 6-6 the results for the best fit to both discharge and groundwater level are compared for the model with IGF data as modelled by MORIA and the model with IGF data derived from the IGF relations. The same parameter set is used, gained from the calibration in section 6.2.3. As can be seen, the NS efficiency to the groundwater level drops by 3 % and 8 % for the model with the MLR analysis and Nederrijn relation respectively. Surprisingly, the NS efficiency to the discharge increases by 3 % to 0.74. The product of the NS efficiencies drops by 5 % to 0.53.

From these results it appears that the model with IGF relation is a good fit for both discharge and groundwater level. The results do not differ significantly from the data as modelled by MORIA.

### 6.4.2 WALRUS model without IGF

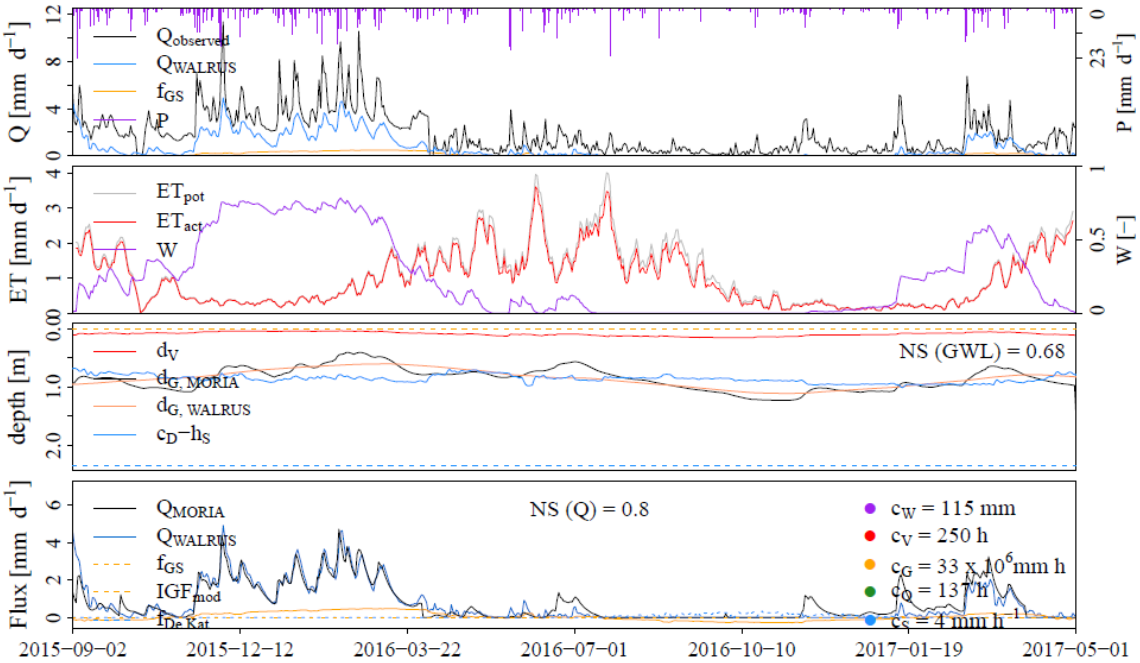


**Figure 6-11, output of the WALRUS model for the period 9-2015 – 4-2017 without an IGF flux.**

In Figure 6-11 the top plot shows the discharge data as provided by Rivierenland in black, the bottom plot shows the discharge as modelled by MORIA in black. The curve fit to the discharge is very good until June 2016. The fit with the groundwater level is poor, only the broad rising and lowering of the groundwater level is modelled without any fluctuations. This is due to the high $c_V$ value, which is the "vadose zone relaxation time" in hours (Brauer et al., 2017). This influences the exchange between the vadose zone/unsaturated zone and the groundwater reservoir. If this value is high, the change in water flowing from the unsaturated zone to the groundwater reservoir or vice versa is small. This results in very little fluctuation over short timeframes.

## 6.5 Spread

As the best fit model does not have a perfect fit with the data from MORIA, the best fit in WALRUS is insufficient to confidently predict every outcome. It is therefore better to additionally show a spread in which the actual values lie, as the best fit is only an approximation.

After the calibration via the Monte Carlo analysis, the WALRUS model is run for all parameter sets with an NS value equal to or higher than the set boundary of 0.65 for both groundwater level and discharge as modelled by MORIA. The resulting datasets are saved separately and loaded into Python. In python, the maximum and minimum values of the groundwater level and discharge modelled by WALRUS for all specified parameters is saved in a separate column for each timestep.

The default file for creating figures in WALRUS is changed to incorporate the spread between minimum and maximum values as a band, as well as plotting the outcome of the best fitting parameter set as a line.

### 6.5.1 Spread with IGF relation

The resulting spread for the WALRUS model with the IGF relation is shown in Figure 6-12.

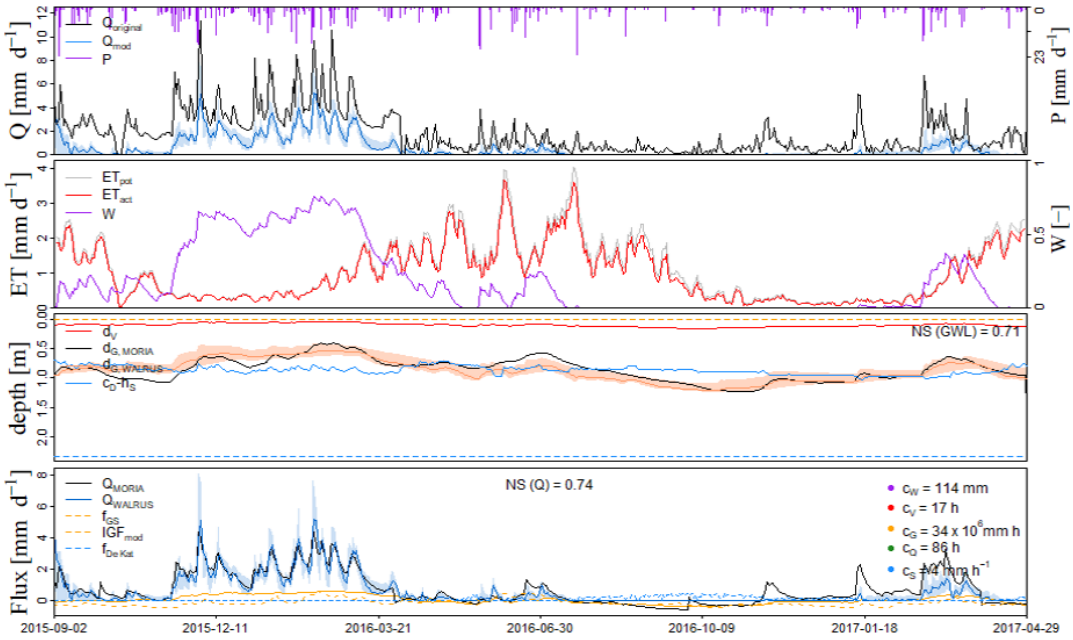


**Figure 6-12, WALRUS model with IGF relation, with spread**

The spread does not cover the entire course of the groundwater level data from MORIA. This can be due to spatial variations taken up by MORIA but that are not taken up by WALRUS. At the end of the dry period even the maximum values of the spread still do not cover the discharge as modelled by MORIA. The rest of the discharge is covered by the spread, making for a good fit outside the end of the dry periods. This can perhaps be mitigated by lowering the NS boundary for which parameter sets are taken in with the spread, but this would increase the model uncertainty.

## 6.5.2 Spread without IGF

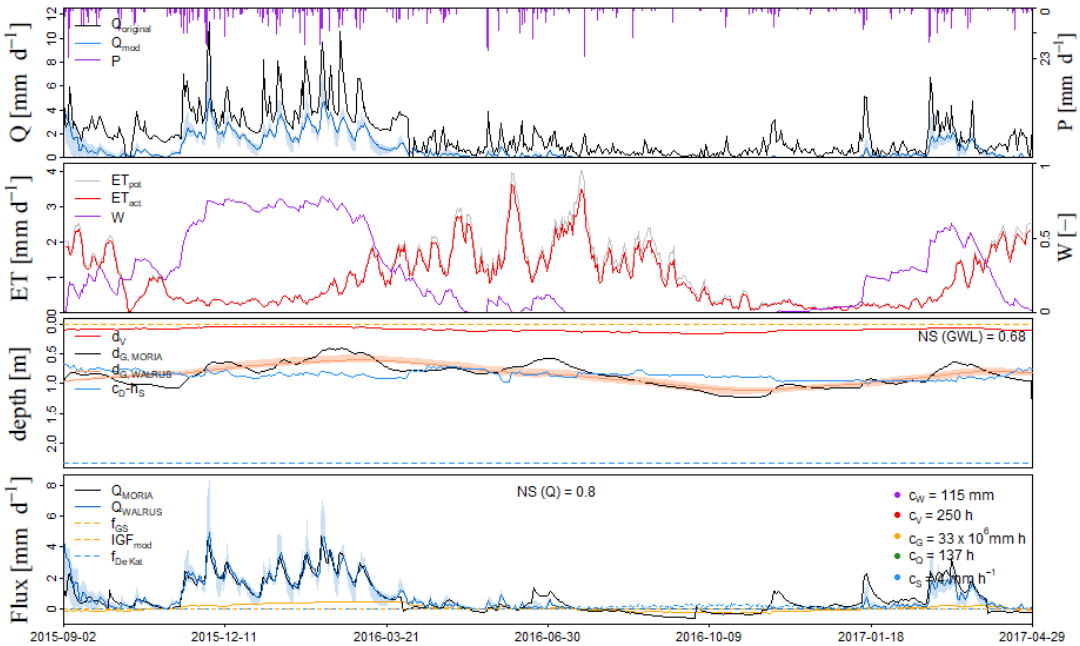


**Figure 6-13, WALRUS model without IGF, with spread**

Comparing Figure 6-12 to Figure 6-13 shows that the groundwater level, even with the spread, is modelled poorly in WALRUS without IGF data as only the long-term rise and fall of the groundwater level is modelled. A wider spread should be used, meaning lowering the boundary for parameter sets to be taken in with the spread.

## 6.6 Model validation

The models with the best fit parameters as determined in section 6.4 are validated using data of the hydrological year of 2017. The validation is first run for the model with IGF data as modelled by MORIA, then for the IGF data as modelled by the best outcomes of the MLR and SLR analyses. Validation is used to determine the predictive capabilities of the model, a model that performs well during calibration but poorly during validation means that the model is wrong due to for instance parameter equifinality.

### 6.6.1 With IGF as modelled by MORIA

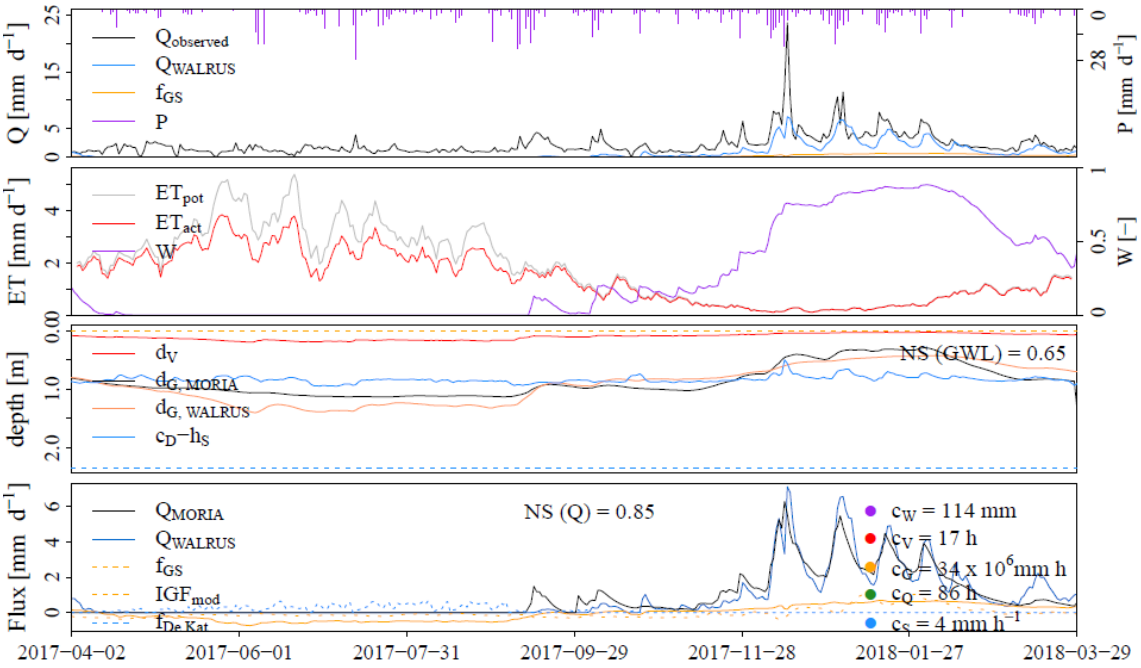


**Figure 6-14, outcome WALRUS model for the validation period 4-2017 – 4-2018 with IGF as modelled by MORIA.**

Figure 6-14 shows the validation of the WALRUS model with IGF as modelled by MORIA. The resulting NS efficiencies of 0.65 for the groundwater level and 0.85 for the discharge show that the model holds up well for the validation period, as a NS efficiency of 0.65 is considered “Good”. The drop in NS efficiency of 0.12.

## 6.6.2 With IGF relation

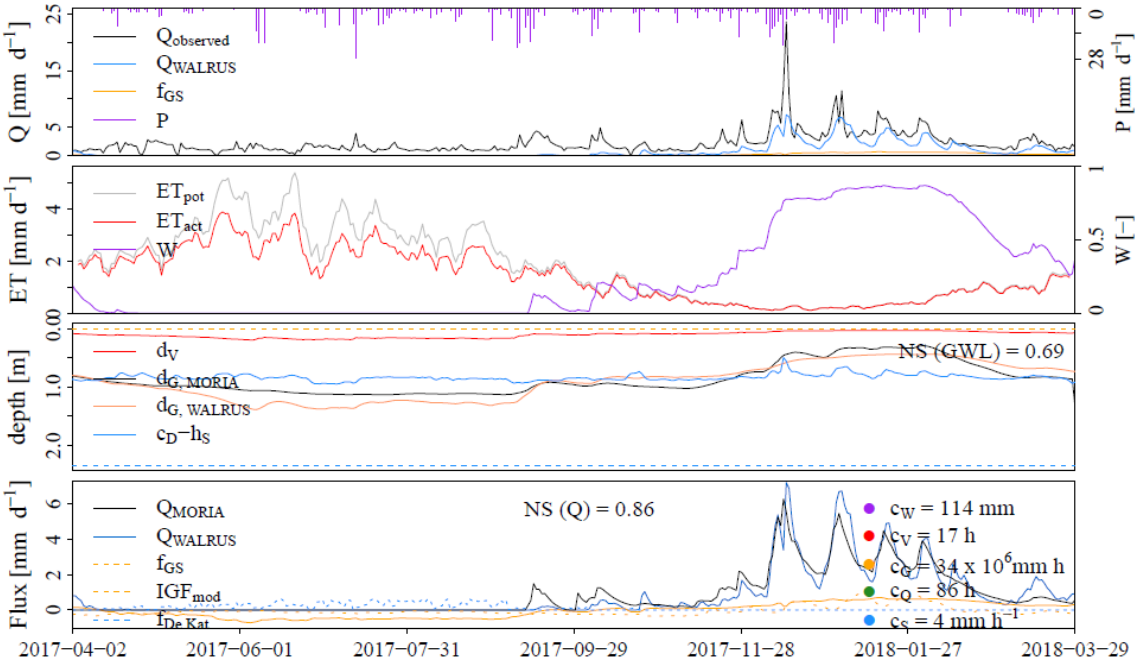


**Figure 6-15 outcome WALRUS model for the validation period 4-2017 – 4-2018 with IGF as modelled by the IGF relation according to the MLR.**

Figure 6-15 shows the validation of the WALRUS model with IGF modelled by the MLR. Comparing the resulting NS efficiencies to those in Figure 6-14 shows that the NS efficiencies increase for both the groundwater level and the discharge compared to the data as modelled by MORIA.

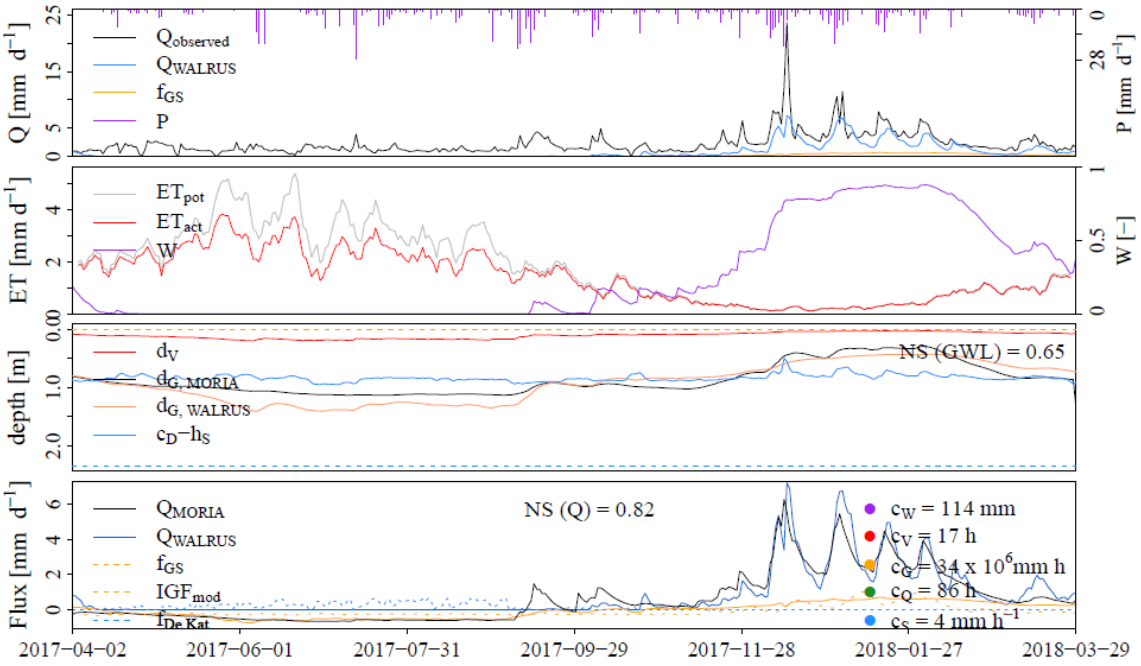


**Figure 6-16, outcome WALRUS model for the validation period 4-2017 – 4-2018 with IGF as modelled by the IGF relation with Nederrijn**

Figure 6-16 shows the validation of the WALRUS model with IGF modelled by the IGF relation with the Nederrijn level. Comparing Figure 6-16 to Figure 6-14, it can be seen that the model with the relation behaves equally to the model with IGF data directly from MORIA.

### 6.6.3 Without IGF

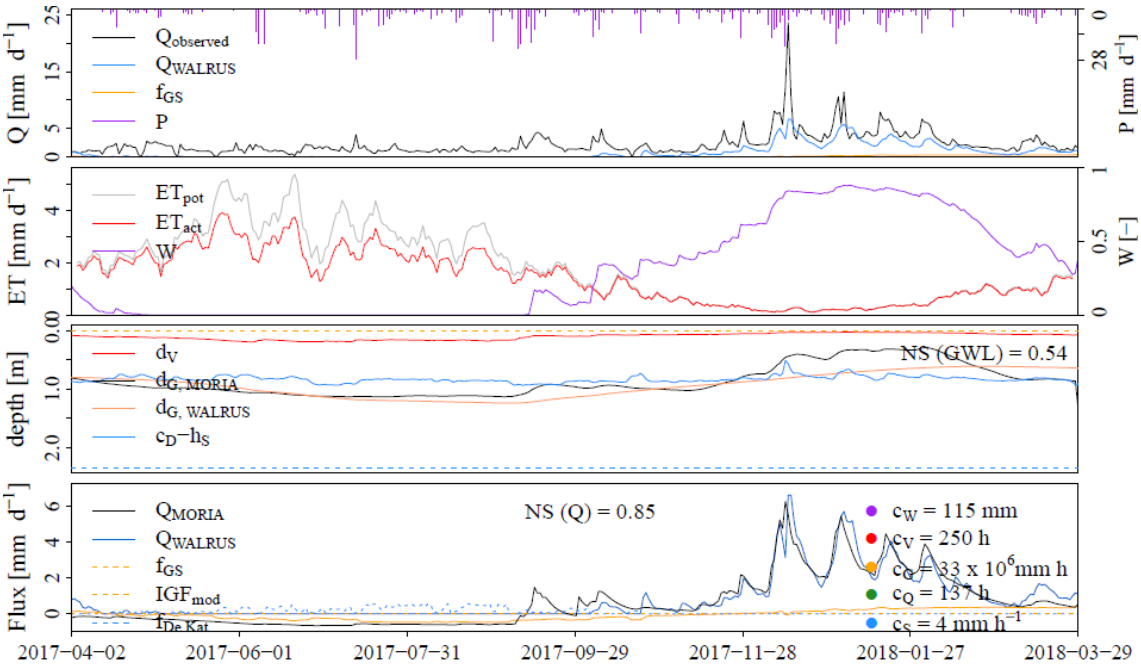


**Figure 6-17, outcome WALRUS model without IGF**

Figure 6-17 shows the validation of the WALRUS model without IGF. As can be seen, the NS efficiency of the groundwater level as modelled by WALRUS to the groundwater level as modelled by MORIA (NS (GWL)) is 0.54 for the model without IGF. Comparing the NS efficiency to the groundwater level to the outcome of Figure 6-14 and Figure 6-16, the NS to the groundwater level drops significantly more for the model without IGF than for the model with IGF. For both models, the NS efficiency to the discharge remains roughly the same.

## 6.7 Comparison

The best fitting parameter set for the model with the IGF relation models the groundwater level better than the best parameter set for the model without IGF. Despite not having a large difference in Nash-Sutcliffe (NS) efficiency, when comparing Figure 6-9 and Figure 6-10 with Figure 6-11, the model without an IGF flux (Figure 6-11) has less variable course and only follows the broad, seasonal change in groundwater level. The models with IGF relation (Figure 6-9 and Figure 6-10) follows the daily variation from the data from MORIA more closely. The maximum NS efficiency to the groundwater level as modelled by MORIA is significantly lower for the model without IGF flux than with IGF flux, both for the best fit model when calibrated only to the groundwater level and for the best fit for both groundwater and discharge. The parameter set with the best fit without IGF does have a higher NS efficiency to the discharge as modelled by MORIA compared to the model with the Nederrijn relation from the SLR analysis.

The poor fit to the groundwater level for the model without IGF data relative to the models with IGF data continues when looking at all parameter sets above a certain NS efficiency (≥ 0.65, which is considered “good” according to Moriasi et al. (2007)).

For either scenario, the model performs poorly when modelling the discharge after a dry period (a period where the groundwater level is below the maintained surface water level). It appears that the WALRUS model takes some time to ‘recover’ from this until providing discharge via quickflow. The model will therefore underestimate the discharge during these times.

Although the discharge as modelled by MORIA is not measured discharge and might be inaccurate, it is assumed that the discharge as modelled by MORIA approaches reality. This is necessary to calibrate the model to the quickflow parameter $c_Q$. It also has the benefit that calibrating to two parameters and combining them decreases the uncertainty of the model.

During validation, both the model with and without the IGF flux have a "very good" fit with the discharge as modelled by MORIA. The model with IGF data as modelled by the IGF relation with the Nederrijn has a NS efficiency of 0.82, compared to the slightly higher NS efficiency for the model without IGF of 0.85. The highest NS efficiency is reached by the model with IGF data as modelled by the MLR, which is 0.86. These numbers are comparable however, and their difference can be considered negligible. However, the model with the IGF relation to the Nederrijn has a NS efficiency to the groundwater level of 0.65 (deemed "good", according to Moriasi et al. (2007)), compared to the NS efficiency to the groundwater level of the model without IGF of 0.54 (deemed "satisfactory", according to Moriasi et al. (2007)). The model with the IGF as modelled by the MLR analysis has the highest NS efficiency to the groundwater level, with a value of 0.69. This is an improvement of 28 % when compared to the model without IGF. This shows the improvement of the WALRUS model by adding the IGF flux.

## 6.8 Chapter summary

A WALRUS model was created for the Maurikse Wetering, which was calibrated to both the average groundwater level and the discharge as modelled by MORIA. This was done for both the model with and without an IGF flux.

The best outcome of the multiple linear regression analysis in chapter 5 and the best outcome of the simple linear regression analysis in chapter 5 were set to replace the modelled IGF data from MORIA. Both these WALRUS models and the WALRUS model without an IGF flux were validated using data for the hydrological year of 2017. The results were then compared to each other, which shows the improvement of the WALRUS model by adding the IGF flux.

This comparison showed that the WALRUS model without an IGF flux has a higher Nash-Sutcliffe efficiency for the groundwater level as modelled by MORIA than the WALRUS model without an IGF flux. The models with IGF can also be considered more realistic, as without an IGF flux the model only shows a seasonal change in groundwater level without short-term variation, whereas the model with IGF does show short-term variation. This means that while it is not absolutely necessary to add the IGF, as a functioning WALRUS model can be created without IGF flux for this catchment, adding IGF data does improve the model significantly, both in terms of realism and overall efficiency.

# 7 Conclusion

This chapter summarizes the findings presented in this thesis and the conclusions that are drawn.

A common approach to estimate the intercatchment groundwater flow (IGF) to a catchment is to equate the net IGF to the 'missing' water in the water balance of the catchment. In order for the water balance of the Maurikse Wetering catchment to close, the actual evaporation in the catchment for 2017 has to be between 0% and 20% of the precipitation in 2017 (depending on the KNMI station used for meteorological data). Methods like the Budyko curve, a relation between actual and potential evaporation ratios which is followed by every catchment in the world, show that for 2017 this percentage should be much higher. The difference between these percentages shows that a data variable is incorrect. Since the precipitation and potential evapotranspiration data correspond to expected values, the error is expected to be in the discharge data. The erroneous discharge data appears to stem from the erroneous data from the tilting weirs in the Maurikse Wetering, which show weir levels below the minimum weir level possible. For this reason, equating the to the "missing" water in the water balance will not work for this catchment. The discharge estimates at the siphon beneath the Amsterdam Rijnkanaal are too low, as by these estimates hardly any water is being generated by the Maurikse Wetering catchment.

According to the groundwater model MORIA, the net IGF amounts to -60 to +90 mm per year. Taking the hydrological year of 2017, the commonly used method of equating the IGF to the "missing" water in the water balance does not hold up for the Maurikse Wetering catchment.

The MORIA results show that the general direction of the groundwater flow in the catchment is fixed throughout the year. This general direction is from the Nederrijn and Waal, through the catchment and finally exiting at the downstream western end of the catchment. Variations in groundwater flow direction are primarily caused by variations in the water level in the Waal and Nederrijn. Along some parts of the catchment border, for instance in the Upper Linge area, these variations in flow direction cause either a net gain due to IGF or a net loss, depending on the water levels in the Nederrijn and Waal. During high water levels in the Nederrijn and Waal, all catchment borders except for the downstream western area see incoming IGF. The net vertical flux, from the second aquifer to the upper aquifer, has the same course as the net horizontal flow. In the hydrological years 2013 to 2017, there are two distinct periods in the course of the modelled net IGF data. The transition between these two periods occurs around June 2015. Around June 2015 the average water level in the Waal drops while the level in the Nederrijn remains constant.

For the first period, from April 2013 to July 2015, the simple linear regression (SLR) analysis did not provide a satisfactory result when relating the modelled net IGF data to independent variables in the catchment or from the water levels in the Waal and Nederrijn. In the second period, from July 2015 to April 2018, a linear relation was found between the net IGF flux and the Nederrijn. This relation had a coefficient of determination (R-squared) of 0.773, meaning the curve-fit for this relation compared to the modelled data from MORIA is deemed 'very good' if the same standards are applied as for Nash-Sutcliffe efficiencies (Moriasi et al., 2007).

According to the multiple linear regression (MLR) analysis, the net IGF depends on the Waal level, groundwater level, precipitation, storage deficit in the unsaturated zone and the water level in the

Maurikse Wetering. The resulting MLR has an adjusted R-squared of 0.632, which is deemed "sufficient". If the MLR analysis is repeated for the period from July 2015 to April 2018 the resulting MLR has an adjusted R-squared of 0.855, which is considered 'very good'.

To see the effect that the IGF has on a conceptual hydrological model, a model for the Maurikse Wetering is built in the conceptual hydrological model WALRUS and is calibrated for both the situation with IGF and when the IGF flux is ignored. For use in the WALRUS model, the relation found between the net IGF to the Maurikse Wetering catchment and the water level in the Nederrijn via the SLR analysis is used as well as the outcome of the MLR analysis for 2015 – 2018. The Nederrijn relation is included as this requires a single variable and the relation has a "very good" fit for the period July 2015 – March 2018, this regression is thus seen as both effective and more robust than the MLR when it comes to predictive modelling. The model is calibrated to the average groundwater level as modelled by MORIA as well as the discharge as modelled by MORIA. The latter is required to get an estimation for the WALRUS parameter cQ, which the groundwater reservoir and thus calibration according to the groundwater level is insensitive to. The parameters were calibrated by selecting the parameter sets with the highest Nash-Sutcliffe efficiency.

The best fitting parameter set for the WALRUS model with the IGF relation models the groundwater level better than the best parameter set for the WALRUS model when it is assumed to be hydrologically isolated (meaning zero IGF). The WALRUS model with IGF as modelled by the MLR analysis has a Nash-Sutcliffe (NS) efficiency to the groundwater level of 0.75, whereas the hydrologically isolated model (without IGF) has a NS efficiency of 0.68. This means that the model with the IGF as modelled by the MLR analysis is better at modelling the groundwater level. The WALRUS model with the Nederrijn relation from the SLR analysis has a NS efficiency of 0.71. Despite not having a large difference in NS efficiency to the groundwater level, when comparing the outcomes visually the model without an IGF flux has a less variable course and only follows the broad, seasonal change in groundwater level. The models with IGF relation follow the daily variation from the data from MORIA more closely. The parameter set with the best fit does have a higher NS efficiency to the discharge as modelled by MORIA, as the model with IGF relation has a NS efficiency to the discharge of 0.74 and the model without IGF has a NS efficiency of 0.8.

For either scenario, the WALRUS model performs poorly when modelling the discharge after a dry period (a period where the groundwater level is below the maintained surface water level). It appears that the WALRUS model takes some time to 'recover' from this until providing discharge via quickflow. The model will therefore likely underestimate the discharge during these times. Despite this, both scenarios have a "very good" NS efficiency when looking at the discharge as modelled by MORIA, with the WALRUS model without IGF having a slightly higher NS efficiency to the discharge as modelled by MORIA. The poor fit to the short-term change in groundwater level for the model without IGF data relative to the model with IGF data continues when looking at all parameter sets above a NS efficiency towards the groundwater level ≥ 0.65, with the model without IGF only showing a broad seasonal change in groundwater level. In contrast, the WALRUS model with the IGF flux has a better short-term fit.

The improvement of the WALRUS model by adding the IGF flux is shown again in the validation of the WALRUS models using the hydrological year of 2017, where the model with the IGF as modelled by the Nederrijn relation has a NS value to the groundwater model of 0.65, compared to the NS value to the groundwater level of 0.54 for the model without IGF. The IGF as modelled by the MLR analysis is even better, with a NS value to the groundwater level of 0.69. The difference between these values is significant enough to state that the model with IGF as modelled by the relation with the Nederrijn significantly improves the WALRUS model for the Maurikse Wetering. This proves that, while a conceptual hydrological model can be created without IGF data, the incorporation of the IGF can significantly improve conceptual hydrological modelling.

# 8 Discussion

A lack of data is a common problem in hydrological modelling. As the observed KNMI station is not within the Maurikse Wetering catchment, the precipitation data will often be inaccurate. Similarly, spatial variations and local events of the precipitation are therefore often missed by these KNMI stations. With the available data, any statement concerning the spatial variation of meteorological data would be unreliable. As such, the precipitation data from KNMI station Herwijnen is assumed to be spatially uniform over the Maurikse Wetering catchment.

The apparently false discharge data caused by errors in the weir level data can be caused either by an error during data conversion or a false reference level. As the tilting weirs recently saw a conversion to a different operating system, this is where the error might have occurred. Either in the form of a wrong reference level or a conversion factor. When comparing the observed discharge data to the modelled discharge data, the course of the two is rather similar. This suggests either a constant or linear offset in weir level data to actual weir level, as opposed to completely unreliable data with no relation to reality. This would suggest that the data can be corrected relatively easily. Perhaps the original data can be located, or a case study can reveal the offset.

The fact that the exchange between the second and upper aquifer has the same course as the horizontal IGF suggests that this exchange is influenced by the same variables as the horizontal IGF. This can be related to the fault lines or the sand lanes in the area.

MORIA requires a considerable amount of data in order to run. The difference between the periods before and after the shift in IGF around June 2015 may be the result of errors in MORIA. As the MORIA model was run for the entire time frame in one sitting and was thus not subjected to change between runs (something which might occur if for instance the MORIA data consisted of combining annual runs performed a year in-between, where an update to MORIA can result in different outcomes) the chance of such an occurrence is decreased. It is therefore assumed that the MORIA results are a correct approximation of the reality. This means that the change in course occurring around June 2015 is due to changes in variables, either by natural processes or by human intervention. The average Waal level drops during this period. This suggests a correlation between the IGF and the interaction between the Waal and Nederrijn levels. Because of the discontinuous relation between the water levels in the Nederrijn and Waal, this will be difficult to determine. It needs to be verified if the MORIA data differs before and after June 2015 because of a change in modelling. If this is true, the most reliable data needs to be determined. From the relations found, this would likely be the period after 7-2015 as this relation explains the IGF best with the available parameters which likely influence the IGF. This is one of the main reasons that the MLR is performed thrice, once for the entire range of data, once before and once after the shift in the course of the modelled IGF data.

If the MORIA was not subjected to changes, the reason for the difference in periods and the different coefficients for the predictor variables from the three different MLR analyses can be due to several reasons. A first reason can be changes in the project area, like an altered cross-section for the Waal river as a result of the 'Room for the River' project. A second possible reason is that there are nonlinear relations between one or more variables and the IGF. A third possible reason is that an important predictor variable can be missing in this analysis. Examples of possible missing

variables are the groundwater level in the upstream/downstream catchment, or the groundwater level of the Utrechtse Heuvelrug. From the analysis of the groundwater flow direction it appears that the Utrechtse Heuvelrug moraine might play a bigger role than was originally thought. A fourth possible reason is that spatial differences plays an important role. Should this shift occur due to for instance physical changes to the Waal, then the relation after 7-2015 should be used as the physical aspects of the variables change because of this. If the shift is due to another occurrence, like continuous low discharge in the Waal and low groundwater levels because of this, then the MLR for the entire data range stands. Looking at the analysis of the groundwater flow direction, the most probable cause is the influence of the Utrechtse Heuvelrug moraine, which is outside of the study area.

Looking at the direction of the groundwater flow, the upstream area can have a significant effect on the IGF to the Maurikse Wetering catchment. Looking at the quantity of the right sided flux versus the front sided flux, the upstream catchment has a more constant course and can be a stabilising factor as opposed to the more variable front sided flux, which is more subjected to variations caused by variations in the water level in the Nederrijn and Waal. The effect of the upstream area cannot be determined by simply adding a delay in for instance the Waal level, as it is unknown how the Waal and Nederrijn rivers influence this upstream area and what the dampening effect will be as peak flows travel through the soil. This would require a separate case study of the upstream area, which is not in the scope of this research. The same is true for the downstream area the area to the west of the Maurikse Wetering catchment, where the groundwater level will influence the outgoing IGF. A separate study is needed for this as well. Upstream of the Maurikse Wetering the Nederrijn has a higher level due to locks which will influence the geohydrology of the area, and sandlanes can have a significant effect. It is also not known how far back the upstream area will influence the IGF towards the Maurikse Wetering. This will require a wider study.

In the MLR for the period April 2013 – June 2015, the poor curve fit can be partially explained by the little variation in the IGF data. As the R-squared value is determined in part by the difference from the mean, residuals have a more pronounced effect on the R-squared value of a dataset with low variations. In the MLR for the entire time frame, the groundwater level relative to the ground level has a negative coefficient. This would contradict the formula of Darcy, as the pressure difference would drop with decreasing groundwater levels, increasing IGF.

This research serves as a basis for further research into IGF for catchments without a detailed groundwater model like MORIA, as this would prove that creating a relation between the IGF and other variables in the catchment like surface water levels through a MLR analysis is possible. This would otherwise be impossible to prove without sufficient data and, as it is thought that smaller catchments can have significant IGF fluxes, being able to estimate the IGF to other variables will be very useful in practices like predictive modelling. As MORIA is a detailed 'bottom-up' model, there is a lot of data required for a similar model in other catchments. This creates problems for data-poor regions and is probably a reason why IGF is so often ignored.

If reliable discharge data at Buren can be found, this study can be used to prove the viability of the common method of modelling the IGF, namely equating the IGF flux to the missing water in the water balance. As the difference in storage $\Delta S$ is hard to accurately quantify for entire catchments for short time periods, a relation between the IGF and measurable variables (which will vary per catchment) is preferable.

# 9 RECOMMENDATIONS & FURTHER RESEARCH

It is advised that the Rivierenland Water Board tries to determine what caused the error in the weir level data, as it appears that this is the sole reason for the erroneous discharge data. This should be done for practical reasons, for instance water resource management in the Maurikse Wetering, but will also help the research towards IGF. This has to be done for all tilting weirs in the catchment, including the inlet from the Oude Rijn at De Kat.

Due to the complex network of artificial canals and (unmonitored) weirs to levelling areas, the water balance is difficult to model for the Maurikse Wetering catchment. As all water upstream of the Amsterdam Rijnkanaal must pass through the culvert beneath the Amsterdam Rijnkanaal, continuously measuring the water level downstream of the culvert and calibrating the discharge to the difference between the upstream and downstream measurements will provide reliable discharge measurements of a clearly defined area.

Another improvement to discharge measurements can be made by calibrating the weir at Buren, but not closing the fish ladder while doing so. The weir at Buren was calibrated in 2017 (Mulder & Maartense, 2017), however the fish ladder was closed during calibration. This gives the best estimate for the water flowing through the weir at Buren. However, this method decreases the accuracy for the discharge through the Maurikse Wetering when the fish ladder is not closed.

With reliable discharge data it can be seen if the IGF is equal to the missing water in the water balance. If this proves true, this research serves as a basis for further research into IGF for catchments without a detailed groundwater model like MORIA, as this would prove that creating a relation between the IGF and other variables in the catchment like surface water levels through a MLR analysis is possible. This would otherwise be impossible to prove without sufficient data and, as it is thought that smaller catchments can have significant IGF fluxes, being able to estimate the IGF using other variables will be useful in practices like predictive modelling. This relation can be created by doing a MLR analysis, using the missing water in the water balance (set equal to the IGF) to variables in or around the catchment, for instance the water level in adjacent rivers, the precipitation and the groundwater level of the catchment. The resulting MLR can then be used to estimate the IGF in predictive modelling.

If the water balance does not close with the addition of IGF, this will prove that the common approach of equating the IGF to the missing water in the water balance is at the least not always correct. This would create a problem, namely that there is a missing flux or that the other processes are improperly modelled. This would mean that more effort needs to be put into fluxes like the actual evaporation or the spatial variation of precipitation to close the water balance.

The reason for the shift around June 2015 should be researched further, starting with ensuring that this shift is not due to a change in MORIA. If it turns out that no changes occurred in MORIA, the reason for this shift in the data can be researched. From the analysis of the direction of groundwater flow and the quantity of IGF, this appears to be due to the groundwater level in the Utrechtse Heuvelrug moraine. For this reason, the study area should be expanded to incorporate this area.

Looking at iMOD, several issues were encountered while using this program. To improve the user friendliness of iMOD, it is advised to add a 'cancel' option when loading in data or running a module. Now, forgetting to change a desired setting for instance can result in a delay of multiple hours, as the user can either wait for the model to finish the run or do a forced shutdown, which requires all data to be loaded in again after reopening iMOD which can be time consuming.

Furthermore, it is preferable that wrong settings result in an error message instead of the program shutting down. As this is not an uncommon occurrence when settings are entered correctly, probably depending on the computer of the user, this might occur only after several tries. And without an error message describing the source of the error, it can be difficult to find out the wrong (or bugged) setting. For instance, checking the "save fluxes between zones" option results in the program closing unexpectedly during a run. As after a shutdown the data has to be loaded in again, this can be a time-consuming affair. Another option for improving user friendliness lies in the "preview" option in the water balance tool. iMOD opening up to thousands of images one after the other can be frustrating to the user, as each image needs to be closed individually.

# 10 References


Allen, R.G., Pereira, L.S., Raes, D., Smith, M. (1998). Crop evapotranspiration – Guidelines for computing crop water requirements – FAO irrigation and drainage Paper 56. FAO, 1998. ISBN 92-5-104219-5

Bouaziz, L., Weerts, A., Schellekens, J., Sprokkereef, E., Stam, J., Savenije, H., and Hrachowitz, M. (2018). Redressing the balance: quantifying net intercatchment groundwater flows, Hydrol. Earth Syst. Sci. Discuss., https://doi.org/10.5194/hess-2018-370, in review, 2018.

Brauer, C. (2014). *Modelling rainfall-runoff processes in lowland catchments*.

Brauer, C. C., Teuling, A. J., Torfs, P. J. J. F., Uijlenhoet, R. (2014a). The Wageningen Lowland Runoff Simulator (WALRUS): a lumped rainfall-runoff model for catchments with shallow groundwater. Geosci. Model Dev. 7, 2313–2332.

Brauer, C. C., Torfs, P. J. J. F., Teuling, A. J., Uijlenhoet, R. (2014b). The Wageningen Lowland Runoff Simulator (WALRUS): application to the Hupsel Brook catchment and Cabauw polder. Hydrol. Earth Syst. Sci. 18, 4007–4028.

Brauer, C. C., Torfs, P. J. J. F., Uijlenhoet, R. (2018) WALRUS tutorial. Retrieved from https://github.com/ClaudiaBrauer/WALRUS/tree/master/tutorial

Brauer, C., Torfs, P., Teuling, R., Uijlenhoet, R. (2017). *The Wageningen Lowland Runoff Simulator WALRUS 1.10. User Manual*

Cohen, K.M., Stouthamer, E., Hoek, W.Z., Berendsen, H.J.A., Kempen, H.F.J. (2009) Zand in Banen - Zanddieptekaarten van het Rivierengebied en het IJsseldal in de provincies Gelderland en Overijssel. Arnhem: Provincie Gelderland.

De Vries, J. J. (1974). *Groundwater Flow Systems and Stream Nets in the Netherlands*.

Gemeente Buren. (2018). *Gemeente Buren*. Retrieved from https://www.buren.nl/

Genereux, D. P., Jordan, M. T., and Carbonell, D. (2005) A paired-watershed budget study to quantify interbasin groundwater flow in a lowland rain forest, Costa Rica. *Water resources research, 41*, W04011, doi:10.1029/2004WR003635

Genereux, D. P.,Wood, S. J., Pringle, C. M. (2002) Chemical tracing of interbasin groundwater transfer in the lowland rainforest of Costa Rica. *Journal of Hydrology, 258*, 163–178

Hayashi, F. (2000). *Econometrics*. Princeton University Press. ISBN 0-691-01018-8.

Hobbelt, L., Klutman, W., Ter Harmsel, A., Van der Veen, R., & Van de Braak, J. (2018). *Betuwe Synthese grondwatersysteembeschrijving.*

Juras, R., Pavlásek, J., Vitvar, T., Šanda, M., Holub, J., Jankovec, J., & Linda, M. (2016). Isotopic tracing of the outflow during artificial rain-on-snow event. *Journal of Hydrology, 541,* 1145-1154.

KNMI. (n.d.). KNMI - Kennis & uitleg. From https://www.knmi.nl/kennis-en-datacentrum

Lingestreek. (n.d.). Langste rivier in Nederland. Geraadpleegd op 26 juli 2018, van http://lingestreek.nl/rivier-de-linge/

Lomax, R. G. (2007). *Statistical Concepts: A Second Course*. Lawrence Erlbaum Associates.

Moriasi, D. N., Arnold, J. G., Van Liew, M. W., Bingner, R. L., Hamel, R. D., & Veith, T. L. (2007). Model Evaluation Guidelines for Systematic Quantification of Accuracy in Watershed Simulations. *American Society of Agricultural and Biological Engineers*, 50(3), 885–900.

Mulder, M. R., & Maartense, R. (2017). *Capaciteitsmetingen Kantelstuw Buren* (Referentie P16084).

Novotny, V. (2008) Watershed models. *Encyclopedia of Ecology,* 3748-3759, https://doi.org/10.1016/B978-008045405-4.00240-8

Pellicer-Martínez, F., González-Soto, I., & Martínez-Paz, J. M. (2015). Analysis of incorporating groundwater exchanges in hydrological models. *Hydrological Processes, 29,* 4361-4366. doi:10.1002/hyp.10586

Preacher, K. J., Curran, P. J., & Bauer, D. J. (2006). Computational Tools for Probing Interactions in Multiple Linear Regression, Multilevel Modeling, and Latent Curve Analysis. *Journal of Educational and Behavioral Statistics*, *31*(4), 437–448. https://doi.org/10.3102/10769986031004437

Rijkswaterstaat. (2015). Factsheet kribverlaging Waal. Retrieved May 15, 2019, from https://issuu.com/ruimtevoorderivier/docs/factsheet_kribverlaging_waal_tcm174

Rijkswaterstaat. (2019). Rijkswaterstaat Waterinfo – Waterhoogte (t.o.v. NAP) [Dataset]. Retrieved February 11, 2019, from https://waterinfo.rws.nl/

Rivierenland Water Board. (n.d.). Gemaal Maurikse Wetering (v2) [Dataset].

Schuurmans, J. M., & Droogers, P. (2010). *Penman-Monteith referentieverdamping: Inventarisatie beschikbaarheid en mogelijkheden tot regionalisatie* (Report No. 2010-37, ISBN 978.90.5773.491.5). Retrieved from http://edepot.wur.nl/163482

Seltman, H. J. (2018). *Experimental Design and Analysis*.

Shieh, G. (2007). Improved Shrinkage Estimation of Squared Multiple Correlation Coefficient and Squared Cross-Validity Coefficient. *Organizational Research Methods*, *11*(2), 387–407. https://doi.org/10.1177/1094428106292901

Statsmodels (n.d.). StatsModels: Statistics in Python — statsmodels 0.9.0 documentation. Retrieved May 30, 2019, from https://www.statsmodels.org/stable/index.html

Sui, J., & Koehler, G. (2001). Rain-on-snow induced flood events in Southern Germany. *Journal of Hydrology, 251,* 205-220.

Swierstra, W., & Kerckhoffs, T. (2018). *Inbouwen REGIS II v2.2 in MORIA* (BG1132WATRP1811291318).

Tanis, K. (2017, December 14). Sluis in Arkelsche Dam dicht vanwege hoog waterpeil. *AD*. Retrieved from https://www.ad.nl/rivierenland/sluis-in-arkelsche-dam-dicht-vanwege-hoog-waterpeil~abe1afoc/

Thyne, G. D., Gillespie, J. M., Ostdick, J.R. (1999), Evidence for interbasin flow through bedrock in the southeastern Sierra Nevada, *Geol. Soc. Am. Bull., 111(11),* 1600– 1616.

TNO. (2013). *DINOloket*. Retrieved from https://www.dinoloket.nl/

Veldkamp, J. G., & Wiertz, J. (1997) *Schematisatie van bodembedekking en kwel in Nederland voor SMART/MOVE* (Rapport no. 711901 021). Retrieved from https://www.rivm.nl/Documenten_en_publicaties/Wetenschappelijk/Rapporten/1997/oktober/Schematisatie_van_bodembedekking_en_kwel_in_Nederland_voor_SMART_MOVE

Vermeulen, P. T. M., Burgering, L. M. T., Roelofsen, F. J., Minnema, B., & Verkalk, J. (2018). *iMOD User Manual 4.2.1* (Verson 4.2.1, Revision 54031).

Vermue, H. (2017). *Modellering calamiteitenmodel voor pilotgebied* (Kenmerk WATBF5331-101-N003F1.1).

Vernes, R., Van Doorn, T., Bierkens, M., Van Gessel, S., & De Heer, E. (2005). *Van Gidslaag naar Hydrogeologische Eenheid* (NITG 05-038-B).

Versteegen, F. G. (2017). *Lingesysteem, Toelichting op het Streefpeilenplan* (Reference TL268-1/17-012.646).

Vis, H., & Franssen, M. (2014). *Opstellen RA prestatie-eisen gemaal Maurikse Wetering* (Reference 14.525-P14.007.01-VIH-FRM).

Wasserstein, R. L., & Lazar, N. A. (2016). The ASA's Statement onp-Values: Context, Process, and Purpose. *The American Statistician*, *70*(2), 129–133. https://doi.org/10.1080/00031305.2016.1154108

Wendt, D. E. (2015) Snow hydrology in the Netherlands: Developing snowmelt algorithms for Dutch regional water management modules. Internship report (at HKV), Wageningen University.

Young, P. H. (2000). Generalized Coefficient of Determination. *The Journal of Cost Analysis & Management*, *2*(1), 59–68. https://doi.org/10.1080/15411656.2000.10462406

Zambrano-Bigiarini, M. and Rojas, R. (2013). A model-independent Particle Swarm Optimisation software for model calibration, Environmental Modelling & Software, 43, 5-25, doi:10.1016/j.envsoft.2013.01.004.

Zambrano-Bigiarini, M. and Rojas, R. (2018). hydroPSO: Particle Swarm Optimisation, with Focus on Environmental Models. R package version 0.4-1. URL https://cran.r-project.org/package=hydroPSO. DOI:10.5281/zenodo.1287350

# Appendices

# Appendix A. WATER LEVEL IN THE RHINE

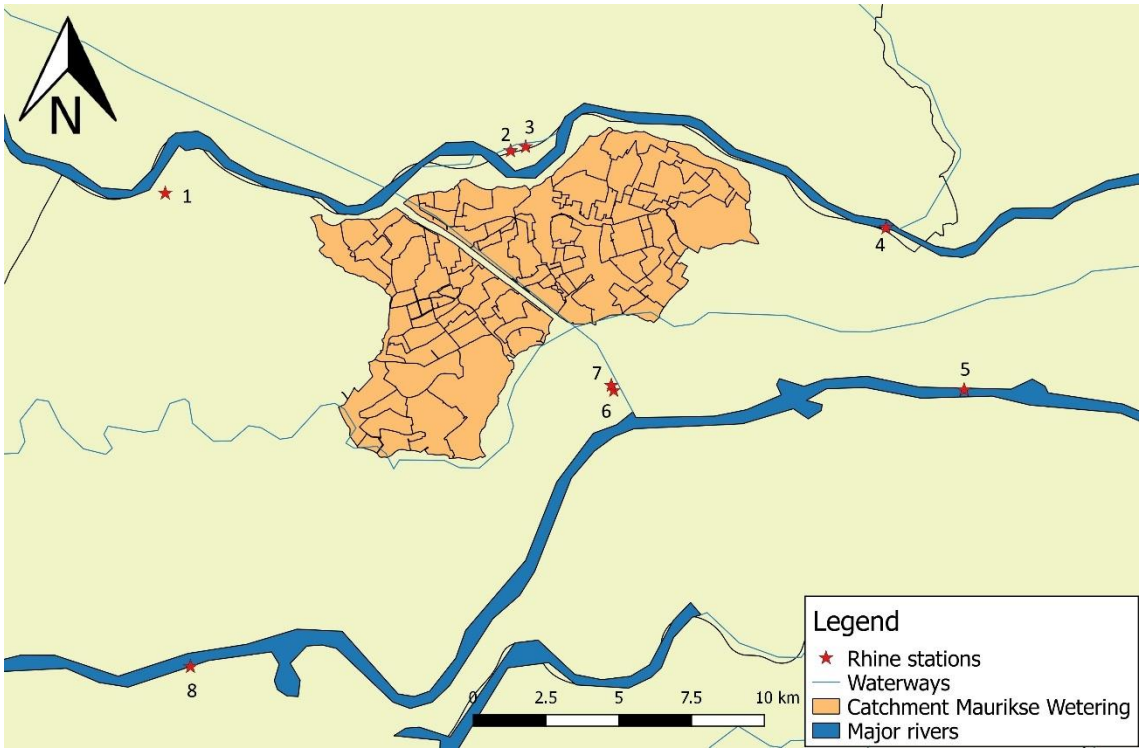


**Figure A-1, actual positions measuring stations Nederrijn and Waal**

The actual position of the different measuring stations is given in Figure A-1. Figure A-2 through Figure A-9 give the water levels in these stations. As can be seen, the Nederrijn stations show a much more stable water level due to the locks present in the Nederrijn.

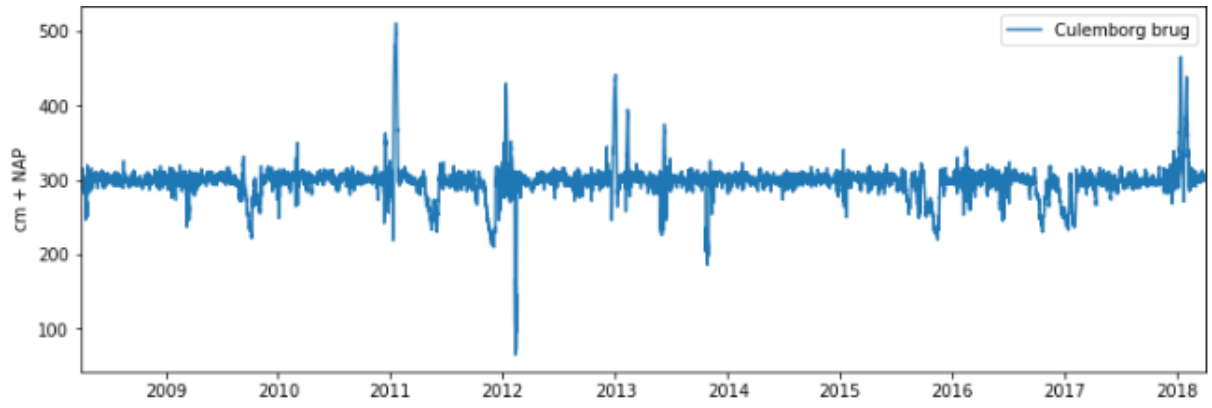


**Figure A-2, station 1: water level at Culemborg (Nederrijn)**

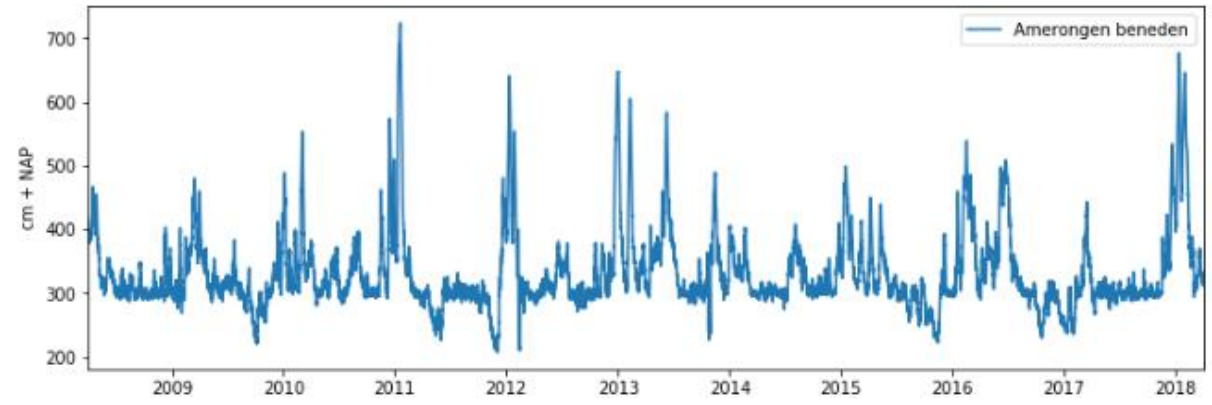


**Figure A-3, station 2: water level at Beneden Amerongen (Nederrijn)**

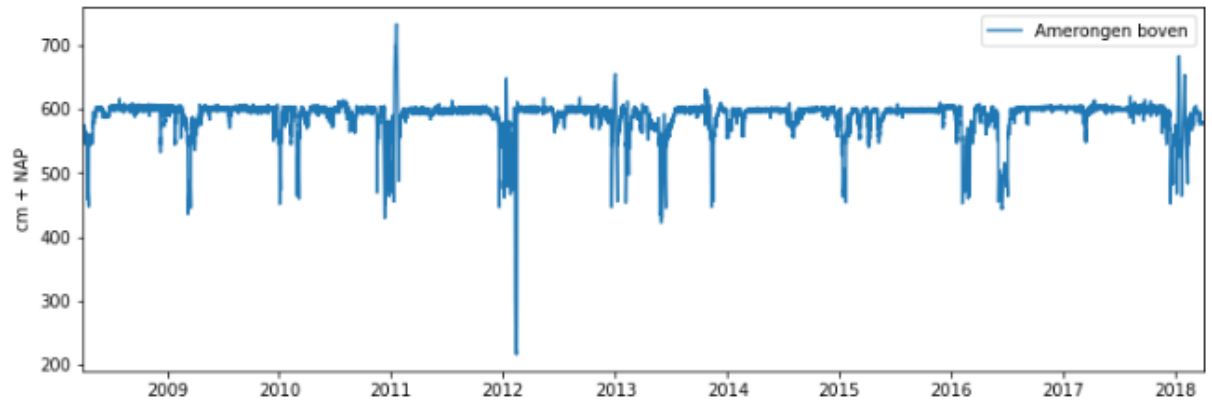


**Figure A-4, station 3: water level at Boven Amerongen (Nederrijn)**

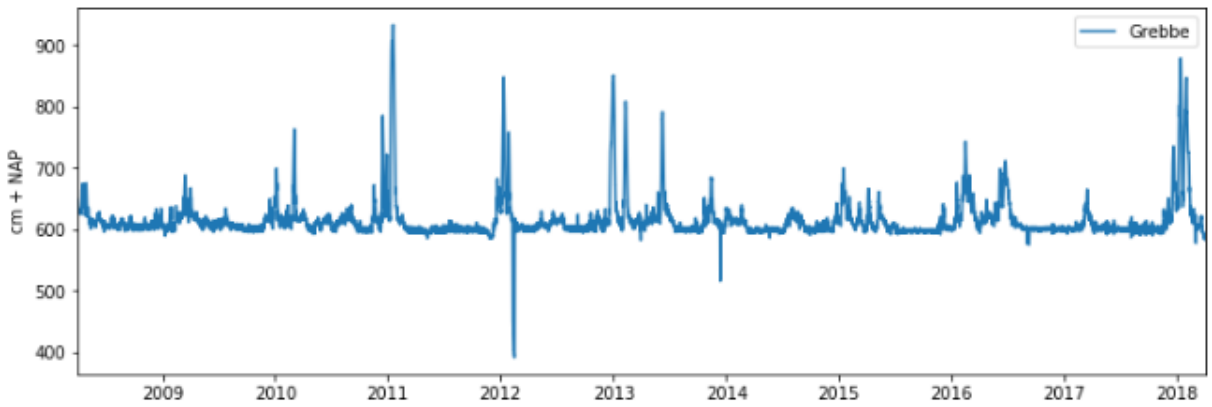


**Figure A-5, station 4: water level at Grebbe (Nederrijn)**

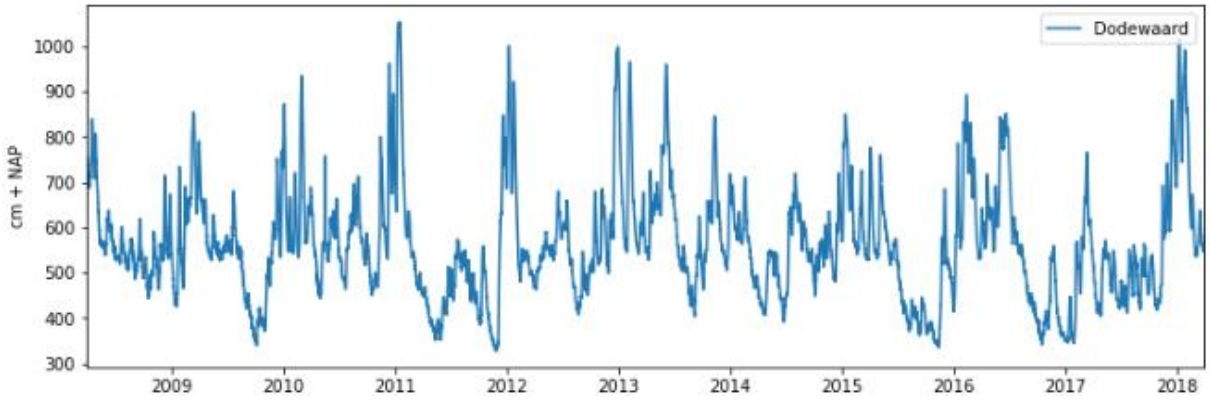


**Figure A-6, station 5: water level at Dodewaard (Waal)**

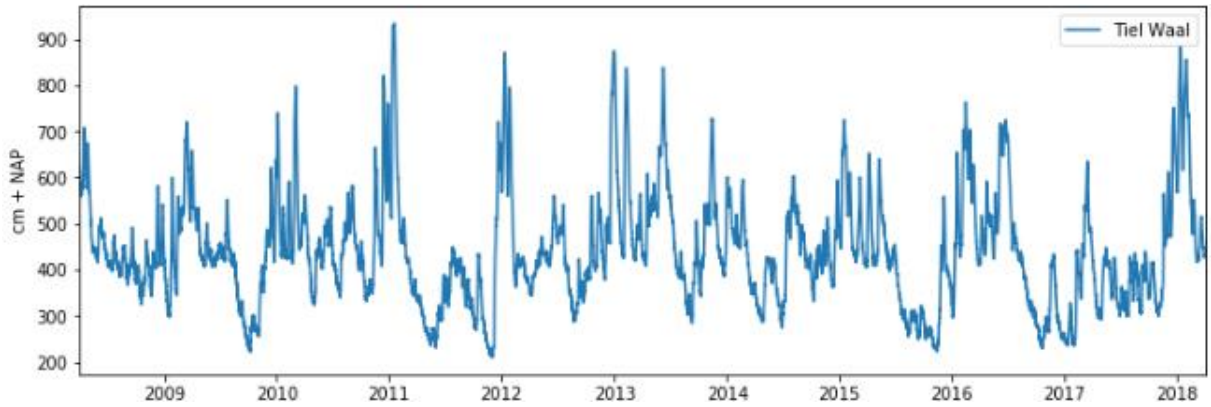


**Figure A-7, station 6: water level at Tiel (Waal)**

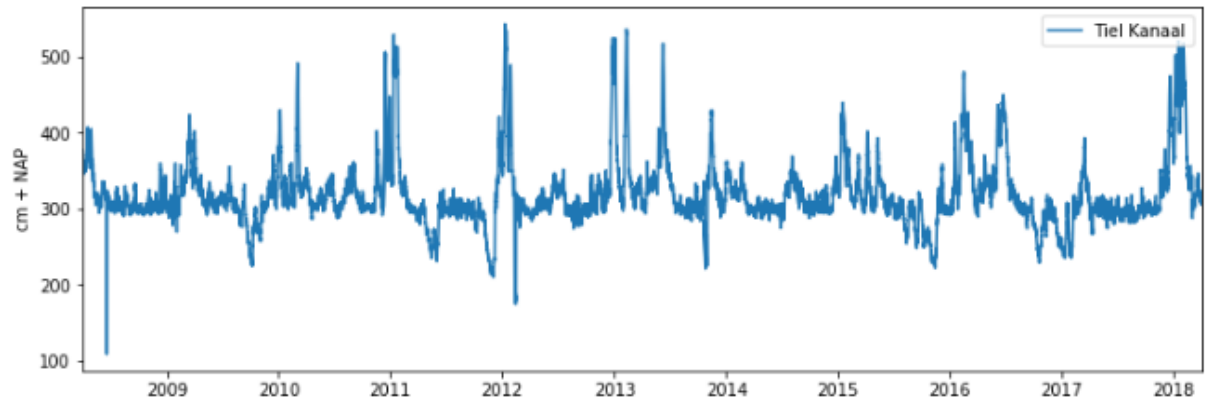


**Figure A-8, station 7: water level at Tiel (Amsterdam Rijnkanaal)**

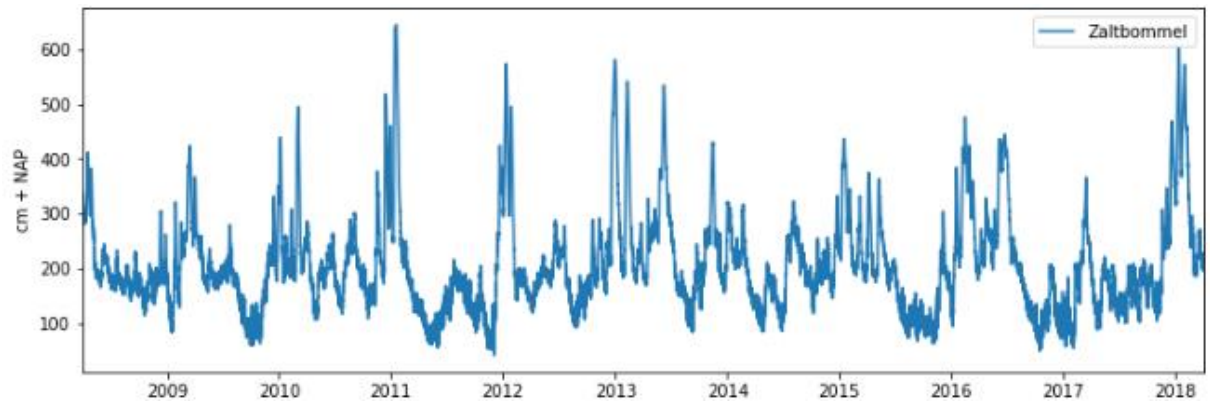


**Figure A-9, station 8: water level at Zaltbommel (Waal)**

# Appendix B. INFLUENCE AMSTERDAM RIJNKANAAL

Although in iMOD the (bugged) option “save fluxes between catchments” was disabled, due to the distance between the eastern and western parts of the catchment by the Amsterdam Rijnkanaal it had to be checked if the fluxes between the two parts would not be counted double. This would show in the (gross) IGF fluxes for each subcatchment. As most groundwater exiting the eastern part passes through the western part in the period 1-1-2014 – 28-2-2014, if these fluxes are taken into account the result this would result in the outgoing FFF and FRF of the eastern catchment to be added to the incoming FFF and FRF of the western catchment. If the analysis is repeated with a single shape in which the Amsterdam Rijnkanaal is taken up in the catchment as shown in Figure B-2, this flux would not be visible as the water never exits the catchment. If the fluxes between the catchment are taken in with the analysis, the difference between the summation of the IGF fluxes should be vastly different between the two resulting timeseries.

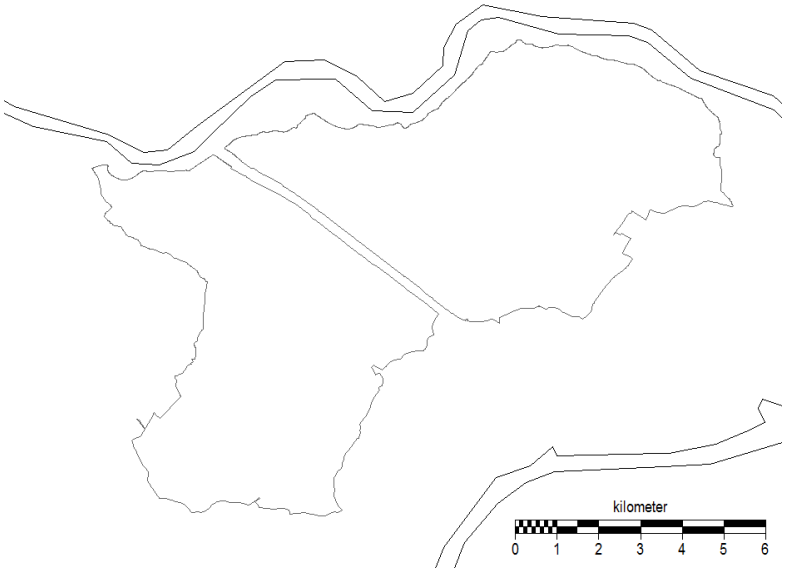


**Figure B-1, Maurikse Wetering catchment borders, with the Amsterdam Rijnkanaal separating the two halves**

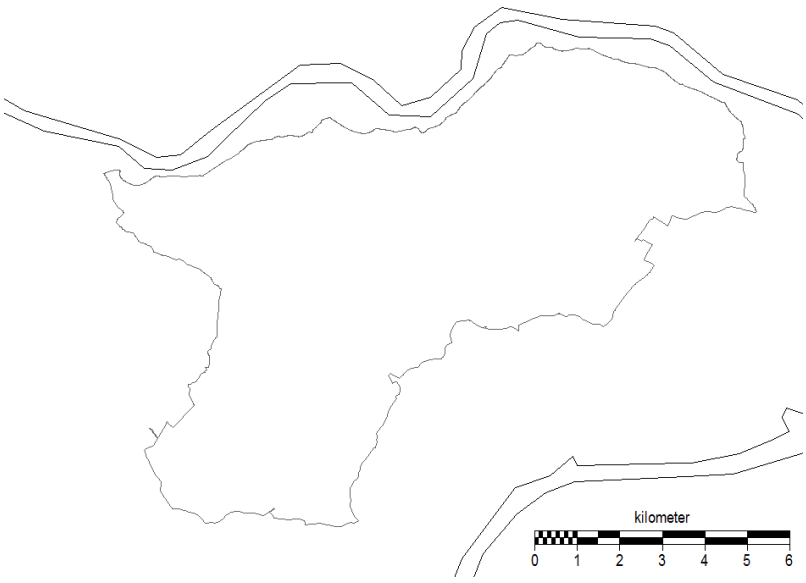


**Figure B-2, Maurikse Wetering catchment with ARK dissolved in catchment shapefile**

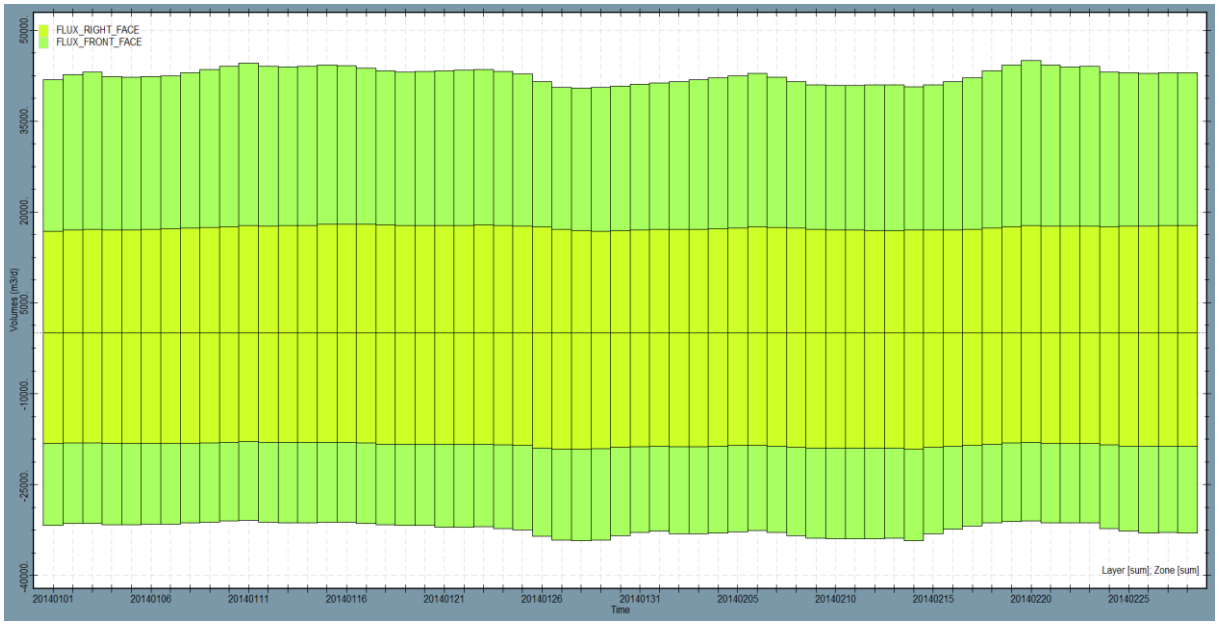


**Figure B-3, horizontal groundwater flux with ARK outside catchment shapefile (default catchment)**

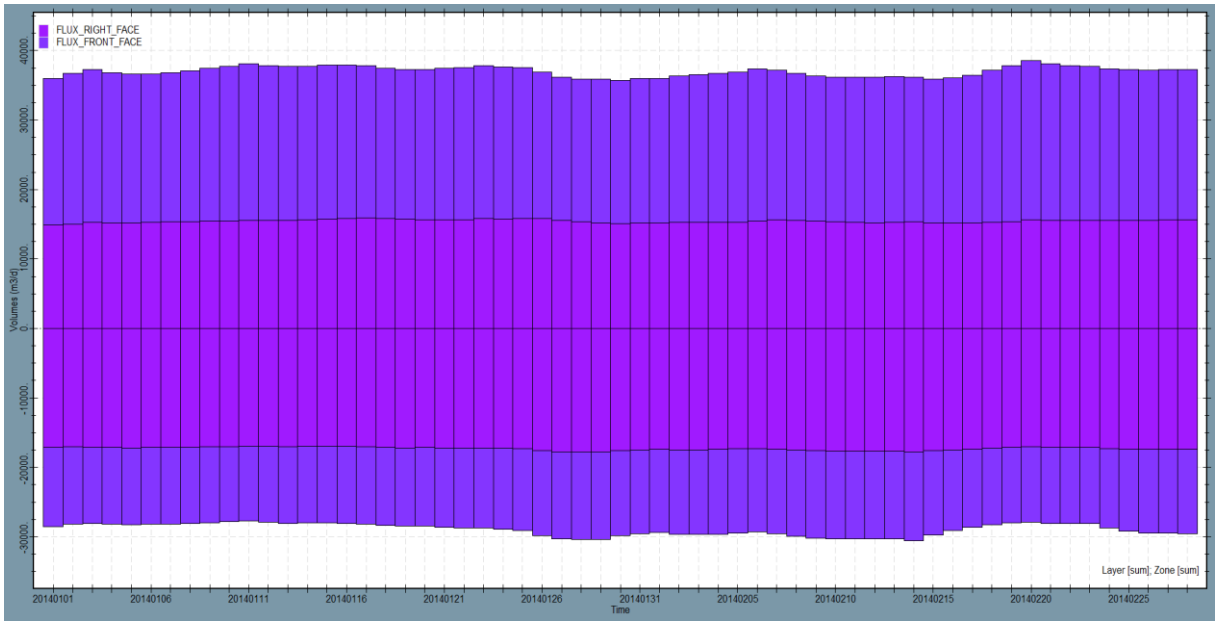


**Figure B-4, horizontal groundwater flux with ARK dissolved within catchment shapefile**

As can be seen in Figure B-3 and Figure B-4, the timeseries show only a slight difference. The flux between the two parts cannot account for the difference between the two timeseries. Therefore it can be concluded that the shapefile being split in two by the Amsterdam Rijnkanaal can be used without fluxes being counted double by iMOD's analysis. The difference is likely caused mostly by the influence of the Amsterdam Rijnkanaal itself.

# Appendix C. CHANNEL DEPTH

The new channel depth $c_D$ has been estimated using SOBEK cross-sections. From 40 cross-sections evenly distributed throughout the catchment this new channel depth $c_{D,1}$ has been set at 2.34 m. This does not consider any sludge in the system, which can be seen in Figure C-1. This will not be a problem as the top of the tilting weir will be above any possible sludge on the channel bed.

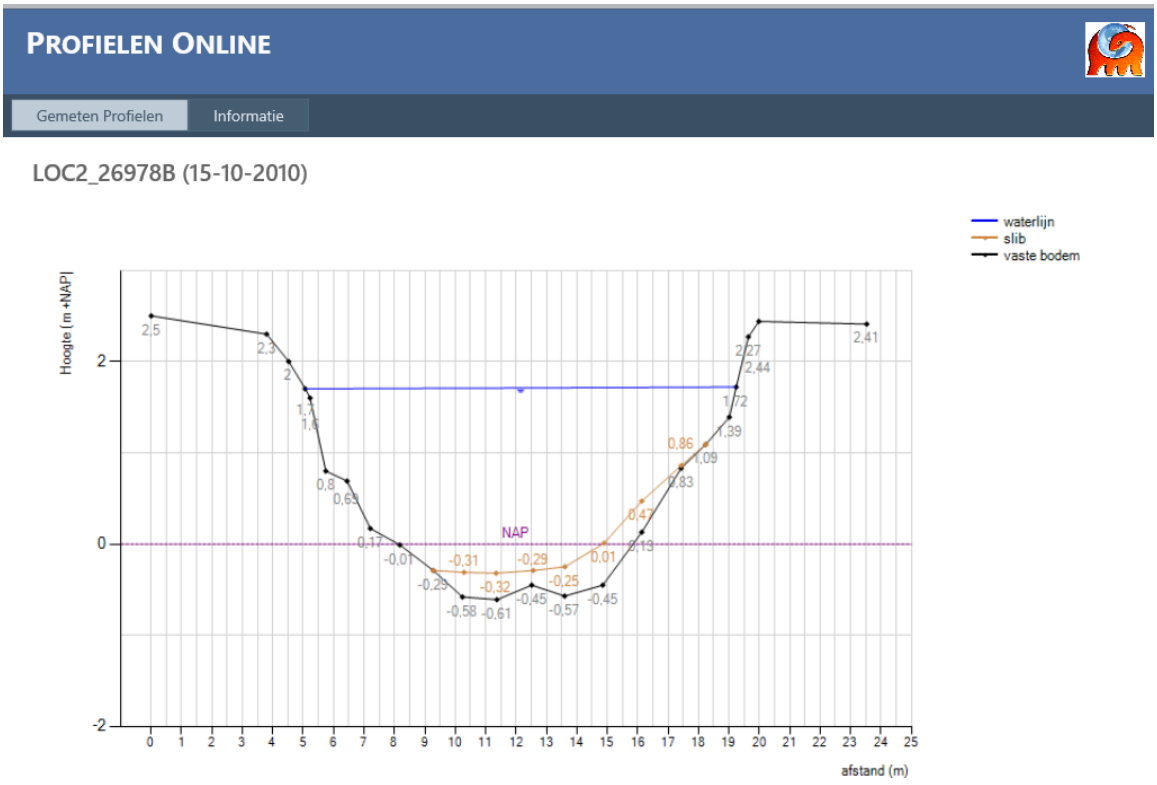


**Figure C-1, cross-section Maurikse Wetering with sludge**

The original channel depth $c_{D,0}$ is 4.05 m with a bottom level of – 1.51 m +NAP. These values are taken from the SOBEK model of the Maurikse Wetering. The cross-section closest upstream to the weir at Buren is given in Figure C-2.

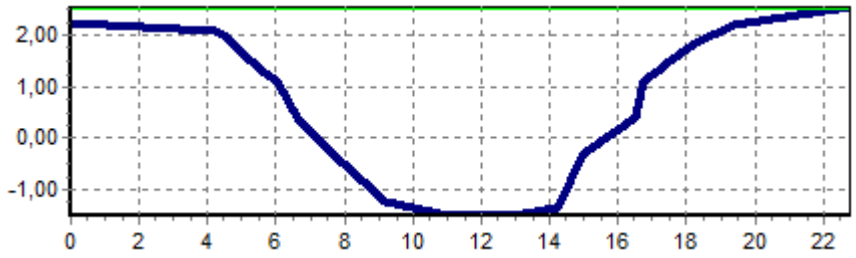


**Figure C-2, cross-section Maurikse Wetering upstream of the weir at Buren**

# Appendix D. WALRUS CALIBRATED TO OBSERVED DISCHARGE

When the model is calibrated to the observed discharge at the weir at Buren, the erroneous discharge measurements become clear. The example in this appendix is for the Maurikse Wetering catchment when it is seen as a hydrologically isolated model, by which there is no external groundwater flux and no external surface water flux. Automatic calibration was done using hydroPSO. HydroPSO is a Particle Swarm Optimization algorithm for the calibration of models. After specifying which model parameters need calibration, hydroPSO will calibrate the model until either an error tolerance or a specified maximum number of iterations is reached (Zambrano-Bigiarini & Rojas, 2018). The model was calibrated to a short period to save time.

The initial groundwater depth $d_{G,0}$, one of the required input parameters for WALRUS, was set at the corresponding depth of the nearby groundwater well BETU20003 at the start of the run. At 1-8-2017 this was 1.406 m below ground level.

As most data are in the hourly format it would be better to have the same for the evaporation. As of now, the KNMI only provides evaporation data on a daily timestep. In order to get hourly evaporation data, the evaporation will be calculated using the Makkink formula:

$$ET_{ref} = \frac{0.65 * \frac{s}{s+\gamma} * K^{\downarrow}}{\lambda * \rho} \quad \text{(D-1)}$$

| Parameter | Symbol | Value | Unit |
|---|---|---|---|
| *Reference evapotranspiration* | $ET_{ref}$ | | m/h |
| *Global radiation* | $K^{\downarrow}$ | | J/m²/h |
| *Slope of vapor pressure* | s | | kPa/⁰C |
| *Psychrometric constant* | γ | 0.066 | kPa/⁰C |
| *Heat of evaporation* | λ | | J/kg |
| *Density* | ρ | 1000 | kg/m³ |
| *Temperature* | T | | ⁰C |

**Table D-1, parameters equation** (D-1)

$$\lambda = (2501 - 2.375 * T) * 1000 \quad \text{(D-2)}$$

$$s = \frac{4098 * \left(0.618 * \exp\left(\frac{17.27 * T_{avg}}{T_{avg} + 237.3}\right)\right)}{\left(T_{avg} + 237.3\right)^2} \quad \text{(D-3)}$$

Here $T_{avg}$ is the average temperature. To compute hourly values, the temperature given by the KNMI for that hour is used. It is assumed that the changes are negligible. For the daily values the average between the highest and lowest daily temperature as given by the KNMI was used.

$$T_{avg} = \frac{T_{max} + T_{min}}{2} \quad \text{(D-4)}$$

This formula for s is somewhat aged. However, to stay close to the given values as computed by the KNMI this formula is used.

A consistent error appears to occur between the sum of hourly evaporation values for one day and the daily value.

$$E_{P,daily} \approx \frac{sum(E_{P,hourly})}{1.1} \qquad \text{(D-5)}$$

This is likely caused by a combination of:

- The course of the temperature over time. Averaging assumes a linear approach but actually the process is more similar to a sinusoid.
- As global radiation only occurs during the day, which is when high temperatures occur, this hourly approach results in a slightly higher value when the 24 hours are summed up as the lower temperatures occurring during the night are left out of the equation as they receive no radiation.

Despite this slight difference in summed amount, the hourly values acquired the method above are assumed to be the correct values.

With this input the WALRUS model can be created.

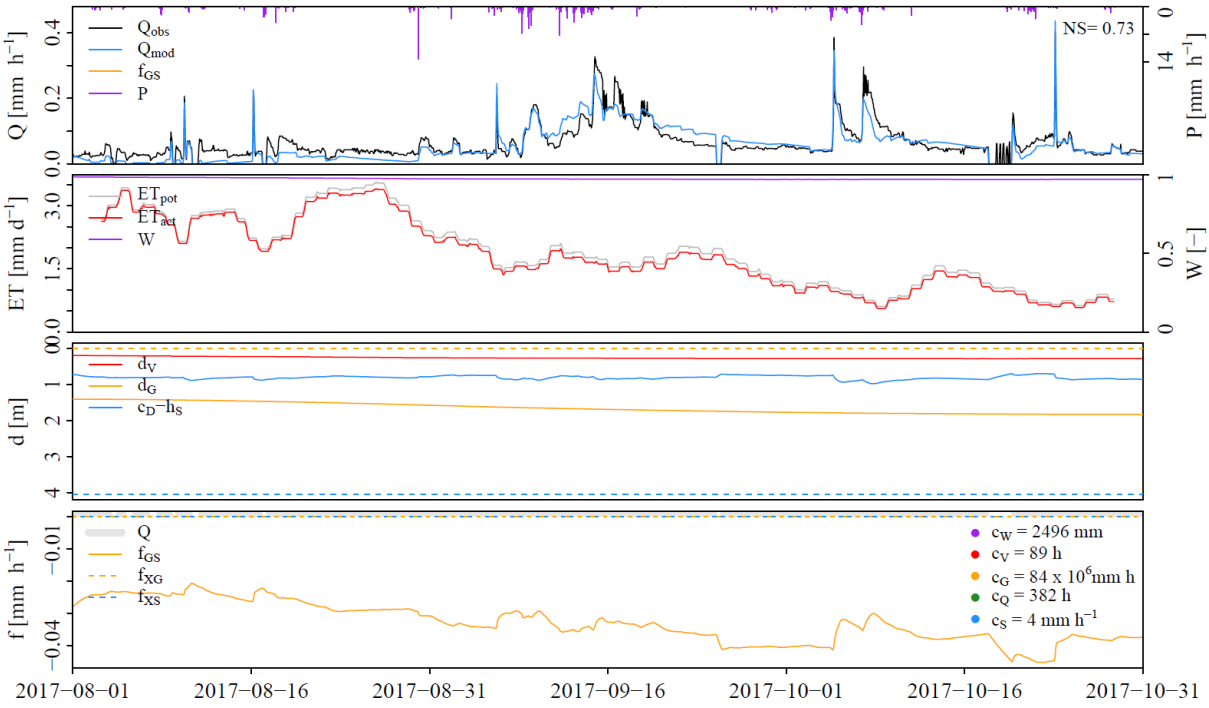


**Figure D-1, WALRUS model with original input and parameters**

As can be seen from the resulting WALRUS figures in Figure D-1, the fit of the modelled discharge to the observed discharge is good with a NS efficiency of 0.73. However, the second, third and fourth plot in Figure D-1 show the errors in this model. In order to fit the observed discharge, all discharge needs to be routed to the surface water via the quickflow. This happens when the wetness W is 1. This effectively means that the surface is impermeable, as the unsaturated/vadose zone is fully saturated. This can be seen in the third plot, where there is no fluctuation only a constant lowering of the groundwater level. The surface water infiltrates to the groundwater reservoir over the entire period, which also should not occur.

# Appendix E. WALRUS PARAMETERS IN LITERATURE

The WALRUS examples from the WALRUS tutorials were used to get a feel of the values of each parameter. This made a first estimation of the parameter values easier.

| Parameter | Cabauw | Berkel | Hupsel | Oude Riet | Bakelse Aa |
|---|---|---|---|---|---|
| *cW* | 110 | 400 | 200 | 250 | 230 |
| *cV* | 14 | 4 | 4 | 10 | 18 |
| *cG (* 10^6)* | 118 | 20 | 5 | 20 | 7 |
| *cQ* | 76 | 20 | 10 | 25 | 30 |
| *cS* | NA | 3 | 4 | 2 | 1.3 |
| *dGo* | 246 | 1500 | 1250 | 350 | 1200 |
| *cD* | 1500 | 2500 | 1500 | 2000 | 1500 |
| *aS* | 0.05 | 0.01 | 0.01 | 0.02 | 0.015 |
| *st* | Cal_C | Sand | Loamy sand | Cal_C | sand |

**Table E-1, values parameters from WALRUS examples**

| Parameter | Maurikse Wetering | Cabauw | Berkel | Hupsel | Oude Riet | Bakelse Aa |
|---|---|---|---|---|---|---|
| *cW* | 114 | 110 | 400 | 200 | 250 | 230 |
| *cV* | 17 | 14 | 4 | 4 | 10 | 18 |
| *cG (* 10^6)* | 34 | 118 | 20 | 5 | 20 | 7 |
| *cQ* | 86 | 76 | 20 | 10 | 25 | 30 |
| *cS* | 4 | NA | 3 | 4 | 2 | 1.3 |
| *dGo* | (varies) | 246 | 1500 | 1250 | 350 | 1200 |
| *cD* | 2340 | 1500 | 2500 | 1500 | 2000 | 1500 |
| *aS* | 0.01 | 0.05 | 0.01 | 0.01 | 0.02 | 0.015 |
| *st* | Loamy sand | Cal_C | Sand | Loamy sand | Cal_C | sand |

**Table E-2, values parameters Maurikse Wetering compared to WALRUS examples from literature**